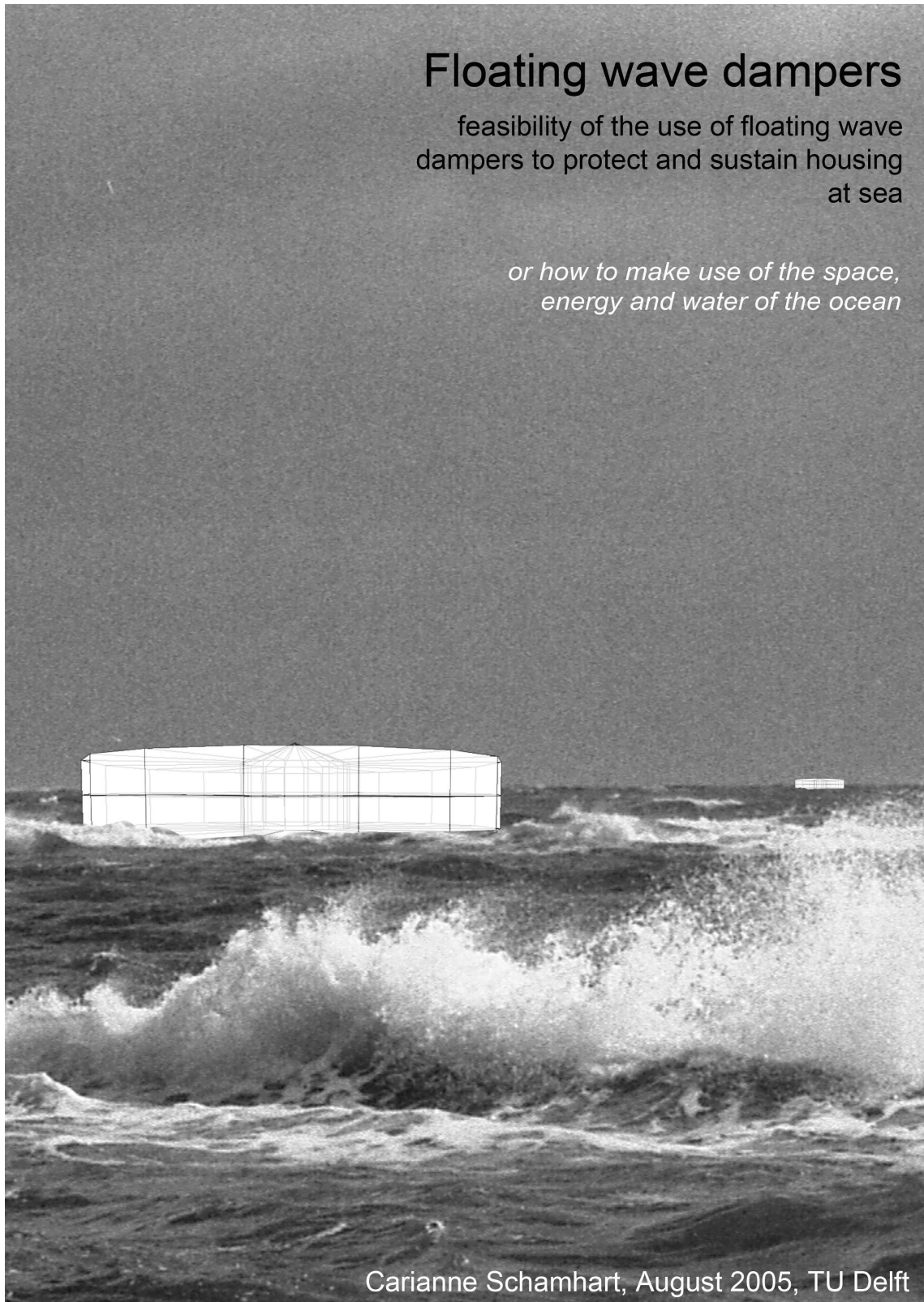# Floating wave dampers

feasibility of the use of floating wave
dampers to protect and sustain housing
at sea

*or how to make use of the space,
energy and water of the ocean*

Carianne Schamhart, August 2005, TU Delft

1

Floating wave dampers

Feasibility of the use of floating wave dampers to protect and sustain housing at sea.

or how to use the space, energy and water of the ocean.

Carianne Schamhart

August 2005, Delft University of Technology

Preface

'The sea is man's final frontier.'[1] This is partly why an aerospace engineering student like me chooses a maritime topic for her Masters' thesis. The innovative character of the assignment appealed to me and I wanted to be involved in developments that can reshape our surroundings.

The assignment is part of a research program initiated by the ecoboat foundation. The objective of the foundation is to find a sustainable answer for the ever increasing need for water, energy and living space. Their solution is referred to as the ecoboat: a floating house at sea that uses the waves for energy and salt water for fresh water. Most research on this project has been done at the Delft university of Technology. Several students have graduated on ecoboat related subjects and several smaller projects have contributed to the program's knowledge. But this thesis is the first research on the technical aspects of living at sea.

The thesis is also part of the university program for sustainable development. The university program includes a certificate ('sustainable engineer') for Masters' students that incorporate sustainable development into their courses. One of the requirements for the certificate is the integration of sustainable development into the Masters' thesis. This thesis is my last step to receive the certificate.

The theoretical information presented may seem excessive to engineers with a maritime engineering background. But most readers will have no knowledge of waves or motions of floating bodies. Therefore this thesis is written for engineers with a basic understanding of dynamics, fluid mechanics, statistics and other general engineering topics.

I would like to thank prof. dr. ir. Th. van Holten and ir. Jessica Holierhoek for giving me the opportunity to choose a subject outside aerospace engineering, prof. dr. ir. J.A. Pinkster and ir. Peter Wellens for their support and their confidence in this futuristic assignment, Frits Schoute for his vision of sea-building nations and Gijs, Anne Loes and Emma for putting up with me these last months.

---

[1]Liberally translated from Jacques-Yves Cousteau (1910-1997).

Contents

Summary

Population growth, urbanization and increasing prosperity. These are the main elements that increase the demand for space, water and energy, especially in large cities. To find a sustainable solution that meets these needs the sea-surface is considered. For coastal metropolises the sea offers an abundance of space, water and energy, but is as yet unaccessible. A research program has been started to enable living at sea with the ecoboat as projected solution. An ecoboat should provide housing, water and energy to its inhabitants in a sustainable manner.

This thesis investigates the feasibility of the use of floating wave dampers to protect an ecoboat settlement. It also investigates the feasibility of ecoboats and dampers as a sustainable form of living. The research to find the damping properties is restricted to the effect of one damper on one ecoboat for one wave propagation direction. The investigation of the sustainability is restricted to household consumption.

Protection

The feasibility of the use of the dampers as a protection system is investigated by comparing the motions of the ecoboat in waves behind a damper with the ecoboat motions in undisturbed waves. To this purpose a basic damper is designed.

The damper requirements are derived from the ecoboat. It should protect an ecoboat of $35m$ diameter, $7m$ total height, $2m$ submerged and located at the coastal zone of the Randstad. The longest 5% of the wave periods at that location are excluded since these require too large wave dampers. Internal stabilization is assumed to reduce the ecoboat motions for these waves. Therefore a design wave regime is selected of $T_2 = 5.75s$ and $H_{1/3} = 4.1m$ and a design frequency of $\omega_0 = 0.85\,rad/s$. The dampers will need to reduce the wave height from these waves.

'Heaving and pitching bodies' is the wave energy conversion principle chosen to convert the wave motion to mechanical motion. This principle is relatively simple and therefore most reliable. It uses the motion of the structure directly to excite an internal mechanism. Therefore the damper can be designed as a float and the motions of the float can be used to calculate the power generation.

The damper geometry is selected based on its damping characteristics and the practicality of its size. Large diameters yield more damping, but also need more height. The resonance frequency of the damper should be equal to the design frequency for maximum damping of the waves. This means that the total height of the damper increases with increasing diameter, since a damper with a larger diameter needs a higher position of the center of gravity to have

7

the pitch resonance peak at the design frequency. Therefore the selected damper geometry is

$$\text{damper geometry:} \quad \begin{aligned} diameter &= 28 \ m \\ draught &= 4.2 \ m \\ total \ height &= 5.45 \ m \end{aligned}$$

The resonance peak of this damper geometry is not a perfect match with the design frequency and the performance of the will improve for a better match. An iterative design approach is required to improve this result.

After the damper geometry is selected the wave regime behind the damper can be calculated. Three different wave regimes are used to illustrate different circumstances of the ecoboat: the design wave regime, the most occurring wave regime and a high load wave regime. The damping of the three motions that are considered for the symmetrical situation, is given in table 1.

	surge $x_{a_{1/3}}$	heave $z_{a_{1/3}}$	pitch $\theta_{a_{1/3}}$
design wave regime [%]	-5.91	-16.07	-31.23
most occurring wave regime [%]	+113.03	+28.12	-46.33
high load wave regime [%]	-17.13	-19.87	-23.83

Table 1: Damping of ecoboat motions

It is clear that the dampers yield a strong reduction of the motions of the ecoboat. Although the surge and the heave motion in the most occurring wave regime are increased, the actual motion remains very small and can therefore be neglected. The largest motion of the ecoboat in all waves is the pitch motion. This motion is also the most uncomfortable motion for inhabitants. Therefore the damping achieved by the damper for that motion is considered most relevant and sufficient to recommend the use of the dampers for the ecoboats' protection.

Sustainability

A sustainable solution should counteract the population growth, increasing consumption and degradation of natural resources by using far more efficient technology. This requires an improvement of (at least) a factor-10 more efficient technology compared to the current situation or a different technology that does not limit the use of resources for a future generation.

The feasibility of the ecoboat and dampers as a sustainable solution to the need for space, energy and water is investigated by comparing the consumption of a land-based with an ecoboat household. The land-based reference building for this comparison is defined with four consumption statistics: average use of electricity, water, natural gas and building materials. These characteristic values are used as an indication of the total differences between sea and land-based living. This comparison should be extended in a next design phase to include all aspects of living at sea for a conclusive answer on the sustainability of the system.

The ecoboat uses the electricity yield of the wave dampers. One wave damper with solar panels on top yields 446437kWh/year for the most occurring wave regime. This is sufficient for the households situated on one ecoboat, but can also supply another 100 land-based households. Fresh water for the ecoboat is made from salt water with reverse osmosis, heating is generated

by electrical heat pumps and the materials are paid for with full cost pricing. This means that all environmental effects are incorporated in the prices so they can be compensated. Table 2 gives the reduction or change in consumption for one ecoboat household.

	reduction of raw materials and energy use per ecoboat household per year
electricity	from renewables
water	from salt water
natural gas (heating)	-100% (-79%)
combined energy need	-56% + renewables
materials	-32% + full cost pricing

Table 2: Reduction of household consumption for the ecoboat

The overall consumption is reduced, but not with a factor-10. However the change to renewable energy, salt water and full cost pricing makes the system sustainable, since these technologies do not limit the use of resources for future generations. It is worth while to consider this solution in a next phase of design.

List of symbols

a — added mass $[kg]$

A — affluence or consumption level

A — exponential function in JONSWAP formula

A_d — area of damper $[m^2]$

A_{kj} — added mass and inertia matrix

A_w — water plane area $[m^2]$

b — damping coefficient

b_{heave} — damping coefficient in heave $[kg/s]$

b_{pitch} — damping coefficient in pitch $[kg\,m^2/s]$

B — center of buoyancy

B_{kj} — damping matrix

c — wave speed of phase velocity $[m/s]$

c — spring coefficient

c_{heave} — spring coefficient in heave $[N/m]$

c_{pitch} — spring coefficient in pitch $[Nm]$

c_g — wave group velocity $[m/s]$

c_{g_h} — wave group velocity at local water depth $[m/s]$

c_{g_∞} — wave group velocity at deep water $[m/s]$

$C_l,\ C_2,\ C$ — unknown constants

C_{kj} — spring matrix

COP — coefficient of performance

d — draft $[m]$

d — draft of damper $[m]$

D — diameter $[m]$

D_d — diameter of damper $[m]$

E — energy per unit sea surface $[J/m]$

E_K — kinetic energy $[J]$

$E_{K_{particle}}$ — kinetic energy of a particle $[J]$

E_P — potential energy $[J]$

F — force $[N]$

F_h — hydromechanical force $[N]$

F_w — wave force $[N]$

F_w^* — approximation of F_w $[N]$

F_{w_k} — wave force in direction k $(k = 1, 6)$ $[N]$

F_z — force in vertical direction $[N]$

g — gravitational acceleration $[m/s^2]$

G	- center of gravity
$\overline{GM}$	- distance between the center of gravity and the metacenter $[m]$
h	- water depth $[m]$
H	- wave height $[m]$
$H_{1/3}$	- significant wave height $[m]$
H_d	- total height of damper $[m]$
H_h	- wave height at local water depth $[m]$
$H_{measured}$	- wave height from measurement $[m]$
$H_{requested}$	- wave height at requested water depth $[m]$
H_∞	- wave height at deep water $[m]$
I	- mass moment of inertia $[kgm^2]$
I	- environmental impact
I_a	- added mass moment of inertia $[kgm^2]$
I_{xx}	- mass moment of inertia about the x axis $[kgm^2]$
I_T	- transverse moment of inertia $[m^4]$
j	- damping ratio [-]
j_{heave}	- damping ratio in heave [-]
j_{pitch}	- damping ratio in pitch [-]
j	- body motion mode (1=surge, 2=sway, 3=heave, 4=roll, 5=pitch, 6=yaw)
k	- wave number $[rad/s]$
k	- direction of force (1=surge, 2=sway, 3=heave, 4=roll, 5=pitch, 6=yaw)
k_n	- wave number of measurement n $[rad/s]$
K_{sh}	- shoaling coefficient $[-]$
$K_{sh_{measured}}$	- shoaling coefficient from measurement site $[-]$
$K_{sh_{requested}}$	- shoaling coefficient at requested water depth $[-]$
$\overline{KG}$	- distance from keel to center of gravity $[m]$
$\overline{KM}$	- distance from keel to metacenter $[m]$
L	- length of float $[m]$
m	- body mass $[kg]$
m_{nz}	- moment of heave response spectrum
m_{0z}	- area beneath heave response spectrum
m_{2z}	- moment of inertia of heave response spectrum
M	- metacenter
M_{kj}	- mass and inertia matrix
M_y	- Moment around y-axis
n	- reference to specific measurement
$\vec{n}$	- normal vector
n_k	- direction parameter
N	- number of observations
O	- origin of earth-bound co-ordinate system
p	- pressure $[N/m^2]$
p_0	- air pressure at sea level $[bar]$
P	- population
$P(z)$	- undefined function of z
$\overline{P}_{heave}$	- average available power in heave $[Watt]$
Q_{warmth}	- heat to building $[J]$ or $[kWh]$

$Q_{natural\ gas}$ - calorific value of natural gas $[J]$ or $[kWh]$
RMS - root mean square
S_0 - mean wetted surface $[m^2]$
S_z - energy spectrum $[m^2/s]$
S_ζ - wave spectrum $[m^2/s]$
SWL - sea water level
t - time $[s]$
T - wave period $[s]$
T - technology
$\overline{T}$ - average wave period $[s]$
T_2 - zero-crossing wave period $[s]$
T_{2x} - significant response period for surge $[s]$
T_{2z} - significant response period for heave $[s]$
$T_{2\theta}$ - significant response period for pitch $[s]$
T_p - spectral peak period (JONSWAP: $T_p = 1.287 \cdot T_2$) $[s]$
u - velocity component in x $\frac{dx}{dt}$ $[m/s]$
v - water particle velocity $[m/s]$
$\vec{v}$ - velocity vector $[m/s]$
v_w - vertical wave velocity $[m/s]$
v_f - vertical float velocity $[m/s]$
w - velocity component in z $\frac{dz}{dt}$ $[m/s]$
W - average work done per wave period $[Watt]$
W_h - power at local water depth $[Watt]$
W_∞ - power at deep water $[Watt]$
$W_{electric}$ - work applied to system $[kWh]$
x, y, z - co-ordinates
x_0, y_0, z_0 - earth-bound co-ordinates
$x_{a_{1/3}}$ - significant surge amplitude $[m]$
x_b, y_b, z_b - body-bound co-ordinates
z_a - amplitude of heave motion $[m]$
$z_{a_{1/3}}$ - significant heave amplitude $[m]$

β_{heave} - additional damping in heave $[kg/s]$
β_{max} - maximum additional damping
β_{pitch} - additional damping in pitch $[kg\,m^2/s]$
γ - peakedness factor JONSWAP formula
Δt - small time step $[s]$
$\Delta\omega$ - small frequency step $[rad/s]$
ϵ_n - random phase angle of n-th measurement $[deg]$
$\epsilon_{z\zeta}$ - random phase angle $[deg]$
ζ - wave profile
$\zeta(t)$ - vertical displacement or wave elevation
ζ^* - effective wave elevation $[m]$
ζ_a - wave amplitude $[m]$
$\zeta_{a_{1/3}}$ - significant wave amplitude $[m]$

ζ_{a_n}	- wave amplitude of n-th measurement $[m]$
ζ_n	- vertical displacement of n-th measurement $[m]$
η	- efficiency $[-]$
θ	- pitch
$\theta_{a_{1/3}}$	- significant pitch amplitude $[rad]$
λ	- wave length $[m]$
μ	- angle between wave propagation direction and x_b $[deg]$
ρ	- density $[kg/m^3]$
ρ_d	- density damper $[kg/m^3]$
ρ_{sea}	- sea water density $[kg/m^3]$
σ	- standard deviation
σ	- step function of ω for JONSWAP formula
σ_ζ^2	- variance
ϕ	- roll
$\phi_d,\ \phi_w$	- co-ordinate dependent part of Φ_d and Φ_w
Φ	- potential
Φ_d	- potential due to diffraction of incoming wave
Φ_j	- potential due to the six body motions $(j = 1, 6)$
Φ_w	- wave potential
τ	- measurement time $\tau = N \cdot \Delta t$ $[s]$
ψ	- yaw
ω	- circular wave frequency $[rad/s]$
ω_0	- resonance frequency $[rad/s]$
ω_d	- resonance frequency of damped system $[rad/s]$
ω_n	- circular wave frequency for n-th measurement $[rad/s]$
ω_p	- spectral peak frequency $[rad/s]$

∇	- nabla
∇	- submerged volume of structure $[m^3]$

Chapter 1

Introduction

In the near future population growth and urbanization will increase the size of the worlds major cities beyond their physical capacity, where the limits of the natural capacity have usually long been reached. Space, energy and water will be the main deficits for these areas. The ecoboat foundation has been working on a program to enable human habitation of the sea-surface where space, water and energy are plentiful but as yet unaccessible. This should yield a sustainable form of living that meets the needs of coastal metropolises. Their solution is called the ecoboat and is intended to be a floating living unit of one or more households that is self sustaining in fresh water and electricity.

This thesis will investigate the feasibility of the use of separate, floating wave dampers to protect an ecoboat and the feasibility of the dampers as part of a sustainable form of living at sea. The investigation of the opportunities of the dampers to protect an ecoboat is is restricted to the functionality of one damper for one wave propagation direction. The dampers are intended to surround the ecoboats and create an enclosed area of calm water, but the restricted investigation should present sufficient information for the current phase of design. The feasibility of the dampers as part of a sustainable solution for the need for space, energy and water is investigated by comparing the consumption of land-based households to ecoboat households. This comparison gives a first indication of the opportunities of living at sea. It should be extended to include all aspects of living at sea for a conclusive answer wether living at sea is a sustainable form of living or not.

To investigate the feasibility of the use of the dampers the mathematical description of the wave environment is explained in chapter 2 and the mathematical description of floating structures in chapter 3. Chapter 4 introduces the ecoboat and the ecoboat foundation and derives the requirements for the dampers from the location choice and ecoboat characteristics and objectives. With these requirements the available energy conversion principles are investigated in chapter 5 to find the most suitable principle for the ecoboat damping system. Chapter 6 uses this principle for a primary design of a damper and compares the waves behind the damper with the undisturbed waves to find the effect of the damper. Finally in chapter 7 the ecoboat and dampers are placed in their broader context of global trends and sustainable objectives. The combination of the damping properties derived in chapter 6 and the sustainability characteristics of the combination of dampers and ecoboat found in chapter 7 yields the feasibility of the use of the dampers for the ecoboat.

Chapter 2

Wave environment of floating structures

This chapter will present a mathematical representation of waves. This representation will be used to model the wave environment of the ecoboat and the dampers at a certain location. The reader is presumed to be acquainted with this part of wave theory in the following chapters, because the concepts in this chapter are fundamental to the argumentation presented there.

Section 2.1 discusses the properties of wind generated waves depending on their physical appearance and circumstances and distinguishes between regular and irregular waves. Regular waves are discussed in section 2.2. Their mathematical representation is introduced with its use in linear potential theory, the impact of water depth on wave properties is evaluated and the definition of wave energy is given. Next section 2.3 discusses the different aspects of irregular waves based on statistics. Statistical averages are combined in wave energy spectra and standard wave spectra are introduced to derive wave energy spectra in the absence of full measurement data.

2.1 Wind generated waves

Waves at sea can be generated by astronomical forces (tides), motions of a structure in water, earthquakes or submarine landslides (tsunamis) or interaction of wind and sea-surface. Only wind generated waves are considered in this thesis.

Wind generated waves can be divided in two categories: 'sea' and 'swell'. 'Sea' is a train of waves driven by the prevailing local wind field [6]. These waves have relatively sharp crests (highest points of the wave) and show very irregular behavior; propagation direction, wave height and period are all unpredictable in time. 'Swell' are waves which have propagated out of the area and wind in which they were generated [6]. Waves can travel long distances from their source to other regions and during this travel the waves become more regular. This means that the crests become rounder and longer and wave height, period and propagation direction become more predictable. In normal circumstances a combination of these two exists at any given time. Therefore the sea surface has to be modeled as an irregular wave pattern.

An important concept to work with this mostly irregular behavior of waves is the superposition principle. This states that the irregular pattern of waves can be seen as a superposition of many regular waves each with its own amplitude, length, period and propagation direction. The combination of these different simple waves yields the irregular pattern that can be seen at sea. Figure 2.1 gives a graphical representation of this principle.
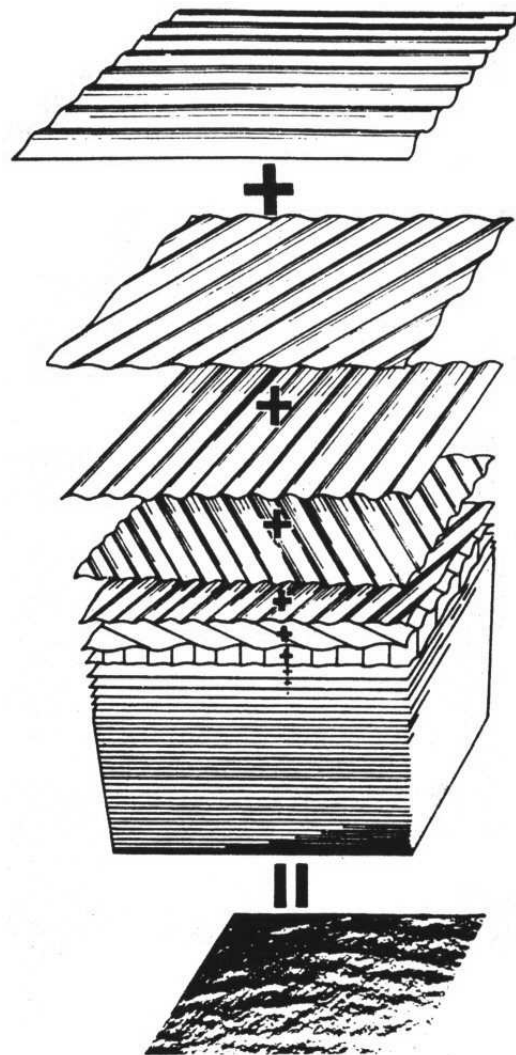

Figure 2.1: Superposition of many regular waves to create an irregular pattern [5]

Therefore it is important to understand the properties of simple, regular waves in order to be able to model the sea surface.

2.2 Regular waves

Regular waves are single, harmonic waves. They can be described with sine or cosine functions and the mathematics associated with vibrations. Paragraph 2.2.1 will introduce the definitions to describe waves and give the sign conventions, paragraph 2.2.2 will cover the basics of linear potential theory with the applicable boundary conditions, paragraph 2.2.3 treats the different aspects of changing water depth on wave properties and paragraph ?? gives the expressions to estimate wave energy.

2.2.1 Definitions

A regular wave is defined with respect to the still water level (SWL), the water depth h $[m]$ and coordinates x and z. The main properties are the wave length λ $[m]$, amplitude ζ_a $[m]$ and the wave height $H = 2 \cdot \zeta_a$ $[m]$ as indicated in figure 2.2.
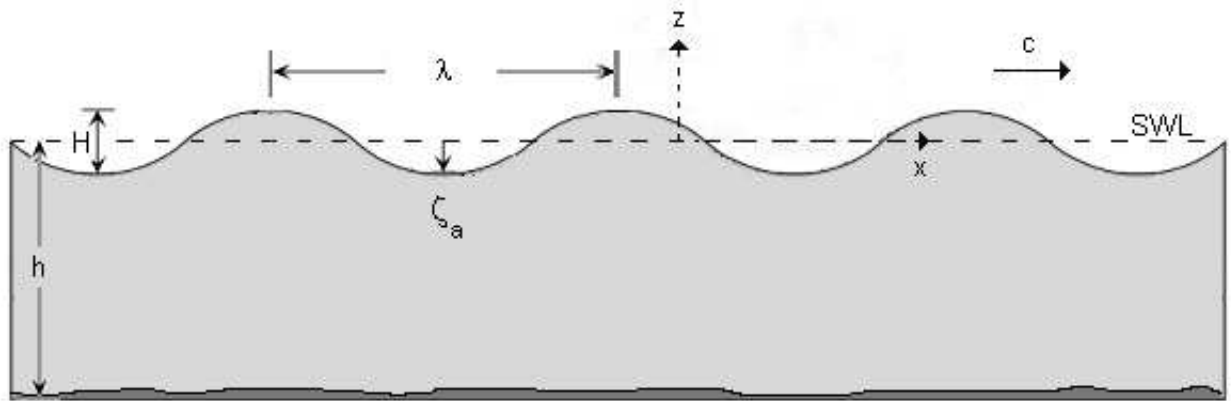

Figure 2.2: Definition of waves

Waves at sea are propagating waves, that means that if figure 2.2 is evaluated in time the wave pattern will move to the right. The time required to travel one wave length is the wave period T $[s]$. Because a regular wave can be represented with a sine or cosine, it is practical to convert wave length and period to angular arguments as

$$
\begin{aligned}
k\lambda = 2\pi &\Leftrightarrow k = \frac{2\pi}{\lambda} \\
\omega T = 2\pi &\Leftrightarrow \omega = \frac{2\pi}{T}
\end{aligned}
\tag{2.2.1}
$$

in which k [rad/m] is the wave number and ω [rad/s] is the circular wave frequency. The last important wave property is the speed or phase velocity c [m/s]

$$
c = \frac{\lambda}{T} = \frac{\omega}{k}
\tag{2.2.2}
$$

Using these expressions the wave profile (shape of the wave at the surface) is equal to

$$\zeta = \zeta_a \cos(kx - \omega t) \tag{2.2.3}$$

2.2.2 Linear potential theory of waves

Potential theory is used to derive the velocity potential of waves. The combination of the velocity potential with boundary conditions yields wave characteristics such as the relation between wave length, height and water depth and the particle motion within a wave.

For potential theory all flows are considered incompressible, irrotational, non-viscous, continuous and homogeneous. Most of these assumptions rarely impose restrictions on the use of this theory for water, but viscosity and rotation should be considered more carefully. If surface friction becomes important, viscosity and rotation effects can not be neglected anymore.

The velocity potential $\Phi(x, y, z, t)$ is given as a scalar function at each point in the fluid. The derivatives of the velocity potential are equal to the velocity components of the fluid particle. The waves are linearized before they are used in potential theory. Therefore all terms in the equation of motion with the steepness squared should be a magnitude smaller then the other terms and should be ignored. Physically a low wave steepness ($\frac{H}{\lambda}$) implies a relatively great length and a small height making the wave crest round. Usually the theory for linear waves is accurate for a wave steepness of $H/\lambda = 1/50$ or less.

A linearized wave profile resembles a sine or cosine and the motion of the water particles depends on their position with respect to the water surface. Since a single wave is considered there is only one propagation direction and thus only the variations in the x-z plane need to be included. Therefore the wave velocity potential is

$$\Phi_w(x, z, t) = P(z) \cdot \sin(kx - \omega t) \tag{2.2.4}$$

in which P(z) is an undefined function of z.

The velocity potential should fulfil four requirements, but only the first three are used to find a more detailed expression for the velocity potential. The fourth is used to find the relation between wave length, wave period and water depth in paragraph 2.2.3.

1. Continuity equation or Laplace equation
2. Sea bed boundary condition
3. Free surface dynamic boundary condition
4. Free surface kinematic boundary condition

Ad 1. Since the fluid is incompressible, homogeneous and only the $x - z$ plane is considered the continuity equation is

$$\frac{\partial u}{\partial x} + \frac{\partial w}{\partial z} = 0 \tag{2.2.5}$$

for potential flow this can also be expressed as the Laplace equation

$$\nabla^2 \Phi_w = \frac{\partial^2 \Phi_w}{\partial x^2} + \frac{\partial^2 \Phi_w}{\partial z^2} = 0 \tag{2.2.6}$$

If equation 2.2.4 and equation 2.2.6 are combined a first solution for P(z) is found as

$$P(z) = C_1 e^{+kz} + C_2 e^{-kz} \tag{2.2.7}$$

with C_1 and C_2 two undefined constants.

Ad 2. The sea bed is considered 'leak proof'. No water can move through the sea bed therefore the vertical velocity of the water at $z = -h$ is zero

$$\frac{\partial \Phi_w}{\partial z} = 0 \quad \text{for } z = -h \tag{2.2.8}$$

If this condition is substituted in equation 2.2.4 using equation 2.2.7 for P(z), P(z) can be rewritten as

$$
\begin{aligned}
P(z) &= \frac{C}{2} \left(e^{+k(h+z)} + e^{-k(h+z)} \right) \\
&= C \cosh k(h+z)
\end{aligned}
\tag{2.2.9}
$$

Ad 3. At the wave surface the pressure should be equal to the air pressure. Bernoulli's equation for an unsteady irrotational flow can be used with a small wave steepness.

$$p = -\rho \frac{\partial \Phi_w}{\partial t} - \rho g z - \frac{1}{2} \rho v^2 \tag{2.2.10}$$

with p the pressure, ρ the sea water density and v the water particle velocity. Small wave steepness ensures small local fluid velocities v and therefore the contribution of these local velocities squared can be ignored. This means that the Bernoulli equation at the wave surface can be reduced to

$$\frac{\partial \Phi_w}{\partial t} + \frac{p_0}{\rho} + g\zeta = 0 \quad \text{for } z = \zeta \text{ and } p = p_0 \tag{2.2.11}$$

Since $\frac{p_0}{\rho}$ is constant it can be included in $\frac{\partial \Phi_w}{\partial t}$, because it will not influence the velocities derived from the potential Φ_w. If this equation is expanded in a Taylor series and linearized it yields

$$\frac{\partial \Phi_w}{\partial t} + g\zeta = 0 \quad \text{for } z = 0 \tag{2.2.12}$$

The combination of equation 2.2.12 with equation 2.2.4 yields the wave profile

$$\zeta = \frac{\omega C}{g} \cdot \cosh kh \cdot \cos (kx - \omega t) \tag{2.2.13}$$

The wave profile is a combination of a constant term or wave amplitude ζ_a with a harmonic term $\cos (kx - \omega t)$ as presented in equation 2.2.3, therefore

$$\zeta = \zeta_a \cos (kx - \omega t) \quad \text{with} \quad \zeta_a = \frac{\omega C}{g} \cdot \cosh kh$$

This leads to the definition of the wave velocity potential Φ_w for waves with small steepness for all h

$$\Phi_w = \frac{\zeta_a g}{\omega} \cdot \frac{\cosh k(h+z)}{\cosh kh} \cdot \sin (kx - \omega t) \tag{2.2.14}$$

2.2.3 Influence of water depth on wave properties

A change in water depth affects several aspects of waves. The dispersion relationship describes the influence of water depth on wave length and wave period. The relation between water depth and wave length predicts the local particle motions and the shoaling coefficient gives the relation between wave height and water depth.

Dispersion relationship
The relation between wave length, period and water depth known as the dispersion relationship, can be derived with the use of the fourth boundary condition of the velocity potential: the free surface kinetic boundary condition.

Ad 4. The water surface should fulfill a 'no-leak' condition. This means that there is a clear division between water and air and that there is no mixed region in between. Therefore the vertical velocity of the water particles at the surface should be identical to the vertical velocity of that surface itself.

For the limited wave steepness assumed the vertical velocity of the wave surface can be reduced to

$$\frac{dz}{dt} = \frac{\partial \zeta}{\partial t} \quad \text{for } z = \zeta \tag{2.2.15}$$

therefore the vertical velocity of a wave particle at the wave surface is

$$\frac{\partial \Phi_w}{\partial z} = \frac{\partial \zeta}{\partial t} \quad \text{for } z = \zeta \text{ and after linearization for } z = 0 \tag{2.2.16}$$

If the dynamic boundary condition for the free surface (2.2.12) is differentiated with respect to t as

$$\frac{\partial^2 \Phi_w}{\partial t^2} + g\frac{\partial \zeta}{\partial t} = 0 \quad \text{for } z = 0 \tag{2.2.17}$$

and combined with equation 2.2.15, it gives the free surface kinematic boundary condition or Cauchy-Poisson condition

$$\frac{\partial z}{\partial t} + \frac{1}{g} \cdot \frac{\partial^2 \Phi_w}{\partial t^2} = 0 \quad \text{for } z = 0 \tag{2.2.18}$$

The substitution of the equation for the velocity potential (2.2.14) into the Cauchy-Poisson condition (2.2.18) gives the direct relation between the wave frequency ω, wave number k and water depth h or equivalently between wave length λ, wave period T and water depth. The dispersion relationship for arbitrary water depth h is

$$\omega^2 = kg \cdot \tanh kh \quad \text{or} \quad \lambda = \frac{gT^2}{2\pi} \cdot \tanh\left(\frac{2\pi h}{\lambda}\right) \tag{2.2.19}$$

The dispersion relationship can only be solved iteratively or graphically as shown in figure 2.3. The figure also explains the classification of waves in short, long and intermediate waves. 'Short waves' are short relative to the water depth and therefore represent deep water ($h > \lambda/2$). 'Long waves' are long relative to the local water depth and that region is known as

shallow water ($h < \lambda/20$). In these two regions the dispersion relation can be linearized which yields an important simplification of the equations. For the ecoboat most calculations will require the complete dispersion relationship because the ratio between water depth and wave length is mostly in between the two regions, known as 'intermediate water waves' ($\lambda/2 < h < \lambda/20$) and does not allow linearization of the dispersion relationship.
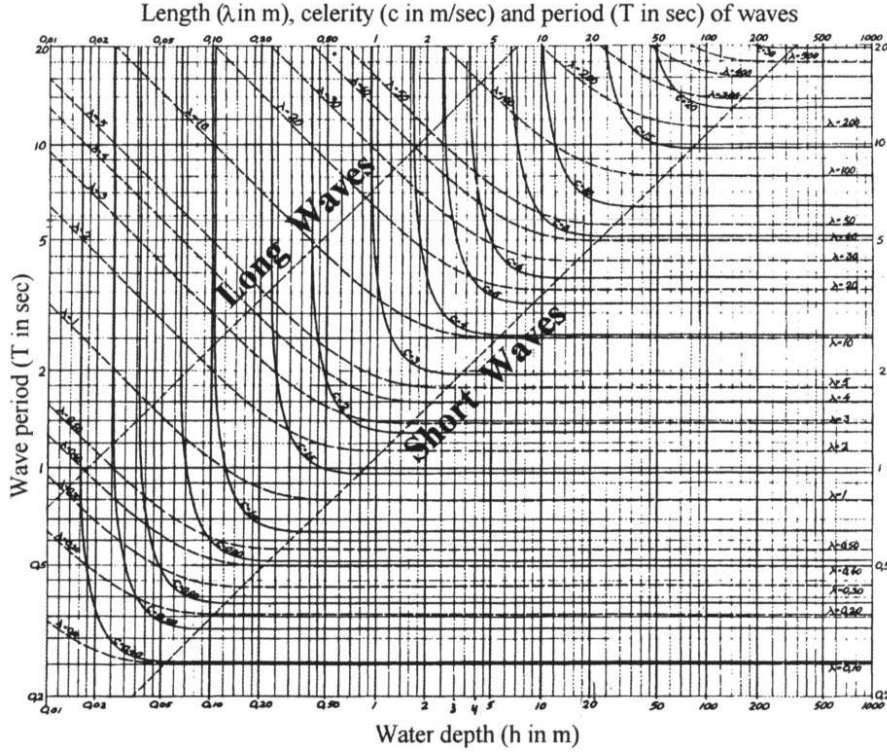

Figure 2.3: Graphical representation of the dispersion relationship [7]

Particle motion
The shape of the internal particle movement changes as a result of the relation between wave length λ and the water depth h. If the velocity potential (2.2.14) and the dispersion relationship (2.2.19) are combined, the velocity components u and w are

$$
\begin{aligned}
u &= \frac{\partial \Phi_w}{\partial x} = \frac{dx}{dt} = \zeta_a \cdot \frac{kg}{\omega} \cdot \frac{\cosh k(h+z)}{\sinh kh} \cdot \cos(kx - \omega t) \\
w &= \frac{\partial \Phi_w}{\partial z} = \frac{dz}{dt} = \zeta_a \cdot \frac{kg}{\omega} \cdot \frac{\sinh k(h+z)}{\sinh kh} \cdot \sin(kx - \omega t)
\end{aligned}
\tag{2.2.20}
$$

Equation 2.2.20 holds for all circumstances but can be simplified for deep and shallow water. For intermediate water depth ($\lambda/20 < h < \lambda/2$) it shows that the particle trajectory is elliptic and both axis of the ellipse (u and w) decrease with depth.

In deep water ($h > \lambda/2$) the velocities can be rewritten as

$$
\begin{aligned}
u &= \zeta_a \cdot e^{kz} \cdot \cos(kx - \omega t) \\
w &= \zeta_a \cdot e^{kz} \cdot \sin(kx - \omega t)
\end{aligned}
\tag{2.2.21}
$$

21

Therefore the particle orbit is circular in deep water and decreases exponentially with depth. In shallow water ($h < \lambda/20$) the velocities are

$$
\begin{aligned}
u &= \zeta_a \omega \cdot \frac{1}{kh} \cdot \cos{(kx - \omega t)} \\
w &= \zeta_a \omega \cdot (1 + \frac{z}{h}) \cdot \sin{(kx - \omega t)}
\end{aligned}
$$

(2.2.22)

Therefore the trajectory of the water particles is elliptic. The horizontal axis (u) of the ellipse remains constant for decreasing water depth, because u is independent of z, while the vertical axis (w) decreases with water depth.

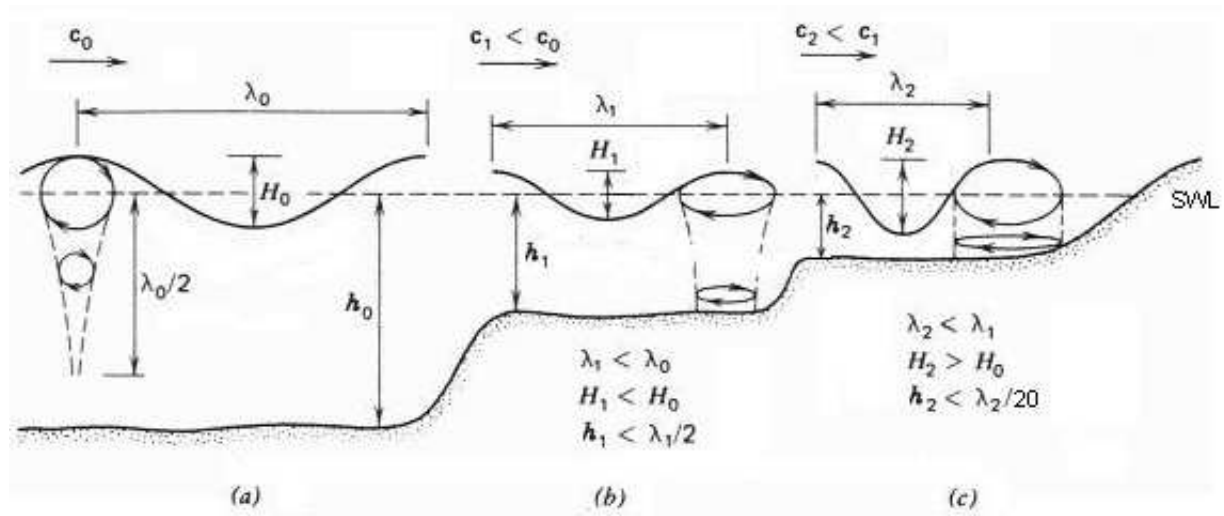The particle movements are illustrated in figure 2.4.

Figure 2.4: Particle movement with water depth [3]

Wave height
The other change with water depth is based on the relation between wave height H and water depth h. Presuming energy conservation, the energy transport through a vertical plane parallel to the wave crests should remain constant [6], therefore the energy transport at deep water should be equal to the energy transport after shoaling at shallower water. Energy transport can be defined as

$$
\bar{W} = E \cdot c_g \quad [Watt]
$$

(2.2.23)

with $\bar{W}$ the average work done per wave period, E the energy per meter wave crest and c_g the wave group velocity. The energy E and c_g are according to reference [7]

$$
\begin{aligned}
E &= \frac{1}{8}\rho g H^2 & [J/m] \\
c_g &= \frac{c}{2} \cdot (1 + \frac{2kh}{\sinh 2kh}) & [m/s]
\end{aligned}
$$

(2.2.24)

Since the energy transport should remain constant the average work per wave period $\bar{W}_h$ at a local water depth should be equal to the average work per wave period before shoaling at deep water $\bar{W}_\infty$. This means that the ratio between deep water and local wave height becomes

$$\bar{W}_h = \bar{W}_\infty \ \Leftrightarrow \ \frac{1}{8}\,\rho g H_h^2 \cdot c_{g_h} = \frac{1}{8}\,\rho g H_\infty^2 \cdot c_{g_\infty} \quad \Leftrightarrow \quad \frac{H_h}{H_\infty} = \sqrt{\frac{c_{g_\infty}}{c_{g_h}}} \tag{2.2.25}$$

This yields

$$K_{sh} = \frac{H_h}{H_\infty} = \sqrt{\frac{1}{\tanh kh \cdot (1 + \frac{2kh}{\sinh 2kh})}} \tag{2.2.26}$$

with K_{sh} the shoaling coefficient, H_h the local wave height, H_∞ the wave height in deep water and h and k the local water depth and local wave number respectively.

The shoaling coefficient can be used to calculate a wave height at a certain water depth from a measured wave regime at another water depth. The ratio between the shoaling coefficient of the measured site and the shoaling coefficient of the requested site is equal to the ratio of the wave height of the two sites.

$$\frac{K_{sh_{measured}}}{K_{sh_{requested}}} = \frac{H_{measured}}{H_{requested}} \ \Leftrightarrow \ H_{requested} = H_{measured} \cdot \frac{K_{sh_{requested}}}{K_{sh_{measured}}} \tag{2.2.27}$$

2.3   Irregular waves

A real sea shows very unpredictable and irregular behavior. Such behavior can be modelled by superimposing regular waves each with its own length, period, height and propagation direction as explained in section 2.1 and illustrated in figure 2.1. Measurement data is used to find the specific regular waves that will result in a representative wave regime.

Paragraph 2.3.1 introduces significant wave height and zero-crossing wave period as two important statistical averages to represent measurement data, paragraph 2.3.2 explains the Fourier analysis used to find energy density spectra as mathematical representation of a specific wave regime and paragraph 2.3.3 discusses standard wave spectra the result of large scale measurement programs to estimate the energy density spectrum if only the significant wave height and zero-crossing period are known.

2.3.1   Statistical averages for wave height and wave period

Wave statistics are based on measurement sequences. A representative measurement sequence takes at least 100 times the longest wave period and will usually take about 15 to 20 minutes. All reference to measurements in this thesis is to measurements in accordance with this condition.

For each measurement sequence the total number of zero-crossings (wave elevation $\zeta(t) =$ Sea Water Level) can be used to find an average wave period. This definition is used for the average 'zero-crossing wave period' T_2. Another definition of an average wave period is the

average peak period. This period is equal to the average period between all the peaks of the measurement sequence. The zero-crossing period has a statistical equivalent in ship motion (see paragraph 3.3) and is therefore used most often, but the peak period is equivalent to the frequency in the transfer function ω_p and is therefore also used. Their relation for JONSWAP measurements is

$$T_p = 1.287 \cdot T_2 \tag{2.3.1}$$

The wave amplitudes from a measurement sequence can be averaged to find an average wave height, but historically wave height was inspected visually and therefore another average is usually given. The significant wave height $H_{1/3}$ is determined as the average of the highest one-third of the wave amplitudes of a sequence. This choice matches the wave height found by visual inspection and there is a direct, simple relation between the significant wave height and the average wave height (see paragraph 2.3.2) and therefore the correspondence to visual inspections is maintained.

Most calculations will be done with the significant wave height $H_{1/3}$ and the zero-crossing period T_2.

2.3.2 Energy density spectra

For a measurement sequence of N observations, there will be N values for the vertical displacement $\zeta(t)$ compared to the mean value of all displacements (the local sea water level). These values (ζ_n) can be averaged to find the average wave amplitude also known as the standard deviation σ or the Root Mean Square (RMS). For large N

$$\sigma = \sqrt{\frac{1}{N} \sum_{n=1}^{N} \zeta_n^2} \tag{2.3.2}$$

The standard deviation σ is directly related to the significant wave amplitude $\zeta_{a_{1/3}}$ or the significant wave height $H_{1/3}$ as

$$\begin{aligned} \zeta_{a_{1/3}} &= 2 \cdot \sigma \\ H_{1/3} &= 4 \cdot \sigma \end{aligned} \tag{2.3.3}$$

Therefore general system and control theory can be used for the significant wave height and period.

If the irregular signal of the measurement is analyzed with Fourier Analysis, the regular waves that make up the system are found. This transformation of a time dependent irregular signal into multiple frequencies in the frequency domain is visualized in figure 2.5.
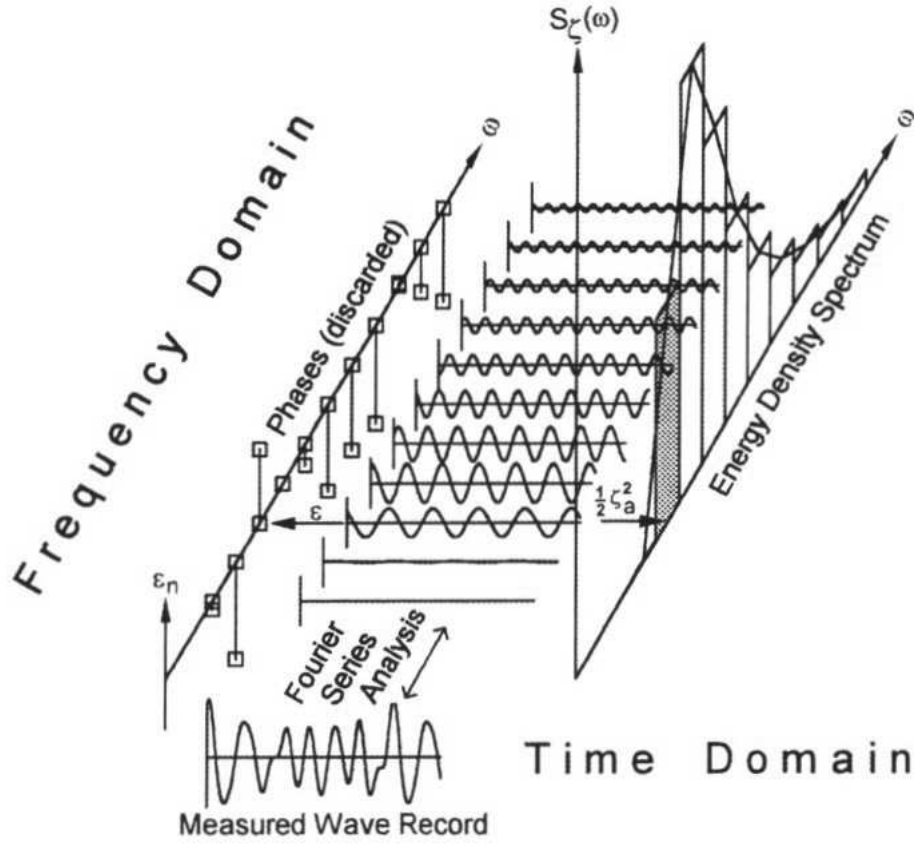
Figure 2.5: Graphical representation of Fourier transformation [7]

The wave elevation in the time domain can be written as the superposition of many regular waves $(n = 1...N)$ in the frequency domain as

$$\zeta(t) = \sum_{n=1}^{N} \zeta_{a_n} \cos\left(k_n x - \omega_n t + \epsilon_n\right) \tag{2.3.4}$$

in which ζ_{a_n} is the wave amplitude component [m], ω_n is the circular frequency component [rad/s], k_n is the wave number component and ϵ_n the random phase angle component [rad].

A Fourier series analysis will result in specific values for ζ_{a_n} and ϵ_n for their specific ω_n. The value of k_n can not be determined from the measurements of only one location, since k is location dependent. But the dispersion relationship (2.2.19) connects k and ω and therefore the combination of equation 2.3.4 and the dispersion relationship yields all unknowns if sufficient Fourier series are included.

In practice average values are used because they summarize the wave properties. Therefore phase angles are usually discarded as indicated in figure 2.5, since they are only required to find the exact water height at a specific time.

The value of ζ_{a_n} in a measurement sequence changes constantly while the mean square value

$\bar{\zeta}_{a_n}^2$ will be almost constant for an irregular signal without prevailing frequencies. The overall average wave amplitude $\bar{\zeta}_a^2$ is a continuous function and the standard deviation squared, the variance, σ_ζ^2 is

$$\sigma_\zeta^2 = \bar{\zeta}^2 = \frac{1}{N} \sum_{n=1}^{N} \zeta_n^2$$

$$= \frac{1}{\tau} \int_0^\tau \left(\sum_{n=1}^{N} \zeta_{a_n} \cos\left(k_n x - \omega_n t + \epsilon_n\right) \right)^2 \cdot dt \quad \text{for } \tau = N \cdot \Delta t \text{ and } \Delta t \to 0 \qquad (2.3.5)$$

$$= \sum_{n=1}^{N} \frac{1}{2} \zeta_{a_n}^2$$

Therefore the wave amplitude ζ_{a_n} can be expressed by a wave spectrum $S_\zeta(\omega_n)$ as

$$S_\zeta(\omega_n) \cdot \Delta\omega = \sum_{\omega_n}^{\omega_n + \Delta\omega} \frac{1}{2} \zeta_{a_n}^2(\omega) \qquad (2.3.6)$$

with $\Delta\omega$ a constant difference between two successive frequencies. Multiplied with ρg this is equal to the equation for wave energy per unit area (2.2.24). Therefore if $\Delta\omega \to 0$ this yields the definition of the wave energy spectrum (see figure 2.5 and figure 2.6)

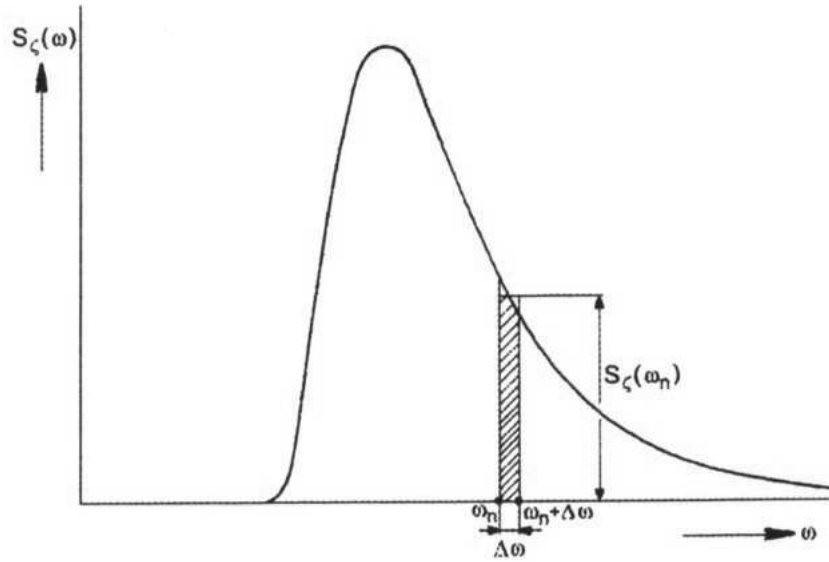$$S_\zeta(\omega_n) \cdot d\omega = \frac{1}{2} \zeta_{a_n}^2 \qquad (2.3.7)$$

Figure 2.6: Energy density spectrum [7]

The area underneath the spectrum is equal to the variance σ_ζ^2 of the wave elevation thus

$$\sigma_\zeta^2 = \int_0^\infty S_\zeta(\omega) \cdot d\omega \qquad (2.3.8)$$

26

The wave energy spectrum is used to summarize the wave properties that have been obtained with measurements. The relation between the variance (standard deviation squared) σ^2 and the area under the spectrum makes it possible to retrieve the significant wave height from a given wave energy spectrum with $H_{1/3} = 4 \cdot \sigma$ as presented in equation 2.3.3.

2.3.3 Standard wave spectra

A wave energy spectrum is location specific. Local winds, currents or obstacles underneath the water surface all influence the local wave regime and usually there will be no complete set of measurement data for a chosen site. World wide the available data is obtained from measuring floats and other measuring equipment and their results are summarized in scatter diagrams. These scatter diagrams give the statistical distribution of wave height and period at a specific site. To find the wave energy spectrum associated with a specific combination of $H_{1/3}$ and T_2 standard wave spectra have been defined.

A standard wave spectrum $S_\zeta(\omega)$ is a function of

$$S_\zeta(\omega) = H_{1/3}^2 \cdot f(\omega, \bar{T}) \tag{2.3.9}$$

This means that the local significant wave height and an average local wave period $\bar{T}$ can be used to find the wave energy density spectrum and that it is not necessary to use a complete set of measurement data.

An extensive study of North Sea wave statistics resulted in the standard wave spectrum known as JONSWAP (Joint North Sea Wave Project).

$$S_\zeta(\omega) = \frac{320\, H_{1/3}^2}{T_p^4}\, \omega^{-5} \cdot \exp\left(\frac{-1950}{T_p^4}\, \omega^{-4}\right) \gamma^A \tag{2.3.10}$$

$$\text{with} \quad \gamma = 3.3\,, \ A = \exp\left(-\{\frac{\frac{\omega}{\omega_p} - 1}{\sigma\sqrt{2}}\}^2\right), \ \omega_p = \frac{2\pi}{T_p}$$

$$\text{and} \quad \sigma \ \text{for } \omega < \omega_p \rightarrow \sigma = 0.07 \text{ or}$$
$$\text{for } \omega > \omega_p \rightarrow \sigma = 0.09$$

T_p is the spectral peak wave period, for the JONSWAP wave spectrum it is related to the zero-crossing period with $T_p = 1.287\, T_2$, γ is the peakedness factor, A an exponential function of ω, ω_p the spectral peak frequency and σ a step function of ω.

Chapter 3

Motion of floating structures in waves

This chapter will introduce the mathematical representation of motions of floating structures in waves as developed for ship motions. This theory will be used to evaluate the reactions of the ecoboat and dampers to the wave environment at the chosen location. In the following chapters familiarity with the mathematical principles of ship motion will be assumed.

The definitions and conventions are presented in section 3.1. Next section 3.2 will evaluate the behavior of structures in regular waves while section 3.3 will use wave and response spectra to investigate the interaction of structures in irregular waves. Section 3.4 gives a description of the computational tool DELFRAC and a verification of the applicability of this program.

3.1   Definitions

Three points of a floating body are of special interest in the analysis of ship motions. The center of gravity G depends on the mass distribution of the body. The center of buoyancy B is located at the center of the submerged part of the structure. The metacenter M defines the rotation point of the body comparable to the aerodynamic center of an airfoil. These three points are used for other definitions and their location indicates the degree of stability of the structure.

Ship motions are defined with respect to the center of gravity G. The translations in x, y and z are known as surge, sway and heave and the rotations around the x, y and z-axis are referred to as roll ϕ, pitch θ and yaw ψ respectively. The assumption of small angles is made during linearization, therefore the sequence of the angles can be neglected. The ship motions are illustrated in figure 3.1.

The front end of a ship is known as the bow, the rear end as the stern. Looking forward, the right side is 'starboard side' and the left side 'port side'. These conventions will also be used for the floating structures of this thesis.

To describe the motions of the floating structures relative to the waves two coordinate systems
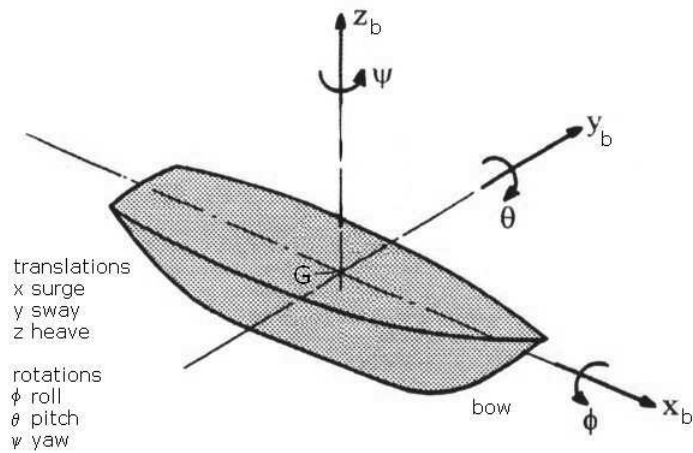
Figure 3.1: Definition of ship motion in 6 degrees of freedom [7]

are used, both right handed orthogonal systems.

Earth-bound coordinate system $O(x_0, y_0, z_0)$
The x_0, y_0-plane of the earth-bound coordinate system is level with the still water surface. The origin is a projection of the center of gravity of the non moving structure in the x_0, y_0-plane. The positive x_0-axis points in the direction of the wave propagation and the positive z_0-axis points upward as illustrated in figure 3.2.

Body-bound coordinate system $G(x_b, y_b, z_b)$
The body-bound coordinate system is parallel to the earth-bound system if the body is at rest. The origin is at the center of gravity with the positive x_b-axis directed to the bow side, the positive y_b-axis to port side and the positive z_b-axis upward. The horizontal angle between the wave propagation direction and the body-bound x-axis is defined as μ (see figure 3.2).

3.2 Motion in regular waves

'The dynamics of rigid bodies and fluid motions are governed by the combined actions of different external forces and moments as well as by the inertia of the bodies themselves.' [7]

This section will explain the interaction between floating structures and regular waves. To be able to evaluate the different loads individually the superposition principle is used as explained in paragraph 3.2.1. With the superposition principle both wave loads and motions can be evaluated individually to illustrate the basic principles. This is used in paragraph 3.2.2 to find the equations of motion. Paragraph 3.2.3 evaluates the response motion of a structure to waves.
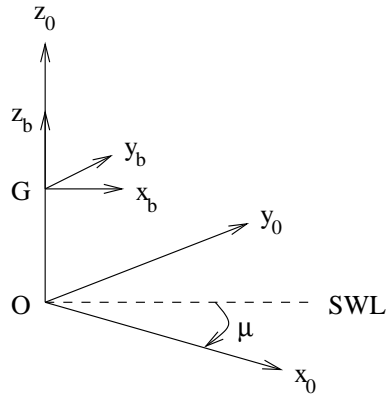
Figure 3.2: Definition of an earth-bound and body-bound coordinate system at rest

3.2.1 Loads superposition

To be able to evaluate the different loads individually the superposition principle should be applicable. This means that the ship motions should be linearized, therefore all rotations (ϕ, θ and ψ) are presumed small and given in radians so $\sin\phi \approx \phi$ and $\cos\phi \approx 1$.

If a structure is floating in waves the motion can be split between an oscillation of the structure in still water and a restraining force on the structure in waves, as illustrated in figure 3.3.
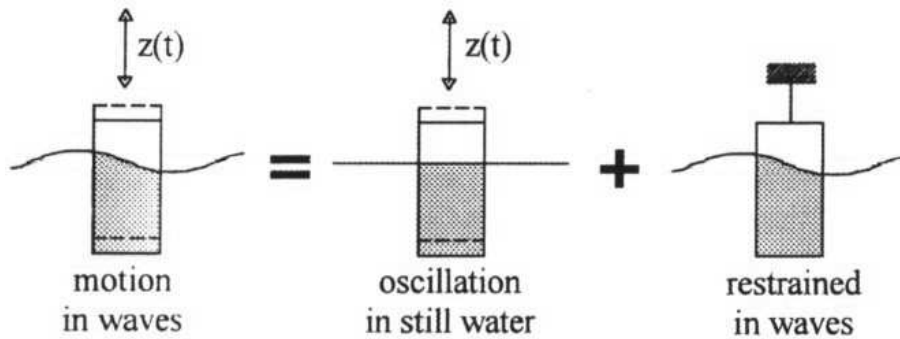

Figure 3.3: Superposition of hydromechanical and wave loads [7]

To make this division two assumptions are made. First it is assumed that the oscillations of a rigid structure in an undisturbed fluid-surface yield the hydromechanical forces and moments. The other assumption is that the incoming waves on a restrained structure produce the wave exciting forces and moments. If these forces and moments are combined they equal the motions of the structure in waves. Therefore the structures are presumed rigid so only rigid body modes need to be considered, the fluid-surface is presumed undisturbed and the restraint complete.

3.2.2   Equations of motion

A vertical cylinder is chosen to illustrate the equations of motion of a floating structure. This shape is analytically transparent and resembles the shape of the ecoboat and the damping structures. The water is assumed ideal and thus to behave as in potential flow.

With the use of the superposition principle the vertical motion can be written as

$$\frac{d}{dt}(\rho \bigtriangledown \cdot \dot{z}) = \rho \bigtriangledown \cdot \ddot{z} = F_h + F_w \qquad (3.2.1)$$

with ρ the water density $[kg/m^3]$, $\bigtriangledown$ the displaced volume of the body $[m^3]$ and F_h and F_w the hydromechanical force $[N]$ and the exciting wave force $[N]$ respectively.

hydromechanical force
The hydromechanical force can be evaluated by oscillating the cylinder in still water. If the initial load is removed the remaining (decaying) motion should fulfil Newton's second law. For heave this is illustrated in figure 3.4 and can be written as

$$\begin{aligned} m\ddot{z} = F_h &= \text{sum of all forces on the cylinder} \\ &= -mg + pA_w - b\dot{z} - a\ddot{z} \end{aligned} \qquad (3.2.2)$$

with

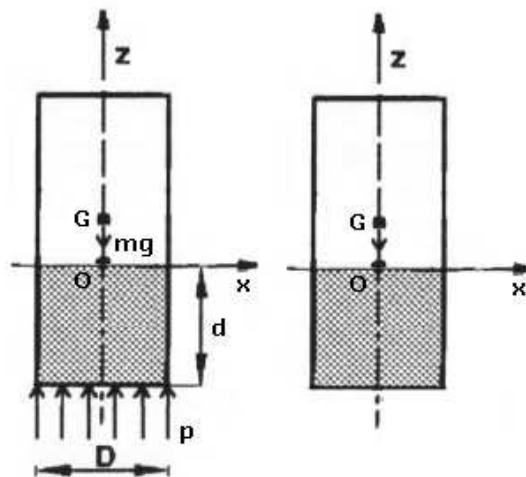|		
m	$=\rho A_w d$	mass of the structure $[kg]$
A_w	$=\frac{\pi}{4}D^2$	water plane area of the cylinder $[m^2]$
D		diameter of the cylinder $[m]$
d		draught (the length of the submerged part of the cylinder at rest) $[m]$
p	$=\rho g(d-z)$	pressure on the submerged part of the structure $[N/m^2]$
b		hydrodynamic damping coefficient $[kg/s]$
a		hydrodynamic mass coefficient $[kg]$

Figure 3.4: Free body diagram and dynamic diagram for hydromechanic heave motion [7]

Archimedes' law states that for static conditions the pressure force on the submerged part of the cylinder should be equal to the weight of the cylinder. Therefore

$$mg = \rho g d A_w \tag{3.2.3}$$

This reduces the equation for the heaving cylinder to

$$(m + a)\ddot{z} + b\dot{z} + cz = 0 \quad \text{with } c = \rho g A_w \tag{3.2.4}$$

The additional mass term a can be interpreted as the mass of the water particles surrounding the cylinder that are accelerated with the heaving motion. It is referred to as hydrodynamic mass or added mass and has a more or less constant value for different frequencies (assuming small diameter compared to wave length). For a vertical cylinder the added mass can be approximated with half a sphere of water of the same diameter as the cylinder. The damping coefficient b [kg/s] is a function of the frequency. A geometrical shape has a specific maximum hydromechanical damping coefficient for a specific frequency.

Thus the hydromechanical forces are the total reaction forces of the fluid on the oscillating cylinder in initially still water

$$m\ddot{z} = F_h \quad \text{with } F_h = -a\ddot{z} - b\dot{z} - cz \tag{3.2.5}$$

exciting wave force
To evaluate the exciting wave forces the vertical cylinder is restraint in its movements and placed in an environment with regular waves (see figure 3.5). For an analytical approach two important simplifications are used: first uniform pressure distribution on the bottom of the structure which implies the use of a small diameter with respect to the wave length and second deep water waves.

(These simplifications impose large restrictions on the use of this theory. Therefore only the essentials will be explained, since diffraction theory as explained in section 3.4 will be used for actual calculations.)

The force on the bottom of the cylinder is equal to the pressure times the surface. If the pressure distribution is assumed constant over the surface the pressure force can be expressed as

$$F = p \cdot A_w \tag{3.2.6}$$

The wave force F_w is defined as the harmonic part of this force F. Therefore a first approximation of this force F_w^* is an integration of the pressures on the structure in the undisturbed wave. This can be written as the spring coefficient from the equation of motion (3.2.4) times an effective wave elevation

$$F_w^* = c \cdot \zeta^* \tag{3.2.7}$$

with $c = \rho g \frac{\pi}{4} D^2$ and for deep water

$$\zeta^* = e^{-kd} \cdot \zeta_a \cos(\omega t) \tag{3.2.8}$$
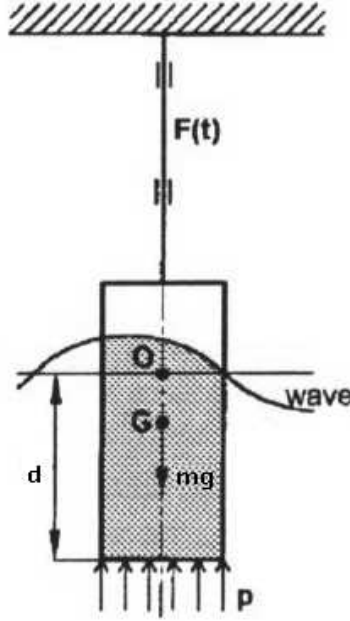
Figure 3.5: Wave loads on restrained structure [7]

Note that the effective wave elevation decreases exponentially with water depth as expected for deep water waves. This equation should be corrected for the diffraction of part of the waves, therefore the total wave force is written as

$$F_w = a\ddot{\zeta}^* + b\dot{\zeta}^* + c\zeta^* \tag{3.2.9}$$

With a and b the hydrodynamic mass and damping coefficient respectively. This means that the wave force amplitude is proportional to the wave amplitude and that the influence of diffraction increases with increasing frequency (see equation 3.2.8). Although this relation is also affected by the frequency dependency of a, b and k.

The equation of motion as given in 3.2.1 can now be rewritten to

$$(m + a)\ddot{z} + b\dot{z} + cz = a\ddot{\zeta}^* + b\dot{\zeta}^* + c\zeta^* \tag{3.2.10}$$

This is the linear equation of heave motion and is applicable for ideal water properties, deep water waves and uniform pressure distribution on the bottom of the structure. In practice the wave forces will be evaluated with diffraction programs like DELFRAC (see section 3.4) that do not impose restrictions on pressure distribution or water depth.

3.2.3 Response to regular waves

The heave response to regular waves can be written as

$$z = z_a \cos(\omega t + \epsilon_{z\zeta}) \tag{3.2.11}$$

33

If equation 3.2.11 is used in equation 3.2.10 with the expression for effective wave elevation from equation 3.2.8 $\zeta^* = e^{-kd} \cdot \zeta_a \cos(\omega t)$ this yields

$$
\begin{aligned}
z_a\{c - (m + a)\omega^2\}\cos(\omega t + \epsilon_{z\zeta}) &- z_a\{b\omega\}\sin(\omega t + \epsilon_{z\zeta}) \\
&= \zeta_a e^{-kd}\{c - a\omega^2\}\cos(\omega t) - \zeta_a e^{-kd}\{b\omega\}\sin(\omega t)
\end{aligned}
\tag{3.2.12}
$$

Apparently there is a direct relation between z_a and ζ_a that can be interpreted as a transfer function: a regular wave component can be transferred to a regular heave component by a multiplication with the transfer function $z_a/\zeta_a(\omega)$. Section 3.3 will show the relation between the wave energy spectrum and the response energy spectrum with the use of this transfer function.

3.3 Motion in irregular waves

The relation between irregular waves and the resulting irregular motion is visualized in figure 3.6. The reaction of the structure on the exciting motions known as the frequency characteristics are comparable to a transfer function of a system.
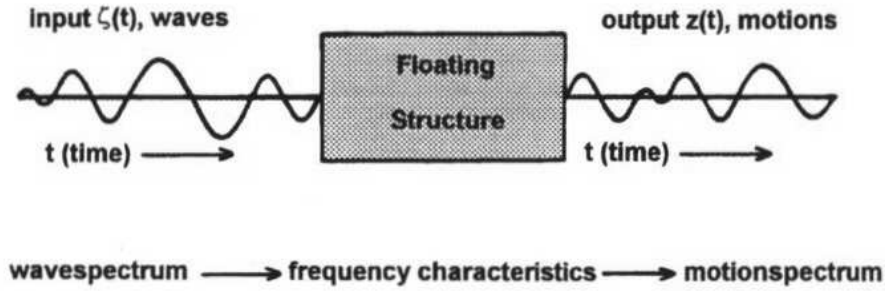

Figure 3.6: Relation between motions and waves [7]

The wave energy spectrum was given in paragraph 2.3.2 as

$$
S_\zeta(\omega) \cdot d\omega = \frac{1}{2}\zeta_a^2(\omega)
\tag{3.3.1}
$$

Analogous to this derivation the energy spectrum of the heave response as given in paragraph 3.2.3 can be given as

$$
S_z(\omega) \cdot d\omega = \frac{1}{2}z_a^2(\omega)
\tag{3.3.2}
$$

If $\frac{1}{2}z_a^2(\omega)$ is rewritten to find the relation between wave energy spectrum and response energy spectrum like

$$
\frac{1}{2}z_a^2(\omega) = \left|\frac{z_a}{\zeta_a}(\omega)\right|^2 \cdot \frac{1}{2}\zeta_a^2(\omega) = \left|\frac{z_a}{\zeta_a}(\omega)\right|^2 \cdot S_\zeta(\omega) \cdot d\omega
\tag{3.3.3}
$$

the response energy spectrum of a motion can also be given as

$$S_z(\omega) = \left| \frac{z_a}{\zeta_a}(\omega) \right|^2 \cdot S_\zeta(\omega) \tag{3.3.4}$$

This means that the wave energy spectrum and the response energy spectrum are directly related by the transfer function of the structure.

To find the significant values of the response energy spectrum the moments m_{nm} of the spectrum are used

$$m_{nz} = \int_0^\infty S_z(\omega) \cdot \omega^n \cdot d\omega \quad \text{with } n = 0, 1, 2, \dots \tag{3.3.5}$$

with $n = 0$ the area underneath the spectrum, $n = 1$ the first moment, $n = 2$ the moment of inertia of the spectral curve and z the heave motion of the response.

This yield the significant heave amplitude

$$\bar{z}_{a_{1/3}} = 2 \cdot \sqrt{m_{0z}} = 2 \cdot RMS \tag{3.3.6}$$

with RMS the root mean square value. The significant amplitude is used as a measure to compare different combinations of structures and wave regimes and is defined as the average value of the highest one-third of the amplitudes.

and the corresponding significant response period T_{2z} for heave as

$$T_{2z} = 2\pi \cdot \sqrt{\frac{m_{0z}}{m_{2z}}} \tag{3.3.7}$$

Since only the amplitudes are affected by the transfer function, the significant response period should be equal to the period of the wave regime. This agrees with the definition of T_{2z}.

3.4 Computational tool DELFRAC for fluid-structure interactions

This section will focus on the boundary conditions and limitations of the computational tool DELFRAC used for the calculations of the fluid-structure interactions of the ecoboat and dampers. In this way the applicability of the program can be demonstrated and recommendations can be made for specific circumstances. DELFRAC is chosen, because it is well documented [9] and since it is developed at the Delft University of Technology, accessible for the purpose of my thesis.

First the theoretical basics are explained in paragraph 3.4.1, next the translation to a numerical model is explained in paragraph 3.4.2 and an indication of the actual use of the program is given in paragraph 3.4.3.

3.4.1 Theory

DELFRAC is developed to compute fluid-structure interactions of structures with a zero mean forward speed. It is a three-dimensional diffraction program using linear 3-d potential theory.

The diffraction of waves is the disturbed wave pattern due to the presence of a body in waves. The diffraction on a body is analogous with the diffraction of light: from every point on a body a spherical front is generated which falls off in intensity away from the forward direction. A continuous series of such actions carries radiation around objects, but with decreasing intensity due to the distribution in space of the energy [32]. The numerical interpretation of this phenomenon is given in paragraph 3.4.2.

Linear potential theory was introduced in paragraph 2.2.2. The main restrictions can be summarized as: all flows are considered incompressible, irrotational, non-viscous, continuous and homogeneous. These restrictions only affect situations with considerable surface friction and those results should be considered more carefully.

The potential of the water surrounding a floating structure can be given by the summation of the potential of the undisturbed incoming wave Φ_w, the potential due to the diffraction of the undisturbed incoming wave Φ_d and the potential due to the six body motions Φ_j (compare paragraph 3.2.2).

$$\Phi = \Phi_w + \Phi_d + \sum_{j=1}^{6} \Phi_j \quad \text{with } j = 1, 2, .., 6 \tag{3.4.1}$$

These potentials should fulfil several boundary conditions. The first three are analogous to the potential theory presented in paragraph 2.2.2. The other two boundary conditions are specific for structures in waves.

1 Continuity or Laplace equation
2 Seabed boundary condition: impermeable to water
3 Free surface kinematic boundary condition: boundary between water and air
4 Mean wetted part of the outside (the hull) of the structure: no leak
5 Radiation[1] condition: energy reduces with increasing distance to source

The first three are equal to the boundary conditions 1, 2 and 4 in paragraph 2.2.2 and 2.2.3 but now expanded to 3-d conditions

Ad 1 $\frac{\partial^2 \Phi}{\partial x^2} + \frac{\partial^2 \Phi}{\partial y^2} + \frac{\partial^2 \Phi}{\partial z^2} = 0$ (compare 2.2.6)

Ad 2 $\frac{\partial \Phi}{\partial z} = 0$ for $z = -h$ (compare 2.2.8)

Ad 3 $\frac{\partial^2 \Phi}{\partial t^2} + g\frac{\partial \zeta}{\partial t} = 0$ for $z = 0$ (compare 2.2.17)

Ad 4. The fourth boundary condition defines the direction of the particle velocity on a point on the hull of the structure

$$\frac{\partial \Phi}{\partial n} = \vec{v} \cdot \vec{n} \tag{3.4.2}$$

with $\vec{v}$ the velocity on a point on the hull and $\vec{n}$ the normal vector of the hull positive into the fluid.

Ad 5. The fifth boundary condition only applies to the body motion and diffraction potentials. It ensures that these potentials will disappear with increasing distance to the structure.

Within linear potential theory wave loads or motions in real sea conditions can be determined by superimposing regular wave results. Therefore input waves can be restricted to regular waves with constant amplitude, direction and frequency without restricting the applicability of the results as long as enough regular waves are computed. For regular waves the linear potential Φ can be written as the combination of a co-ordinate dependent part ϕ and a time dependent part (eg. $e^{-i\omega t}$). If only the co-ordinate dependent part is considered the total fluid potential can be written as

$$\phi = -i\omega \{ (\phi_w + \phi_d)\zeta_w + \sum_{j=1}^{6} \phi_j \zeta_j \} \tag{3.4.3}$$

with
  ϕ_w, ϕ_d co-ordinate dependent part of Φ_w and Φ_d
  ζ_w amplitude of the undisturbed incoming wave (equal to amplitude of diffracted wave)
  $j = 1, 6$ body motion modes (surge=1, sway=2, heave=3, roll=4, pitch=5 and yaw=6)
  ϕ_j potential of the j-th body motion
  ζ_j motion in j relative to the body axes

with the wave potential of the undisturbed incoming wave ϕ_w and wave potential of the diffracted wave ϕ_d, the wave force F_{w_k} can be given as the pressure distribution over the submerged surface as

$$F_{w_k} = -\iint_{S_0} p \, n_k \, dS = -\rho\omega^2 \zeta_w \iint_{S_0} (\phi_w + \phi_d) \, n_k \, dS_0 \quad \text{for } k = 1, ..., 6 \tag{3.4.4}$$

with

  k direction of the force (surge=1, sway=2, heave=3, roll=4, pitch=5 and yaw=6)
  S_0 mean wetted surface (hull) of the structure
  p fluid pressure
  n_k direction parameter of surface element dS for different k

and the (coupled) equations of motion become

$$\sum_{j=1}^{6} \{ -\omega^2(M_{kj} + A_{kj}) - i\omega B_{kj} + C_{kj} \} \, \zeta_j = F_{w_k} \quad \text{for } k = 1, ..., 6 \tag{3.4.5}$$

with

  M_{kj} mass and inertia matrix of the body for mass or inertia coupling in k due to acceleration in j
  A_{kj} added mass and added inertia matrix for the force on the body in k due to acceleration of the body in j
  B_{kj} damping matrix for the force on the body in k due to velocity of the body in j
  C_{kj} spring matrix for the force on the body in k due to motion of the body in j

37

Externally applied damping or spring devices can be modeled by contributions to the B_{kj} or C_{kj} matrices. In this way the effects of additional damping or spring devices can be evaluated prior to their physical design.

A_{kj} and B_{kj} are a function of the water density ρ, the velocity potential of the body motions ϕ_j and their distribution over the submerged surface defined by S_0 and n_k. B_{kj} is also a function of frequency ω. Therefore ϕ_j needs to be calculated to find A_{kj} and B_{kj} and then the motions of the structure can be determined.

Limitations
The theory used restricts the use of DELFRAC to situations with limited surface friction where the influence of rotation and viscosity can be neglected.

3.4.2   Numerical interpretation of the theory

To be able to solve the equations several assumptions are made. First the geometrical shape is discretized in panels as illustrated in figure 3.7 for the ecoboat. Next the body is presumed rigid and all energy concentrated in the ground frequencies. Therefore only first order phenomena are considered.
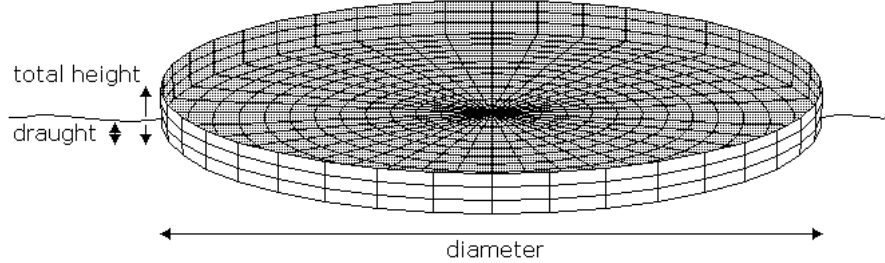

Figure 3.7: DELFRAC model of the ecoboat

The velocity potential due to the motions of the body (ϕ_j) on each panel is calculated by modeling the potentials as pulsating sources in the center point of each panel and calculating the influence of each source on each panel. This description corresponds to the diffraction of waves and is also used to calculate the diffracted waves. The potentials at a specific point on the hull due to one of the motions can now be calculated with

$$\phi_j(X_1, X_2, X_3) = \frac{1}{4\pi} \iint\limits_{S_0} \sigma_j(A_1, A_2, A_3) G(X_1, X_2, X_3, A_1, A_2, A_3) dS$$

$$\text{for } j = 1, ..., 6$$

(3.4.6)

with

ϕ_j velocity potential at an earth fixed point (X_1, X_2, X_3) for the j-th motion

S_0 mean wetted surface of the structure

σ_j source strength at an earth fixed point (A_1, A_2, A_3) on the mean wetted surface due to the j-th motion

G Green's function that can be interpreted as an influence function of the pulsating source located at (A_1, A_2, A_3) on the potential in (X_1, X_2, X_3).

The source strengths are calculated with the boundary condition given in equation 3.4.2 with n_k the direction parameter for the different body motions. The diffracted wave can be calculated in a similar manner with the reflection of the incoming wave as direction.

The calculation of the source strengths yields the potentials ϕ_j and ϕ_d that can be used to determine the added mass and damping coefficients and the wave force. Combined with equation 3.4.5 this yields the required motions.

Limitations
The numerical interpretation limits the results to rigid body modes.

3.4.3 Program use

To find the motions of a structure added mass, damping coefficients and the wave forces should be calculated as explained in the previous paragraphs. Therefore the input is limited to geometrical shape, step size and range of the calculations and the orientation of the incoming waves with respect to the structure.

The input for the ecoboat and dampers is given as

D diameter

d draught

k_{xx} radius of gyration $(\sqrt{\dfrac{I_{xx}}{m}} = \sqrt{\dfrac{1}{4}r^2 + \dfrac{1}{12}l^2})$

$\Delta\omega$ stepsize $(= 0.05\, rad/s)$

ω frequency range $(= 0.05 - 2.0\, rad/s)$

  wave entrance angle $(= 180^o)$

This yields the output of wave forces F_w in amplitude and phase, added mass and damping coefficients per motion and an amplitude and phase for each motion. (All output is in tons.)

Chapter 4

Damper requirements

The purpose of this thesis is to protect and sustain the ecoboat with floating dampers. This chapter will derive the requirements for the dampers that are needed to fulfil this purpose. Paragraph 4.1 will introduce the background of the ecoboat project as a solution for living at sea and evaluate the principles of the ecoboat foundation to find the relating requirements for an ecoboat protection system. Next the requirements that result from the ecoboat are derived: a location is chosen so location characteristics like water depth and wave regime can be determined (4.2), a configuration is chosen for the ecoboat to derive the response frequencies (4.3) and the combination of these location characteristics with the ecoboat response frequencies is used to define the design loads in paragraph 4.4. The different requirements for the protection system are summarized so they can be used for design purposes at the end of the chapter (4.5).

4.1   History and objective of the ecoboat project

The research into sea-based living was initiated by the ecoboat foundation, founded by Frits Schoute in 2000. The foundations' objective is to develop sustainable solutions for the need for water, energy and living space of major cities worldwide. The efforts are focussed on the ecoboat as a combined solution to these needs. The ecoboat should add living space at sea to the inhabitable area of the city and provide energy and fresh water for its inhabitants in a sustainable way. For the comfort of the inhabitants the living space should remain as calm a possible, but wave energy conversion requires motion. Therefore a combination of ecoboats and dampers is currently investigated to . The dampers should provide calm water for the ecoboat and yield energy while the ecoboat provides the required living space.

The long timescale of the project makes it possible to develop and adapt technology to meet these objectives. (See chapter 7 for more information about global trends towards living at sea and the characteristics of sustainable solutions.)

The vision of the ecoboat foundation includes three key principles: small, sustainable and safe. Small means a modular, flexible, simple system. Sustainable leads to floating, because of the rising sea water level and to the choice for an energy conversion system rather then a mere damping system that can fulfil the need for fresh water, electricity and heating. Safe is because safety must be guaranteed for the inhabitants of the ecoboat and a damping system

must ensure this safety requiring a highly reliable, fail safe design.

4.2 Projected location of the ecoboat

The location for the first ecoboat is chosen at the coastal range of the Randstad [1]. This part of the Netherlands is densely populated and has reached its limits in growth. This location choice should not limit the opportunities for the ecoboat in other circumstances, but serve as an example for major cities worldwide, because many coastal metropolis worldwide could benefit from a sea based way of living. Therefore the damping system is designed for near coast North Sea averages, but should be adaptable to different water depths and wave regimes.

Figure 4.1: Measurement-sites at the North Sea [20]

Near coast North Sea is defined as the region within the 12 mile zone that is subject to national legislation. For the Dutch coastal region this zone has a water depth of approximately 20m but the water depth of the first kilometer is less than 8m. Since the first ecoboat will most likely be situated within 2 kilometers off the coast, a water depth of 10m is chosen for design purposes. Compared to other regions this is relatively shallow, therefore deeper water should also be possible.

The scatter diagram used for design is compiled from three different measuring sites along the Dutch coast: Noordwijk, IJmuiden munition depot and Lightship Goeree [20]. Figure 4.1 indicates their position and table 4.1 summarizes the main characteristics of the sites. Compared to other measuring sites these three are situated relatively close to the coast and within the Randstad coastal zone, but the sites still differ from the projected ecoboat location.

---

[1]The Randstad is the combination of the four major cities in the west of the Netherlands (Amsterdam, the Hague, Rotterdam and Utrecht) and the urbanized area in between

Therefore a correction is made with the shoaling coefficient to account for the difference in water depth as introduced in chapter 2 and illustrated in appendix B.

The corrected wave regimes of the three sites are averaged to find the design wave regime. This average of the corrected scatter diagrams of wave height and period is considered representative for a random site within the Randstad coastal area for the given water depth of $10m$. Appendix B shows the scatter diagrams and the corrections for the three sites. This scatter diagram will be used in paragraph 4.4 to determine the design wave regime.

	Projected site	Noordwijk	IJmuiden	Goeree
distance to coast [km]	< 2	10	37	18
water depth [m]	10	18	21	21
shoaling coefficient	0.9732	0.9647	0.9775	0.9775

Table 4.1: Measurement-site characteristics

4.3   Ecoboat configuration

A configuration for the ecoboat is chosen as summarized in table 4.2 and illustrated in figure 4.2.
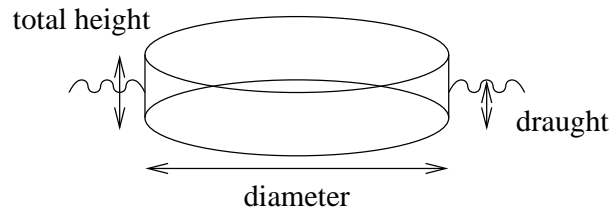
Figure 4.2: Schematic draft of the ecoboat

geometry	cylinder (no directionality)
diameter	$35m$ (ground surface of $\sim 1000m^2$)
draught	$2m$
total height	$7m$
mass	$1962 * 10^3$ kg (see equation 3.2.3)

Uniform mass distribution is assumed, therefore the center of gravity is located at the center axis at half the vessel height $(= 3.5m)$.

Table 4.2: Ecoboat configuration

This size is chosen as a compromise between the ecoboat vision of a small and modular form of living and practical unit size. The shape is evaluated with DELFRAC for the projected water depth (as described in paragraph 3.4) to find the frequency dependent motion response of the structure. For the circular shape no sway, roll or yaw are found for a wave entry direction of 180°. Figure 4.3 shows the relation between wave input and motion output (bode plot) for surge, heave and pitch.
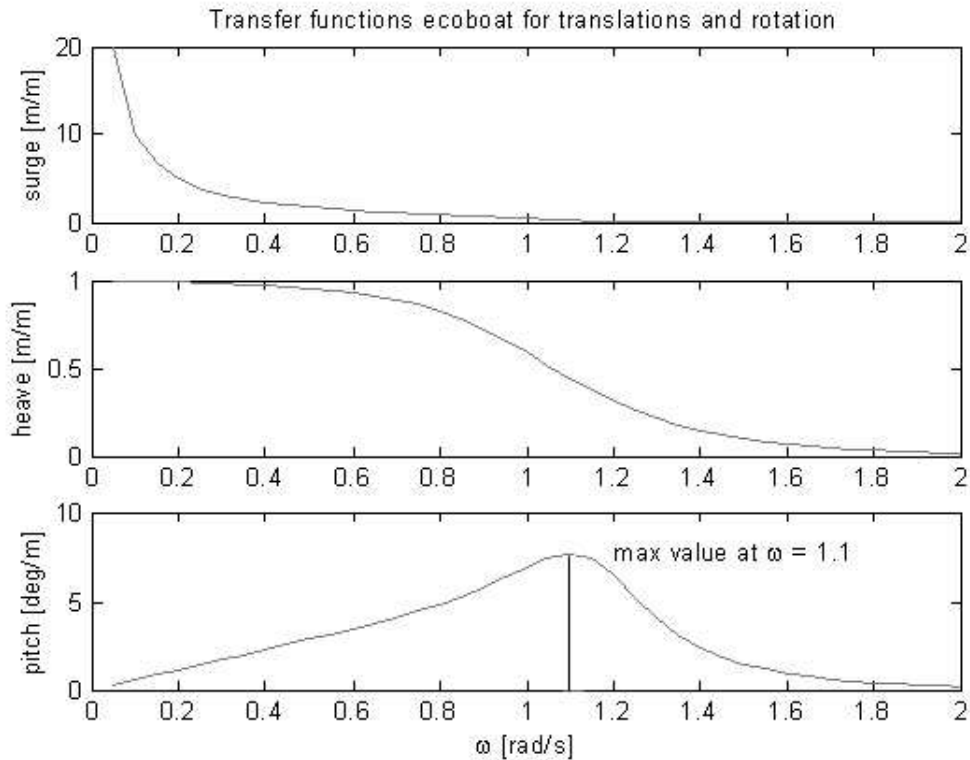

Figure 4.3: Ecoboat transfer functions

The figure shows that the maximum surge motion will occur for the lowest wave frequency present in the waves. The large increase between $\omega = 0$ and $\omega = 0.2\,rad/s$ has no relevance for design purposes, since waves with these frequencies do not occur at the projected location. For heave the wave motion is directly followed by the motions of the structure ($\frac{\zeta_a}{z_a} = 1$) for low frequencies and reduced for higher frequencies. This corresponds to the intuitive feeling that a structure will move with the waves as long as the waves are long relative to the structure itself. It should be noted that there is no resonance peak for heave due to the large hydrodynamic damping of the structure in vertical direction. The pitch motion has a resonance peak at ω=1.1 rad/s and increases the wave input for most of the available wave frequencies. The pitch motion will pose the largest limitations on the functionality of the ecoboat, because it will result in very unpleasant motions for the inhabitants.

The chosen configuration of the ecoboat should be combined with the wave statistics of the projected location to find the responses of the ecoboat and choose a design wave regime.

4.4   Design loads

A rule of thumb for offshore structures indicates that waves are only affected by structures with a diameter of at least 20% of the wave length. The choice of a design wave regime therefore directly affects the size of a damping system, since wave period and wave length are related with the dispersion relation (see chapter 3). If safety is used as a single guideline, the maximum response can be calculated by combining the maximum wave height of different wave periods from the scatter diagram into JONSWAP wave spectra S_ζ and combining those with the ecoboat reaction to the different frequencies $\frac{\zeta_a}{z_a}$. The significant response amplitudes $x_{a_{1/3}}$, $z_{a_{1/3}}$ and $\theta_{a_{1/3}}$ can then be used to compare the resulting motions for different wave spectra. (See chapter 3 for the associated equations.)

If this is done for the ecoboat it becomes clear that the requested structure to protect the ecoboat should be at least 20% of $90m$ if maximum pitch response is used for design. For maximum surge or heave the maximum wave period measured yields $100m$. (See appendix C for the response spectra of the ecoboat to the maximum wave heights from appendix B for a large range of wave periods.) Such structures will only resonate with the waves at less then 0.3% of the time and do not fulfil any of the other requirements of the ecoboat. The limited motions of the damper under normal circumstances will make it difficult to extract energy from the system and the size of the damping system will probably need to be larger then the ecoboat itself to function properly. This does not seem to be a satisfactory solution. Therefore the ecoboat will be presumed to have an internal active stabilization system for the longest 5% of the wave periods and the damping system will provide calm water for the other 95% of the waves.
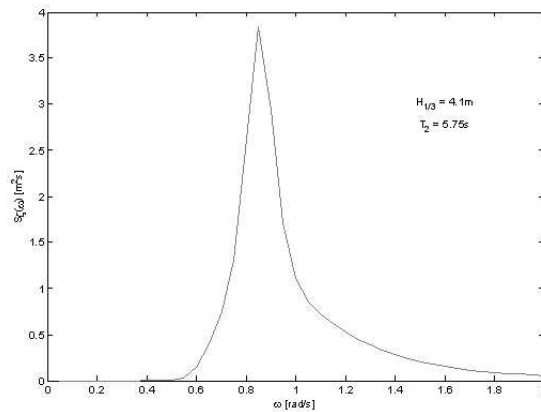

Figure 4.4: Design wave energy spectrum (JONSWAP)

The scatter diagram (see appendix B) shows that the longest wave period that should be affected by the damping system is $T_2 = 5.75s$ and has a maximum wave height $H_{1/3} = 4.4m$. If shoaling is included $H_{1/3} = 4.1m$ (this corresponds to situation D in appendix C). Therefore the design wave regime is $T_2 = 5.75s$ and $H_{1/3} = 4.1m$. This wave period represents about 6% of the waves which is still very limited, but should leave some opportunities for energy

extraction and the size of the damper can remain less then the diameter of the ecoboat since the waves concerned are approximately 50m.

The design wave regime is converted to a JONSWAP wave energy spectrum $S_\zeta(\omega)$ as illustrated in figure 4.4 with the equation (2.3.10) given in chapter 2. The JONSWAP formula is specifically developed for the North Sea therefore and most suitable to simulate the wave conditions.

The combination of the wave energy spectrum with the ecoboat transfer functions is shown in figure 4.5.
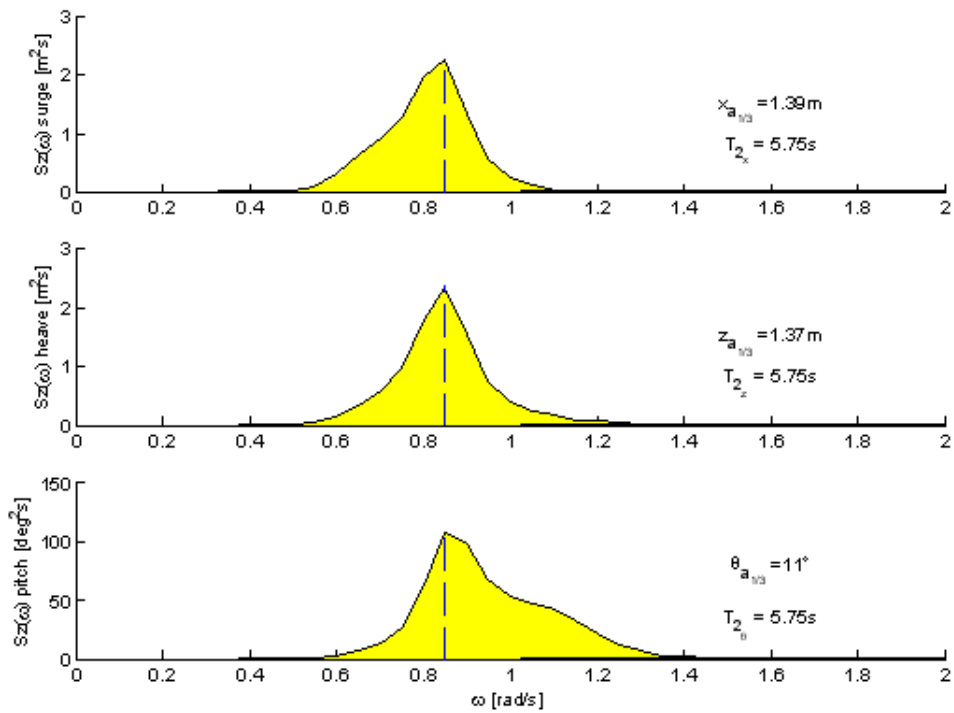
Figure 4.5: Ecoboat response to design wave regime

> *Numerically the JONSWAP formula $S_\zeta(\omega)$ (equation 2.3.10) is calculated for $\omega = 0.05 - 2\ rad/s$ with a step size of 0.05 equal to the range and step size of the DELFRAC output. Next the response spectra $S_x(\omega)$, $S_z(\omega)$ and $S_\theta(\omega)$ are calculated with equation 3.3.4 as*
>
> $$S_q(\omega) = \left| \frac{q_a}{\zeta_a}(\omega) \right|^2 \cdot S_\zeta(\omega) \quad \text{with } q = x, z \text{ or } \theta$$
>
> *in which $\frac{q_a}{\zeta_a}(\omega)$ is given by DELFRAC for surge [m/m], heave [m/m] and pitch [deg/m]. To determine the significant response amplitudes the areas underneath the response spectra (RMS) are calculated with the trapezoid function of MATLAB for a step size of 0.05. The significant response amplitudes can now be given according to equation 3.3.6 with*
>
> $$q_{a_{1/3}} = 2 \cdot \text{RMS } S_q(\omega) \quad \text{with } q = x, z \text{ or } \theta$$

The ecoboat response spectrum shows the resulting motions of the ecoboat with $x_{a_{1/3}}$, $z_{1/3}$ and $\theta_{a_{1/3}}$ the significant response amplitudes and T_{2_x}, T_{2_z} and T_{2_θ} the significant response periods equal to the design zero-crossing wave period T_2. The damper will have to decrease these motions over all frequencies to decrease the load on the ecoboat. The significant response amplitudes can therefore be used as a measure of the effectiveness of the damper if they are combined with the value of the extremes.

The peak value of the motion spectra is used to choose a design frequency of the system. A damper will be most effective at its resonance frequency ω_0 since larger motions are easier to convert to energy than small motions. It is assumed that a damper will also damp higher frequencies than its design frequency, but will not damp lower frequencies very well. This assumption will be verified in chapter 6. The peak of the different motion spectra is at $\omega = 0.85\ rad/s$ as indicated in figure 4.5 and is equal to the peak in the JONSWAP wave energy spectrum. This frequency will be used for design as resonance frequency.

It should be noted that the pitch motion is relatively large with a response amplitude of 11°compared to the surge and heave motion. Therefore the pitch motion will be critical for the design of the dampers. It is important to reconsider the ecoboat configuration at a next design phase, because a different combination of diameter, draught and height could yield a stabler ecoboat as a starting point.

The design wave regime and the consequent design frequency should be re-evaluated at the beginning of each design phase, because a change or further specification of the location should be accompanied with an adaption of the wave regime and the wave regime has a large impact on the outcome of the design.

4.5   Summary of damper requirements

The requirements for the ecoboat damping system are a combination of the vision of the ecoboat foundation with the specific requirements of the projected ecoboat configuration and chosen location. The requirements due to location and configuration of the ecoboat should be reconsidered at the beginning of each design phase.

The ecoboat configuration has a cylindrical geometry, a diameter of 35m and a total height of 7m (5m above and 2 beneath sea water level). To create calm waters for this structure the dampers should limit the wave height for the 95% of the incoming waves. The longest wave periods are excluded, because they require very large structures for damping. Therefore an active stabilization system is presumed present on the ecoboat itself that can reduce the motions of the ecoboat for the longest wave periods.

Table 4.3 gives a summary of the requirements for the damping structure of the ecoboat divided between the sources of the requirements and their numerical value.

Ecoboat vision	
small	modular, flexible, simple
sustainable	floating, energy conversion system
safe	reliable, fail safe, multiple load cases
Location	
water depth	10m
design wave regime	$T_2 = 5.75s$
	$H_{1/3} = 4.1m$
	$\lambda = 50m$
Ecoboat motions	
resonance frequency	$\omega_0 = 0.85\ rad/s$
significant motion amplitude	surge $x_{a_{1/3}} = 1.39m$
	heave $z_{a_{1/3}} = 1.37m$
	pitch $\theta_{a_{1/3}} = 11°$
damper diameter	$> 10m$ and $< 35m$

Table 4.3: Requirements for the damping system

Chapter 5

Wave energy conversion principles

The existing wave energy conversion system designs show a remarkably high diversity of conversion principles. Therefore this chapter presents the different available principles and their opportunities as a damping system for the ecoboat. The different principles are presented and compared to the requirements as given in paragraph 4.5 in paragraph 5.1 so paragraph 5.2 can select the most promising principle.

5.1 Basic energy conversion principles

Wave energy converters can be divided in basic energy conversion principles based on their method of energy absorption. The conversion principles 'heaving and pitching bodies', 'oscillating water columns' and 'pressure devices' primarily use the changing water level as energy source. 'Surging-wave energy convertors' and 'particle motion convertors' use the rotating motion of the water particles, while 'overtopping devices' use the horizontal propagation of waves to fill a basin to extract energy. In the next paragraphs the different basic energy conversion principles will be explained, each with its advantages and limitations.

To explain and compare the different systems a simple sinus shaped wave is assumed with wave length λ and height H as defined in chapter 2.

5.1.1 Heaving or pitching bodies

One of the simplest forms of wave energy conversion is a heaving or pitching body with the energy absorption directly coupled to the motion of the body. Figure 5.1 shows a rectangular float of length L in heave and pitch. The maximum heaving motion will occur for an odd number of half wave lengths compared to the length of the float:

$$\text{Heave}_{max} = \frac{i\lambda}{2L} \quad \text{for } i = 1, 3, 5, \dots \quad if \ \frac{\lambda}{L} \in \mathbb{N} \tag{5.1.1}$$

while there is no heaving motion for an even number of half wave lengths compared to the length of the float, because the upward and downward forces (see figure 5.1) cancel each other

out.

$$\text{Heave}_{min} = \frac{i\lambda}{2L} = 0 \quad \text{for } i = 2, 4, 6, ... \quad if \; \frac{\lambda}{L} \in \mathbb{N} \tag{5.1.2}$$

For a pitching motion this principle reverses. Now an even number of half wave lengths with respect to the length of the float will maximize rotation:

$$\text{Pitch}_{max} = \frac{i\lambda}{2L} \quad \text{for } i = 2, 4, 6, ... \quad if \; \frac{\lambda}{L} \in \mathbb{N} \tag{5.1.3}$$

while an odd number will minimize the pitching motion, because the forces give an equal but opposite moment with respect to the center of gravity (see figure 5.1)

$$\text{Pitch}_{min} = \frac{i\lambda}{2L} = 0 \quad \text{for } i = 1, 3, 5, ... \quad if \; \frac{\lambda}{L} \in \mathbb{N} \tag{5.1.4}$$
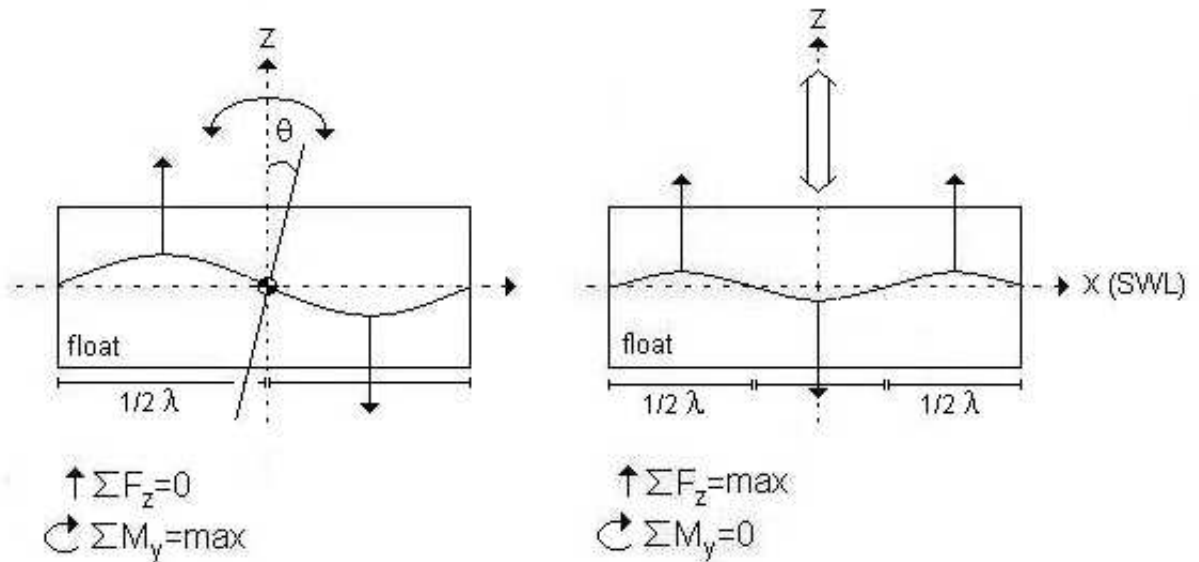
Figure 5.1: Maximum heave and pitch for different wave length

Performance

The maximum energy absorption is directly related to the maximum excitation. If the wave period is equal to the base natural period of the system, the system will resonate with the waves and increase the direct excitation of the waves. Therefore waves with a period equal to the natural period of the floating system give the highest energy absorption. The floating system can have a natural mode in pitch or heave or in both depending on the constraints of the design.

The floating body type of energy converter is limited by this direct relation between optimum performance and resonance conditions. Because a random sea consists of many different

wave lengths and frequencies and the natural mode will not be uniquely excited. Therefore performance is much less than could be expected from calculations with regular waves. Predominant waves can be used to improve performance by matching the natural modes to the waves, especially if the system can adapt its natural modes in response to changes.

The disadvantages of a floating body type of damper are the limited damping of other waves and thus limited overall performance. An other disadvantage of this type of damper is that the excitations of the dampers will increase for severe situations and should therefore be extensively tested for their reliability.

Ecoboat perspective
Floating bodies can be used as a damping system to protect the ecoboat. This would require them to resonate at the design frequency for optimal performance. The design frequency of the ecoboat comprises only 6% of the total wave spectrum, therefore the energy yield will be limited. A major advantage is their relative simplicity in construction and design and the large amount of existing designs of such systems (see appendix A).

5.1.2 Oscillating water column

The basic principle of an oscillating water column is a reversed box: open at the bottom, partly filled with water, partly with air and almost closed at the top (see figure 5.2). The enclosed volume of air is compressed by waves and goes through a small opening at the top that hosts a turbine or other compression driven device. The pressure build up inside the column is comparable to the behavior of a piston: several phases and an equal pressure distribution. If the system is in resonance the internal waves will accelerate and reach a height larger than the exciting wave.
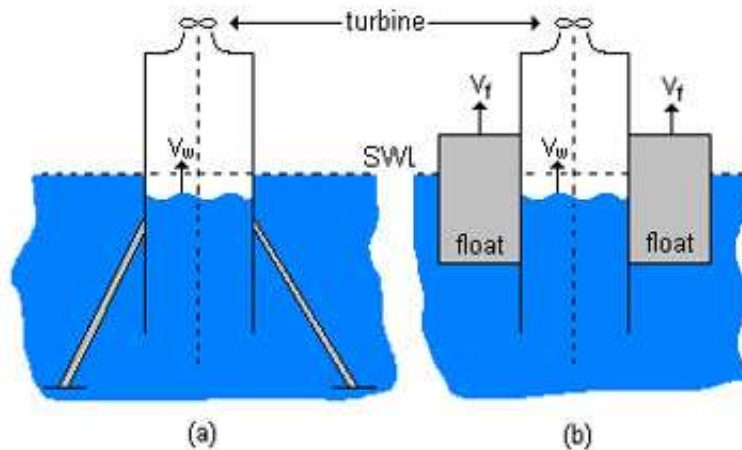

Figure 5.2: Oscillating water column with fixed and floating reaction point

performance

For a fixed reaction point (see figure 5.2 (a)) the optimal performance is obtained if the system is in resonance with the predominant waves. For a floating system (see figure 5.2 (b)) the airflow is determined by the heaving motion of the floating structure and the internal wave motion. An energy absorption graph will now have two peaks one for the natural heaving mode of the floating system and one for the resonance of the water-air column. Maximum absorption is obtained if these two resonances coincide.

ecoboat perspective

The ecoboat vision limits possible solutions to floating systems. Therefore only the floating oscillating water column is considered for the ecoboat protection system. The two resonance frequencies (from the floating system and from the water-air column) can be used to damp the design frequency. They can coincide for maximum damping at that frequency but can also be used separately to broaden the performance range and damp both the design frequency and the highest yield frequency for a combination of protection and performance.

5.1.3 Pressure devices

Pressure devices use the alternating pressure underneath the water level. This pressure is a combination of the change in water level (hydrostatic pressure) and the rotating movement of the water particles (dynamic pressure). The largest contribution to the pressure variation is created by the difference in water mass between a wave crest and a wave trough and the dynamic pressure caused by the rotation of the water particles is usually neglected (McCormick [3] and Shaw [12]). The pressure variation is largest near the surface and decreases rapidly with increasing depth as described in chapter 2, thus reducing the operating zone for pressure devices.

Figure 5.3 shows a basic design. This design is at equilibrium if the piston shaped moving part has a neutral buoyancy and the upward pressure on the plunger is equal to the downward pressure due to the wave motions on the piston. At equilibrium the force on the piston will directly be transferred to the plunger.

performance

The performance of a pressure device is limited its submerged position. To keep the structure submerged the top of the system should be at least half a wave height deep at all times. Therefore storm waves should be used for the design of the neutral position. In addition the position of the structure decreases during a stroke of the system. Since the wave force decreases with water depth the low neutral position and the decreasing forces during a stroke are a severe limitation on the performance.

An important advantage of pressure systems are the limited off-design loads. Because of their submerged position waves do not break on the structure and the system will remain in relatively calm conditions even during major storms.

ecoboat perspective

The water depth at the ecoboat location of $10m$ makes it very difficult to design a floating submerged pressure device. In combination with the limited performance expectations, pressure devices are not considered as a solution for the ecoboat damping system.
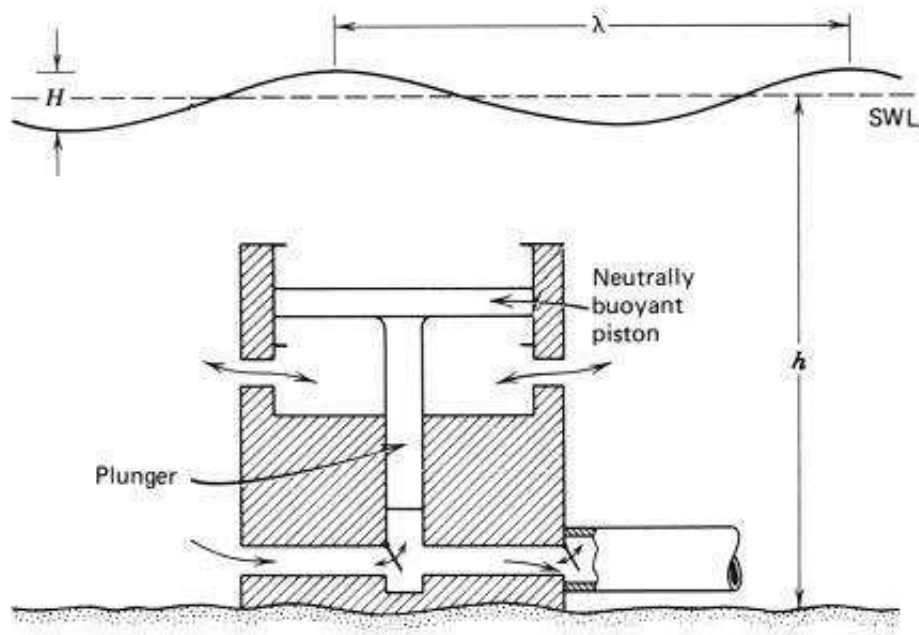
Figure 5.3: Pressure devices

5.1.4 Surging-wave energy converters

Surging-wave energy converters use the constant horizontal movement of the water particles in shallow water ($h < \lambda/20$) as described in section 2.2.3.

ecoboat perspective
The projected site for the ecoboat is near shore to off shore with a water depth of 10m. Using the given definitions for water depth this results in a circular particle motion for waves with a wavelength of 20m or less, elliptical but decreasing with depth for wavelengths between 20 and 200m and elliptical with a constant horizontal component for wavelengths over 200m. This means that only storm induced waves will show such behavior and a device specifically developed for these conditions is not likely to perform best overall. Therefore surging-wave energy converters are not considered a possible solution for the ecoboat and will not be further investigated.

5.1.5 Particle motion converters

Particle motion converters use the rotating movement of the water particles as an exciting source. In deep water this orbit is approximately circular with a maximum radius of half the wave height H tangent to the surface. The particle velocity and the corresponding rotation radius decrease exponentially with depth (see figure 2.4). The rotating motion of the particles is in phase with the wave period resulting in a relatively slow motion with a small radius (1/2 H).

performance

The performance of a particle converter depends on the force exerted by the dynamic pressure and the resistance experienced underneath the water. A rotating device like a water wheel is turned by the difference in dynamic pressure between the blades, because the dynamic pressure varies along the wavelength λ as illustrated in figure 5.4. Where u is the particle velocity.

In normal circumstances λ is long with respect to the wave height H. If the device would be in the same order of size as λ to make use of the change in pressure gradient, the device would be very large. The particles velocity decreases exponentially with depth so the lower blades will not contribute to the rotation but would experience a large resistance. If the device is of the same order of size as the maximum particle orbit, the force due to the difference in pressure gradient would be very small. The combination of small radius with slow rotation imposes large restrictions on the performance and there are no examples of this principle in an advanced state of design (see appendix A)

An interesting development is the design of lift devices. These systems use chambered profiles to increase their rotational motion. At present only very small systems are operational and the difficulties related to larger scales are not yet solved.

ecoboat perspective

The difficulties for this type of energy converter have not been solved yet. Therefore particle motion converters are not considered as a solution for the ecoboat.
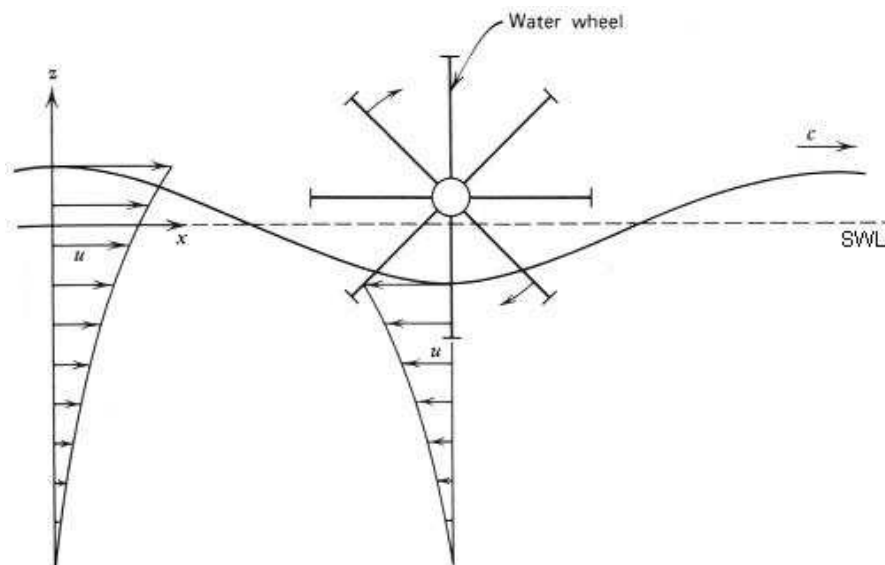

Figure 5.4: Dynamic pressure water wheel

5.1.6 Overtopping devices

Overtopping devices use a ramp to increase the steepness of the incoming waves and fill a higher positioned water basin. After the wave breaks the energy of the wave dissipates into turbulence and thus into heat. The difference in height between basin and sea water level is used to extract energy from the water with a turbine.

performance
The performance of this type of energy converter depends mostly on the size of the structure. The limited energy extraction possibility from the waves should be counter balanced with a large volume of waves flowing through the turbines. This requires large structures to direct the wave motion towards the basin. Figure 5.5 shows the lay-out of an overtopping device known as the wave dragon (see appendix A). In full scale the arms of this energy converter are $50m$ each.

ecoboat perspective
Overtopping devices are considered a possible solution for an 'ecoboat city', but their scale makes them difficult to use at an earlier phase of development since they do not meet the basic requirement of a damper diameter smaller than the ecoboat itself. Another important disadvantage at this design phase is the absence of theoretical and numerical models that can predict the characteristics of the system. Therefore the first damping system of the ecoboat will not use the overtopping principle for energy conversion.
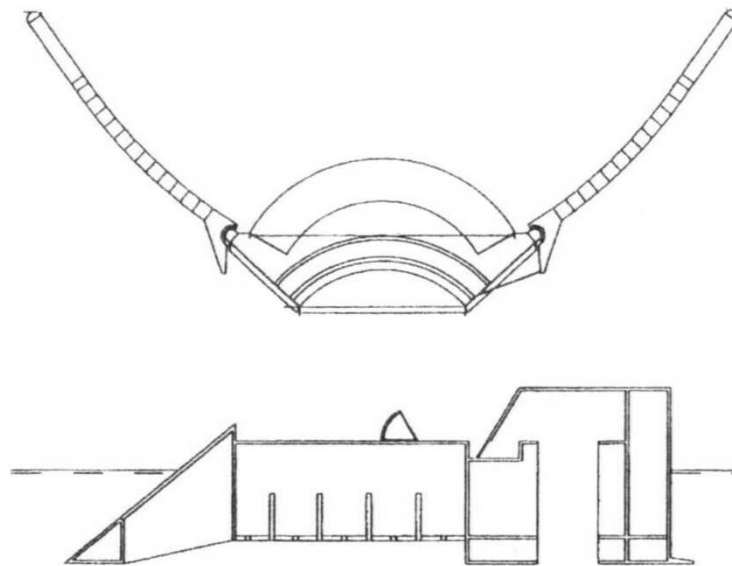

Figure 5.5: Overtopping devices

5.2 Selection of energy conversion principle for the damper

Two energy conversion principles are considered feasible to use for the ecoboat: the heaving and pitching bodies and the oscillating water columns. Both principles can be adapted to the damper requirements (given in paragraph 4.5) in size and resonance frequency and have reached an advanced state of design (as illustrated in appendix A).

The other systems all have specific drawbacks that cannot be solved before the current phase of design of the ecoboat dampers. Floating pressure devices are difficult at the chosen water depth and have very limited performance, surging-wave energy converters are not applicable at the chosen water depth, particle motion converters have not reached a more advanced state of design and overtopping devices are too large for the damping of single ecoboats and can not be designed with the available theoretical models. Overtopping devices should be reconsidered for larger sea settlements if sufficient funding is available to use an experimental design approach. All these systems are not considered feasible at this phase of design.

Heaving and pitching bodies are relatively simple systems. The performance is limited to the match between their resonance frequency and the prevailing wave frequency and can be improved if their resonance frequency can be adapted. The reliability can be relatively high if the design of the mechanical damping separates the sea water and salty air from the moving parts. An important disadvantage is the increase of motion with increasing wave height which makes them vulnerable in storms, but with sufficient mooring they will act as a break-wave and continue to protect the ecoboat. The heaving and pitching bodies are well documented and appendix A shows many examples of existing designs for this conversion principle, therefore sufficient data is available for the current design phase.

Oscillating water columns are more complex systems. The performance can be relatively high, because the oscillating water column has the opportunity to design for two different resonance frequencies providing the opportunity to design for both protection and for yield. Their reliability is affected by the direct contact of the air turbine with the sea environment especially in storms. This is confirmed by the failure of most prototypes in storms. Although the oscillating water columns will always provide some protection as a break-wave with sufficient mooring. Like the heaving and pitching bodies the oscillating water columns are well documented and appendix A shows many examples of existing designs for this conversion principle.

The choice for the energy conversion principle is based on their expected reliability. The differences in the expected performance of the two principles are relatively small and uncertain, since both systems depend on the resonance of the system with a specific wave length. Irregular conditions at sea limit the opportunities for a single interaction of the structure with one wave length, therefore performance of both systems will be mostly limited to direct wave height. Reliability is another main requirements of the dampers (see paragraph 4.5), therefore the expected difference between the reliability of the two principles is chosen to select heaving and pitching bodies for the ecoboat dampers.

Chapter 6

Primary design of a damper for the ecoboat

To demonstrate the opportunities of a damping system for the ecoboat this chapter will design a basic damping system and evaluate its impact on a wave regime and the resulting motions of the ecoboat. A simple cylindrical damper is assumed in order to get a feel for the importance of the main properties like diameter and height. The mechanical damping of the system is modeled with damping coefficients as velocity dependent damping, but is not specified any further.

A geometry trade-off in section 6.1 gives the most suitable geometry that imposes the largest damping on the sea surface. The next section 6.2 adds mechanical damping to this geometry to find the new wave regime for the ecoboat and compare the motions of the ecoboat behind the damper with the motions in undisturbed waves.

6.1 Geometry trade-off

Five different geometries are evaluated to find a suitable geometry for the ecoboat damper. The resonance frequency of each damper is matched to the design frequency to obtain maximum damping and then DELFRAC is used to find the wave pattern behind the dampers. The damper with the highest damping percentage with respect to the incoming waves will be used in section 6.2 for further investigation. It is sufficient to examine the dampers without mechanical damping for the geometry trade-off, because the optimum mechanical damping is directly related to the passive damping as will be explained in paragraph 6.2.1.

Figure 6.1 gives the diagram for the geometry trade-off. At the top the derivation of the design frequency is summarized as done in chapter 4, next the procedure to find the most suitable geometry is given. First five diameters are selected within the boundaries of the damper requirements of paragraph 4.5, these diameters are matched to the design frequency in the heave direction by the choice of their draught (6.1.1). This combination of diameter and draught is run in DELFRAC to find the added inertia that is required to determine the height that will yield pitch resonance for the design frequency (6.1.2). The damping term is

used in paragraph 6.1.3 to predict the relation between diameter and damping. These results are used in paragraph 6.1.4 and paragraph 6.1.5 to compare DELFRAC results to analytical estimations and choose the most suitable damper geometry in paragraph 6.1.6.
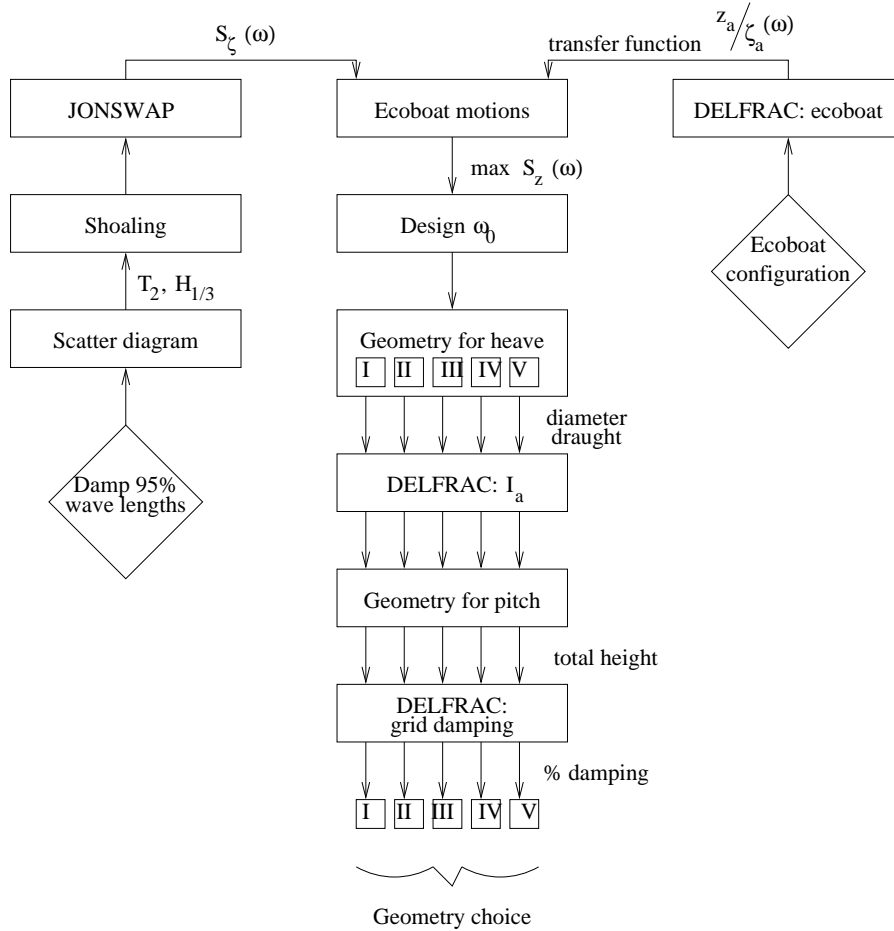

Figure 6.1: Diagram for geometry trade-off

To get a proper feel of the influence of different geometries the maximum range of possibilities is used as given in paragraph 4.5. The minimum diameter is $12m$ due to the water depth of $10m$ as will be demonstrated in paragraph 6.1.1. The maximum diameter is $32m$, because the diameter should be less than that of the ecoboat. This yields the diameters given in table 6.1

geometry	diameter D_d [m]
I	12
II	17
III	22
IV	27
V	32

Table 6.1: Diameter of geometry I-V

6.1.1 Matching the heave frequency: diameter and draught

To get maximum damping at the design frequency the dampers should resonate at that frequency. Therefore both pitch and heave response of the damper should resonate at $\omega_p = 0.85 rad/s$ equivalent to $T_2 = 5.75s$.
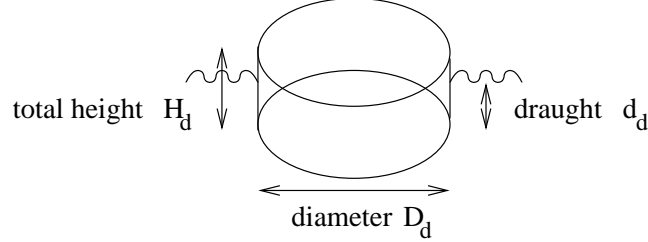
Figure 6.2: Definition of damper geometry

Cylindrical dampers are assumed as defined in figure 6.2 with diameter D_d, total height H_d and draught d_d. The equation of motion for heave for such a system is

$$(m + a)\ddot{z} + b\dot{z} + cz = 0 \tag{6.1.1}$$

with m the mass of the damper, a the added mass of the water, b the damping coefficient and c restoring force or spring coefficient.

Archimedes' law states that the mass of the water replaced is equal to the mass of the body in the water: $m_{\text{damper}} = m_{\text{replaced water}}$

This means that the mass of a damper can be expressed as a function of the diameter D_d and the draught d_d as shown in equation 6.1.2.

$$\left.\begin{array}{c} m_{\text{damper}} = \dfrac{1}{4}\pi D_d^2 H_d \rho_d \\[2mm] m_{\text{replaced water}} = \dfrac{1}{4}\pi D_d^2 d_d \rho_{sea} \end{array}\right\} \Rightarrow d_d = \dfrac{H_d \rho_d}{\rho_{sea}} \quad [m] \qquad \text{for } \rho_d < \rho_{sea} \tag{6.1.2}$$

An approximation of the added mass for heave motion of a cylinder is half a sphere of water [12].

$$a = \frac{1}{12}\pi D_d^3 \rho_{sea} \quad [kg] \tag{6.1.3}$$

This equation does not include the relation between added mass and frequency. This assumption is relatively accurate for the smallest 3 diameters (error$< 20\%$), but becomes less accurate for the larger diameters (see appendix D for the DELFRAC calculations of the added mass compared to the analytical value). This will result in a less accurate calculation of the combination of diameter and draught to achieve heave resonance for the larger diameters. It is recommended that these calculations are reconsidered in a later phase of design.

The mass of the system can now be defined as

$$m + a = f(D_d, d_d) = \frac{1}{4}\pi D_d^2 d_d \rho_{sea} + \frac{1}{12}\pi D_d^3 \rho_{sea} \quad [kg] \tag{6.1.4}$$

The restoring force or spring coefficient c is equal to the change in buoyancy force per unit vertical movement.

$$c = A_d \cdot \rho_{sea} \cdot g = \frac{1}{4}\pi D_d^2 \rho_{sea} g \quad [N/m] \tag{6.1.5}$$

A system in resonance

$$\omega_0 = \sqrt{\frac{c}{m+a}} \Leftrightarrow \omega_0^2 = \frac{c}{m+a} = \frac{\frac{1}{4}\pi D_d^2 \rho_{sea} g}{\frac{1}{4}\pi D_d^2 d_d \rho_{sea} + \frac{1}{12}\pi D_d^3 \rho_{sea}} = \frac{g}{d_d + \frac{1}{3}D_d} \tag{6.1.6}$$

If ω_0=0.85 [rad/s] then the relation between draught and diameter should be

$$d_d = \frac{g}{\omega_0^2} - \frac{1}{3}D_d \Rightarrow d_d = 13.57 - \frac{1}{3}D_d \quad [m] \qquad \text{for } d_d > 0 \tag{6.1.7}$$

Therefore the minimum diameter is indeed $12m$, since this yields a draught of $9.6m$. The water depth of $10m$ restricts the use of any smaller diameters. For the other geometries table 6.2 gives the required draught for heave resonance:

geometry	diameter D_d [m]	draught d_d [m]
I	12	9.6
II	17	7.9
III	22	6.2
IV	27	4.6
V	32	2.9

Table 6.2: Diameter and draught of geometry I-V

6.1.2 Matching the pitch frequency: total height

The equation of motion for pitch can be written as

$$(I + I_a)\ddot{\theta} + b\dot{\theta} + c\theta = 0 \tag{6.1.8}$$

with I the inertia moment about the center of gravity, I_a the added inertia due to the acceleration of water particles surrounding the structure, b the damping coefficient and c the restoring moment or spring coefficient.

The inertia of a cylinder with a homogeneous mass distribution about the x-axis is

$$I_{xx} = \frac{1}{16}mD_d^2 + \frac{1}{12}mH_d^2 \quad [kg\ m^2] \tag{6.1.9}$$

with D_d the diameter of the damper and H_d the total height. The center of gravity is located at half the damper height due to the homogeneous mass distribution.

The added inertia is calculated in DELFRAC for the given geometries, because there are no analytical expressions available for this shape. This calculation presumes the center of gravity to be located at the water level, since the vessel height is and therefore the radius of gyration

k_{xx} is unknown (see paragraph 3.4.3 for DELFRAC input). To find the added inertia for other vessel heights a Steiner transformation is used of the added mass in surge. The pitching movement of a floating cylinder will not be around the center of gravity. Therefore the center of gravity will also experience a surge motion in combination with the pitching motion. This adds to the added inertia in pitch and can be estimated with the Steiner transformation of the added mass in surge to the required position of the center of gravity.

The restoring moment c is given as [6]

$$c = \rho_{sea} g \nabla \cdot \overline{GM} \quad [Nm] \tag{6.1.10}$$

with ∇ the submerged volume and $\overline{GM}$ the distance between the center of gravity (G) and the metacenter (M).

∇ is constant for pitch motions of a structure with straight walls and can therefore be calculated with

$$\nabla = \frac{1}{4}\pi D_d^2 \cdot d_d \quad [m^3] \tag{6.1.11}$$

The distance $\overline{GM}$ can be rewritten as

$$\overline{GM} = \overline{KM} - \overline{KG} \quad [m] \tag{6.1.12}$$

in which $\overline{KM}$ and $\overline{KG}$ are the distance from the metacenter and the center of gravity to the keel (bottom of structure) respectively. The position of the metacenter can be calculated for small angles ($< 10°$) with

$$\overline{KM} = \overline{KB} + \frac{I_T}{\nabla} \quad [m] \tag{6.1.13}$$

In which $\overline{KB}$ is the distance from the keel to the center of buoyancy (B) and I_T is the transverse moment of inertia. The center of buoyancy is located at the middle of the submerged volume. I_T of a circle is $\frac{1}{4}\pi r^4$ $[m^4]$. $\overline{KG}$ is $\frac{1}{2}H_d$.

To match the resonance frequency in pitch ω_0 should be

$$\omega_0 = \sqrt{\frac{c}{I + I_a}} = 0.85 \, rad/s \tag{6.1.14}$$

If the values for I_a are given by DELFRAC and adapted to the vessel height, a graph can be made for different H_d to find the intersection with the requested frequency (see figure 6.3).
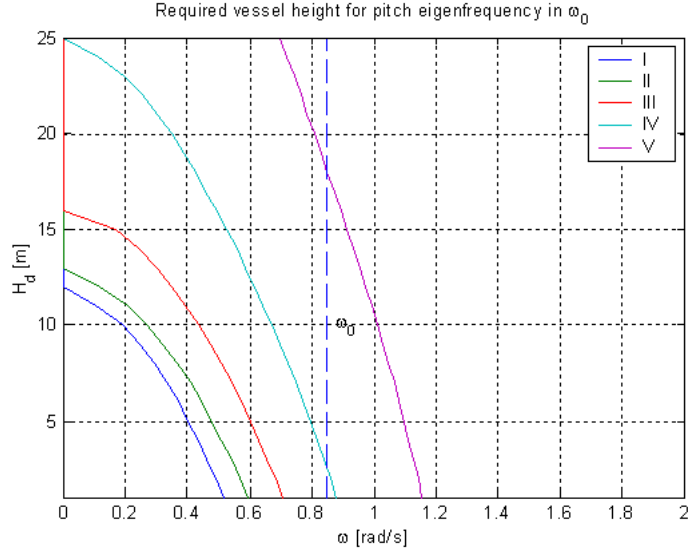
Figure 6.3: Resonance frequencies

Figure 6.3 illustrates the values for $\sqrt{\frac{c}{I+I_a}}$ for $H_d = 0 - 25m$. Geometry I-III do not intersect with the design frequency $\omega_0 = 0.85$. This means that these frequencies will not resonate for the design frequency independent of their height. Geometry IV will resonate with ω_0 but only for a total vessel height of $2.5m$ which is physically unrealistic because the draught calculated in paragraph 6.1.1 is $4.6m$. Geometry V should resonate for a total height of $18m$.

It should be noted that I_a is a function of frequency, while the I_a used for figure 6.3 is equal to I_a for $\omega = 0.85$ and therefore the results in the graph are only correct at the intersection with the design frequency. This approach meets the current objective of selecting a vessel height but should be reconsidered if more insight is required.

Figure should have been used to estimate the required vessel height to obtain pitch resonance, but initial problems have yielded another set of vessel heights that have been used so far. DELFRAC calculations take a long time and can only be done by a few people. Therefore the limited accuracy of these vessel heights is accepted at this stage. The choice of vessel height does not affect geometry I-III since no resonance phenomena will occur according to figure 6.3, coincidentally the choice for the vessel height of the diameter V agrees closely with figure 6.3. Therefore only the resonance characteristics of geometry IV are really affected by this discrepancy. This is taken into account at the selection of the damper geometry in paragraph 6.1.6.

geometry	diameter D_d [m]	draught d_d [m]	height H_d [m]
I	12	9.6	22.8
II	17	7.9	21.5
III	22	6.2	20.1
IV	27	4.6	18.6
V	32	2.9	17

Table 6.3: Diameter, draught and total height of geometry I-V

6.1.3   Prediction of the largest damping with the damping term

To get a sense of the damping properties from the different geometries the damping term is evaluated. According to Ship Hydromechanics by Journee and J. Pinkster [7] the motions in the natural frequency area are dominated by the damping term, with the natural frequency area defined as

$$\frac{c}{m+a} \lesssim \omega^2 \lesssim \frac{c}{a} \quad \Rightarrow \quad \frac{g}{d_d + \frac{1}{3}D_d} \lesssim \omega^2 \lesssim \frac{g}{\frac{1}{3}D_d} \tag{6.1.15}$$

An energy conversion mechanism will need a stroke and a repetitive movement to damp, therefore the damping applied should keep the system within the resonance area. This means that

$$\omega_d \approx \omega_0 \quad \Rightarrow \quad \sqrt{\frac{c}{m+a} - \frac{b^2}{4(m+a)^2}} \approx \sqrt{\frac{c}{m+a}} \tag{6.1.16}$$

To achieve this $\frac{b^2}{4(m+a)^2}$ should be small. This can be achieved by a small value for b, but also with a large value for $m+a$. A small value of b limits the opportunities for energy extraction from the system, therefore the value of $m+a$ should be maximized. If equation 6.1.7 is used to derive a relation between draught and design frequency the total mass can be rewritten to

$$m + a = \frac{1}{4}\pi D_d^2 \rho_{sea} \frac{g}{\omega_0^2} \tag{6.1.17}$$

Therefore $m+a$ is maximal for the largest D_d, this means that geometry V should yield the strongest damping.

6.1.4 Transfer functions of the dampers

The geometries I-V as given in table 6.3 are run in DELFRAC to find their transfer functions. These transfer functions demonstrate the characteristics of the different geometries as illustrated in figure 6.4.
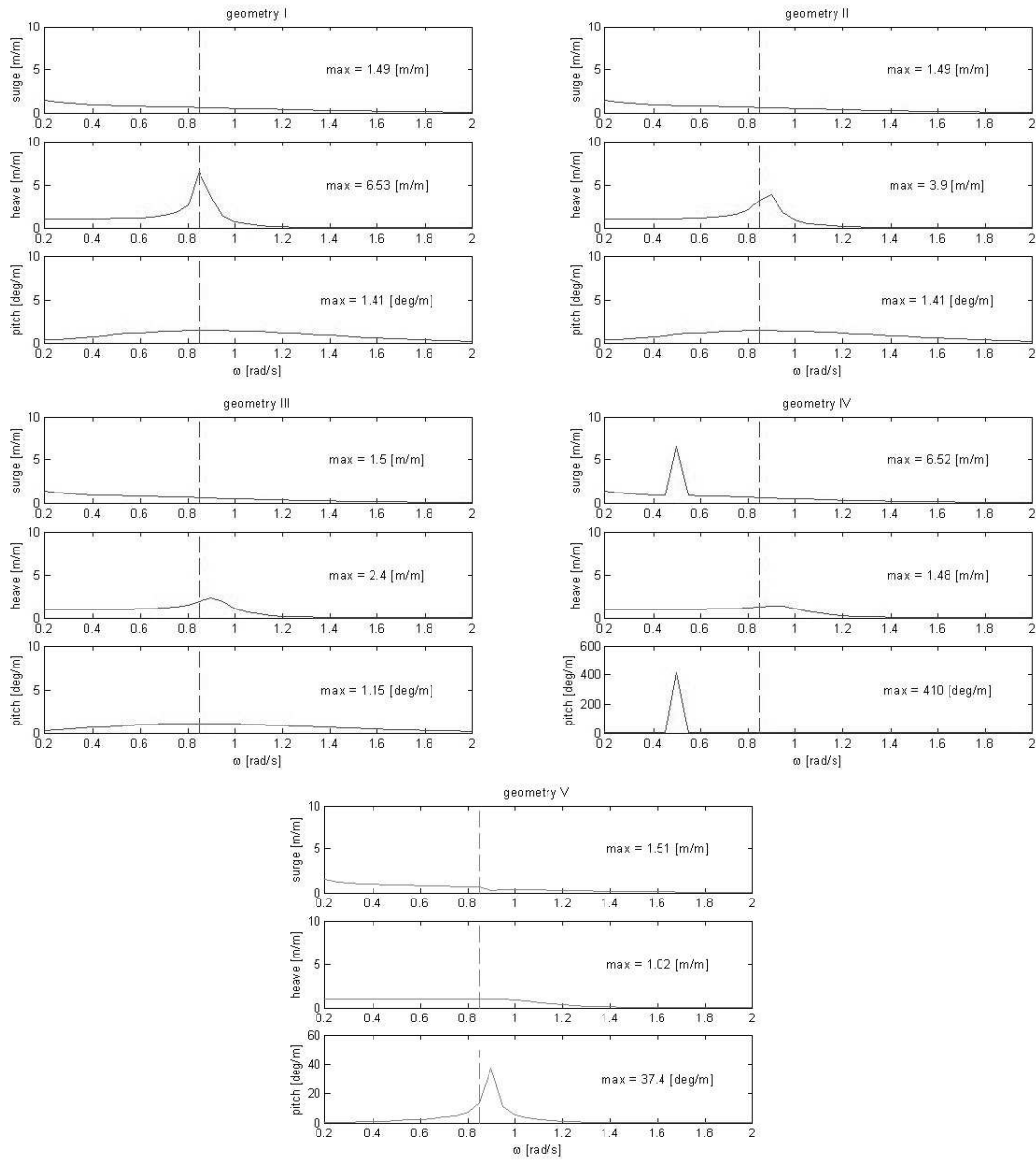

Figure 6.4: Transfer functions in surge, heave and pitch of geometry I-V

Geometry I, II and III have a resonance frequency for heave, but do not show resonance in surge or pitch. Geometry IV has a very high peak for both surge and pitch and a small peak for heave, while geometry V has no resonance for surge or heave, but does have a clear

resonance peak for pitch.

Surge
The surge motion is very limited for all geometries except IV. In IV there is a sharp peak at the same frequency as the peak of the pitch response. These two are coupled, because the pitch motion yields a surging motion for the center of gravity. The distance between the point of rotation and the center of gravity is so large that the center of gravity also experiences a horizontal motion (surge) due to the pitch motion of the vessel as a whole. The surge of the complete vessel remains very limited, comparable to the surge motion of the other geometries.

Heave
Resonance in heave becomes smaller with increasing diameter with a minimal peak for geometry IV and no resonance peak for geometry V. Apparently the damping becomes stronger for larger D_d. This corresponds to calculations of the damping ratio $j_{heave} = \frac{b}{2\sqrt{c(m+a)}}$ that show that the damping ratio increases with diameter D_d. Appendix E shows the damping ratio in heave for the different geometries.

The resonance peak of geometry I is a very accurate match with the design frequency, but geometry II, III and IV are less accurate. To improve these results the DELFRAC (frequency dependent) value for the added mass could be used to calculate the draught (see appendix D for the difference between DELFRAC and the analytical estimates of the added mass).

Pitch
The particular behavior of the different geometries in pitch corresponds to their behavior in figure 6.3 for their specific heights. There is no resonance frequency for geometry I, II and III at their height and indeed no resonance phenomena can be seen. Geometry IV should resonate at approximately 0.4 rad/s according to figure 6.3 for the calculated vessel height of 18.6m. This is reasonably close to the demonstrated 0.5 rad/s if the frequency dependency of I_a is taken into account. For geometry V the resonance frequency is so much closer to the projected 0.85 rad/s that the error in I_a becomes small enough to be negligible. Indeed, figure 6.3 and figure 6.4 both predict a resonance frequency of 0.9 rad/s. To improve this result an iterative procedure should be used to find the vessel height that yields exact resonance with the design frequency.

If the damping ratio for pitch $j_{pitch} = \frac{b}{2\sqrt{c(I_{xx}+I_a)}}$ is calculated it shows a decrease with diameter. This also confirms that the smaller diameters will demonstrate little pitch motion while the larger diameters will have a clear pitch resonance peak. Appendix E gives the damping ratio for pitch for geometry I-V. The high peak of geometry IV can also be explained with the damping ratio. For low frequencies the damping ratio becomes zero, therefore the resonance peak is only limited by the step size of the calculations in DELFRAC. Physically zero damping is impossible and to improve the results additional damping should be applied in DELFRAC. This can only be done by experienced engineers that have seen sufficient experimental data to estimate such damping effects. This case demonstrates one of DELFRACs' limitations as referred to in section 3.4.

6.1.5 Wave pattern behind the dampers

To compare the influence of the different geometries on the wave pattern a grid is defined. It stretches over an area of approximately 50 to $100m$ ($4704m^2$) and comprises 1250 calculation points in order to give a good indication of the wave pattern behind the damper. In comparison, the damper areas are between 113 and $804m^2$ equal to 2.4 or 17.1% of the grid size and the ecoboat is $962m^2$ (20.4%). This size and number of calculated points should be sufficient to view most effects. Figure 6.5 shows the relative size and position of the grid and damper geometry III.
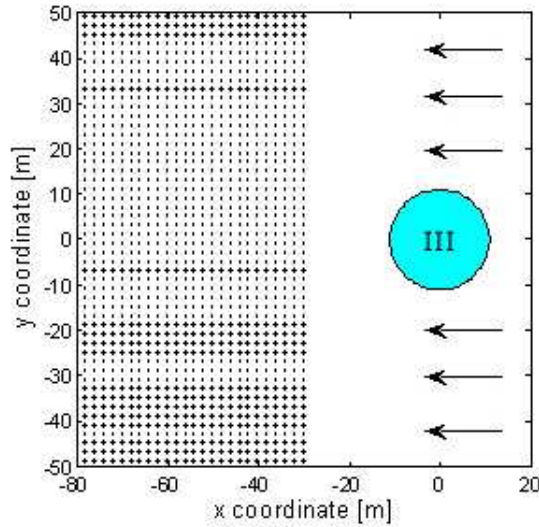
Figure 6.5: Situation sketch of grid points and damper geometry III

The significant wave height ($H_{1/3}$) and zero crossing period (T_2) are chosen to compare the damping of the waves at the grid points. This makes it possible to use the averaged values as a new wave regime for the ecoboat in section 6.2. Figure 6.6 shows the undisturbed wave height at the grid points as a blue square in the first figure. The other figures show the distribution of the significant wave height at the grid point in the presence of damper I, III and V.

The three wave patterns indicate the effects of the five geometries. As expected the pattern is symmetric about the center line, since both the damper and the incoming waves are symmetric about the centerline. The wave height at the centerline is higher than at the sides of the centerline and the wave height increases at the side of the grid. This could be explained with the phases of the waves made by the damper and the incoming waves. If the phases coincide the waves increase each other, if they differ $\frac{1}{2}\pi$ there is maximum damping. This effect becomes stronger if the damper makes higher waves and therefore becomes stronger for the damper with the largest hydrodynamic damping. Making waves is equivalent to wave damping since all energy is conserved for the current systems with only passive damping.

The figure shows that all dampers limit the wave height, but that the larger diameters show a steeper decline than the smaller ones. If the damping of the wave height is averaged over
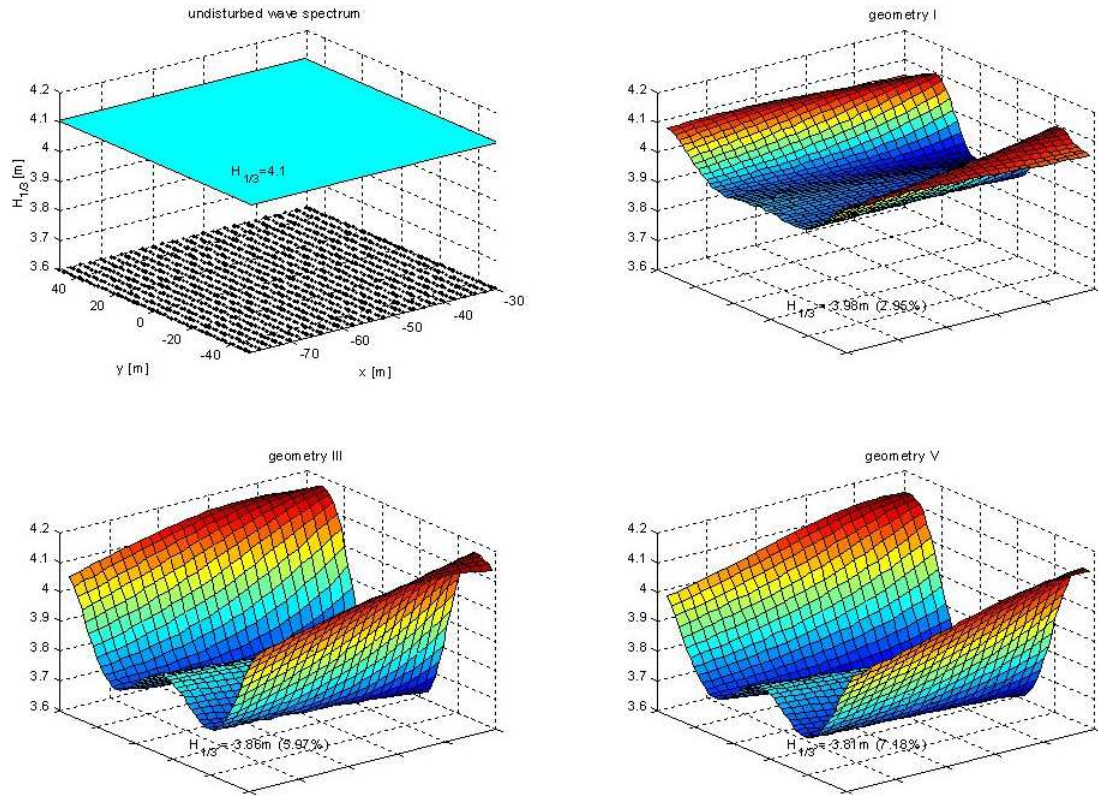
Figure 6.6: Wave height behind damper for geometry I, III and V

the grid this relation becomes even more evident as illustrated in table 6.4. Larger diameters yield more damping. This corresponds to the conclusion of paragraph 6.1.3 that predicted a direct relation between diameter and maximum damping capabilities.

geometry	wave height $H_{1/3}$ [%]
I	-2.96
II	-5.13
III	-5.97
IV	-6.04
V	-7.18

Table 6.4: Reduction in average wave height of geometry I-V

If the wave period is examined behind the five geometries as illustrated in figure 6.7, it shows that the average wave period becomes longer. This confirms the hypothesis that longer wave periods are not damped by the dampers and shorter periods are. The average wave period T_2 will then become longer.
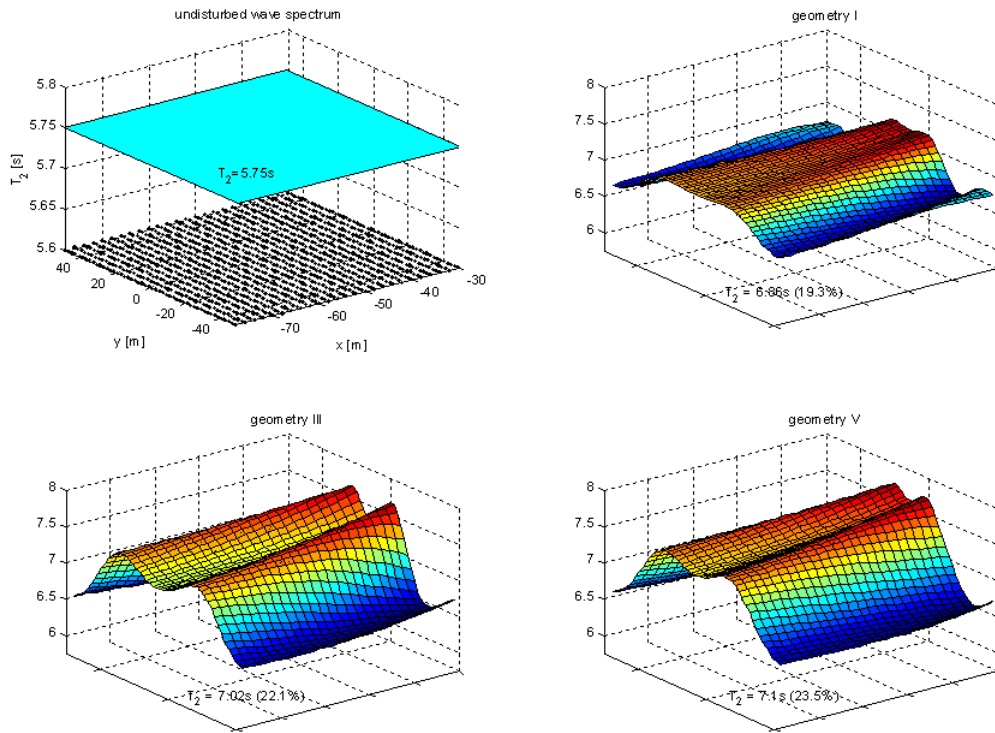
Figure 6.7: Wave period behind damper for geometry I, III, and V

Table 6.5 gives the average wave period for the grid. It can be seen that the increase in wave period is stronger for the larger diameters.

geometry	wave period T_2 [%]
I	+19.30
II	+20.80
III	+22.12
IV	+22.48
V	+23.47

Table 6.5: Increase in average wave period of geometry I-V

6.1.6 Selection of damper geometry

The previous paragraphs have demonstrated that a damper with a large diameter will have the strongest damping characteristics, but also that to match the pitch frequency the structure should become very high for large diameter. Geometry V needs to be approximately $17m$ for

resonance in pitch while geometry IV only needs to be 2.5m. Unfortunately this height is physically unrealistic, because the draught of geometry IV is 4.6m and the total structural height can therefore never be less than that height. Therefore a new geometry is defined as given in table 6.6 that has a diameter between geometry IV and V and will have a physically realistic but limited height to achieve resonance in pitch in the design frequency.

property	value [m]
D_d	28
d_d	4.2
H_d	5.45

Table 6.6: Selected damper geometry

This geometry is evaluated in DELFRAC to find the new transfer functions and the wave pattern behind the damper as demonstrated in figure 6.8 and figure 6.9.
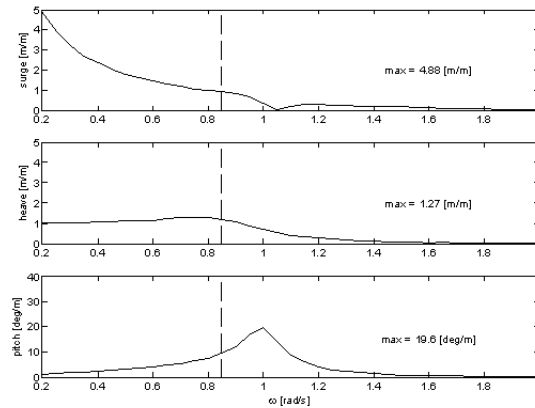
Figure 6.8: Transfer function of chosen geometry

Surge
The surge reaction to low frequencies is stronger than could be expected from the other geometries. This cannot be explained at present, but will have little influence on the results, since design wave spectrum does not include the lowest frequencies. The value of the surge reaction at higher frequencies is comparable to the surge reaction of the other geometries.

Heave
The heave response is in agreement with the other geometries. There is a small increase of the incoming movement with 1.27 [m/m] at the design frequency which is between the heave response of geometry IV and V and the 'peak' is close to the design frequency.

Pitch
The pitch response is comparable to geometry V. The peak is lower and rounder than the peak of geometry V as was expected from the decreasing trend of the damping ratio with increasing diameter for the same frequency (see appendix E). But the match between resonance peak and design frequency is not perfect yet and should be improved in the next design phase.
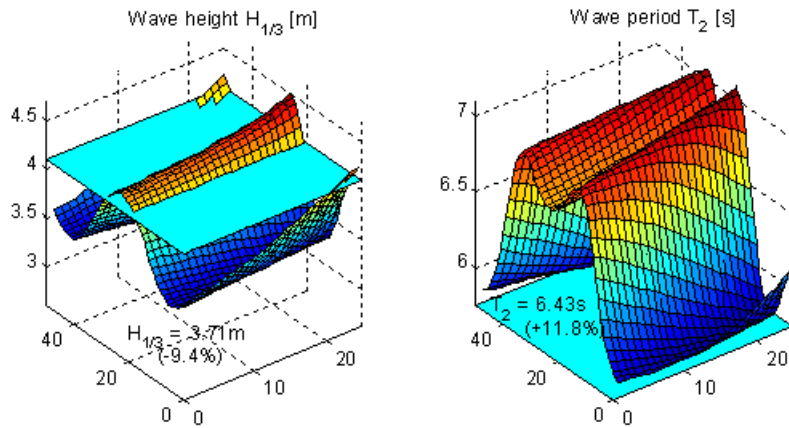
Figure 6.9: Wave height and period behind chosen geometry

The average wave height behind the damper is 9% lower than before. This reduction is more than could be expected from the results of the other geometries, but the most remarkable aspect of figure 6.9 is the distribution of the wave height on the grid. The waves behind the damper at the centerline of the grid actually become higher than the incoming waves. This is a result of the phase difference between the waves initiated by the pitch motion of the damper and the incoming waves. The pitch motion is a-symmetric with respect to the incoming waves and can yield such an enforcement of the waves. DELFRAC does not calculate the phases of the waves initiated by the structure therefore this explanation cannot be confirmed by calculations yet.

The wave period increases with 12% which is very little compared to the other geometries that all show an increase of at least 20%. This cannot be explained yet.

6.2 Wave damping for the ecoboat from the damper

Additional mechanical damping is applied to the geometry found in paragraph 6.1.6. This geometry is evaluated in DELFRAC with and without the additional damping and the effect of the damper on the grid is examined. Three different wave regimes are used to find the effect of the damper in different circumstances. Figure 6.10 gives the diagram used to find the functionality of the damper as wave damper for the ecoboat.
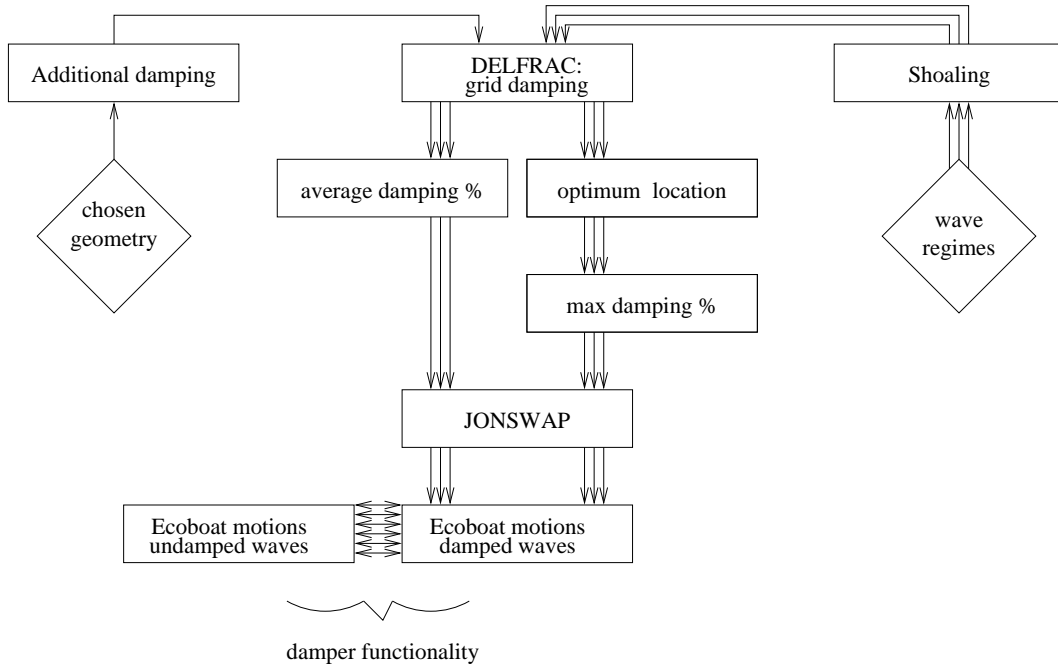

Figure 6.10: Diagram to determine damper functionality

The damping that should be applied to the chosen geometry to yield maximum power, is calculated in paragraph 6.2.1. Three wave regimes are chosen to represent most situations in paragraph 6.2.2. Next the average damping for these wave regimes is determined in combination with a location optimization. This makes it possible to use a local minimum to place the ecoboat. The new wave heights and periods are used in paragraph 6.2.4 to find the new motions of the ecoboat and compared to the undisturbed situation.

6.2.1 Addition of mechanical damping to yield maximum power

The additional mechanical damping that should be applied to yield maximum power is derived by P. Wellens for regular waves [14] as

$$\beta_{max} = \sqrt{\frac{(c - (m + a)\omega^2)^2 + b^2\omega^2}{\omega^2}} \qquad (6.2.1)$$

70

For $\omega = \omega_0$ it reduces to $\beta_{max} = b$ which is often used for approximations and illustrates the direct relation between passive damping and optimal mechanical damping.

Figure 6.8 illustrated that the design frequency is not yet equal to the resonance peak of the system, therefore the more accurate equation (6.2.1) is used to give a first estimation of the optimum damping coefficient in irregular waves. The additional damping constants applied in pitch and heave are

$$\beta_{heave} = 2745 \quad [kg/s]$$
$$\beta_{pitch} = 86007 \quad [kg\,m^2/s]$$

These damping constants are added to the hydrodynamic damping matrix to model internal mechanical damping that depends on the (rotational) velocity of the damper. The damping constants will also be used in paragraph 7.2.2 to calculate the power and energy yield of the damper.

Figure 6.11 shows the effect on the transfer functions in surge, heave and pitch.
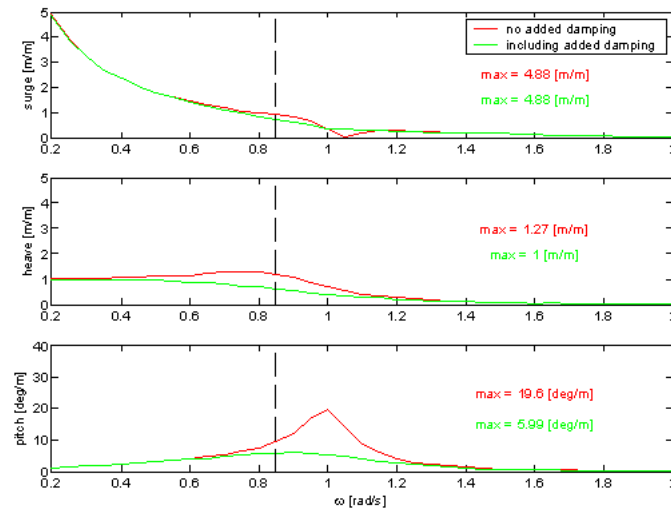
Figure 6.11: Damped transfer functions

At the design frequency of $\omega = 0.85$ the reduction achieved by the additional damping is 21% for surge, 50% for heave and 37% for pitch. The maximum damping for pitch is 69% at the resonance frequency. For an optimized damper in pitch resonance this would be the reduction achieved.

This yields a pattern of the wave height as illustrated in figure 6.12.

The damping effects are increased. The wave height through the middle is strongly reduced now the phase of the waves initiated by the pitch motion has changed with respect to the phase of the incoming waves and the average wave height is reduced from 3.71 to 3.33m (-10%). This leads to a total reduction of the average wave height of 19%. The phase of the initiated waves yields higher waves at the side of the grid than before.
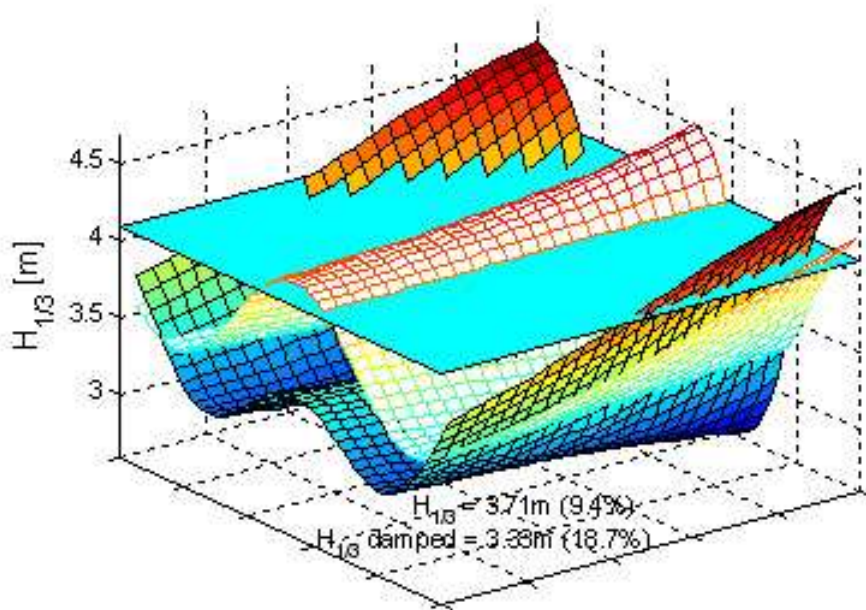
71

Figure 6.12: Effect of additional damping on the wave height behind selected damper

6.2.2 Damping properties in different wave regimes

To demonstrate the effect of the damper on the motions of the ecoboat three different wave regimes are defined. The combination predicts the effect of the damper in most circumstances. The first is the design wave regime as used until now. The second is the most occurring wave regime, this is defined as the prevailing wave period with the average wave height for that period. According to the scatter diagram given in appendix B this is a wave period of T_2=4.25s and an average wave height (including shoaling) of $1m$. The third wave regime represents more severe circumstances than the design wave regime and is referred to as high load wave regime with $T_2 = 6.25s$ and $H_{1/3} = 5.1m$ (including shoaling). The three wave regimes summarized in table 6.7 will demonstrate the effects of low and high waves for the ecoboat.

wave regime	$T_2[s]$	$H_{1/3}\ [m]$
design wave regime	5.75	4.1
most occurring wave regime	4.25	1.0
high load wave regime	6.25	5.1

Table 6.7: Definition of wave regimes

6.2.3 Location optimization of the ecoboat behind the damper

The pattern of wave height behind the damper as illustrated in figure 6.12 has strong variations. Therefore the exact position of the ecoboat within this grid is important for the actual

damping experienced by the ecoboat.

The grid average, used for the selection of the damper geometry, gives only an indication of the new wave regime for the ecoboat. Some more information is found with the average wave height and period at an area of the size of the ecoboat. These local averages give a better indication of the opportunities of the dampers since a local average will be closer to the actual wave regime experienced by the ecoboat than the average of the entire grid. But averages do not take into account the effects of the variation within the area on the ecoboat motions or the interaction effects of damper and ecoboat. In the next design phase the interaction of ecoboat and damper should be part of the DELFRAC calculations. At this stage only the opportunities of the dampers are requested and therefore the local averages are used to find an *optimum location*: the local average with the lowest average wave height.

The local averages are calculated by discretizing the ecoboat to a circle of 253 points and calculating the average of these points for all possible positions of the center point of the circle for which all points of the circle are within the calculated grid. For the given grid the center point of the circle should be at least $18m$ from both sides of the outer edge of the grid. This leaves 186 possible coordinates of the center point between x-coordinate -60 to -50m and y-coordinate -31 and +31m.

Figure 6.13 illustrates the optimum location for the ecoboat for the different wave regimes. The first figure shows a top view with black circles indicating the best position for the ecoboat for different wave regimes. The other figures show the wave pattern for the three different wave regimes with a projection of the optimum location and the coordinates of its center point.

The symmetry of the wave pattern yields two minima for the wave height. For the two longer wave periods (design wave regime and high load wave regime) the optimum location is at $(-50, -17)$ and $(-50, 17)$. The x-coordinate equals the limit coordinate for the center point of the calculations and it would be interesting to enlarge the grid in that direction, although the decrease of wave height in positive x-direction is not very strong. The optimum position for the most occurring waves is closer to the center line of the grid at $(-50, -11)$ and $(-50, 11)$. The first graph in figure 6.13 indicates the relative position of the two minima in a top view. This makes it clear that the optimum locations are close together and a choice within that region will be beneficial for the damping in all circumstances.

This yields the new wave regimes for the ecoboat as presented in table 6.8.

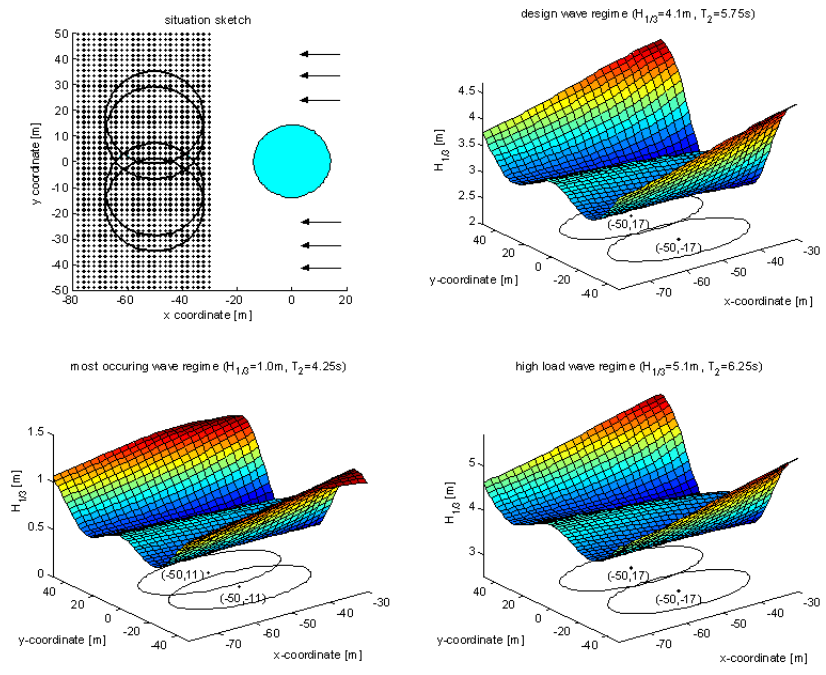|		undisturbed waves	grid average	optimum location
design wave regime	$H_{1/3}$	4.10	3.33	3.05
	T_2	5.75	6.29	6.47
most occurring wave regime	$H_{1/3}$	1.03	0.80	0.63
	T_2	4.25	4.83	6.57
high load wave regime	$H_{1/3}$	5.08	4.24	3.98
	T_2	6.25	6.81	6.47

Table 6.8: New wave regimes for the ecoboat

Figure 6.13: Optimum location of the ecoboat for different wave regimes

6.2.4 New motions of the ecoboat

The wave regimes of table 6.8 are converted to wave spectra with JONSWAP and combined with the transfer functions of the ecoboat to obtain motion spectra for the ecoboat. Figure 6.14 shows the motion spectra for the three different wave regimes with the spectra due to the undisturbed incoming wave regime, the grid average wave regime (referred to as average damping) and the wave regime of the optimum location (referred to as optimum damping).
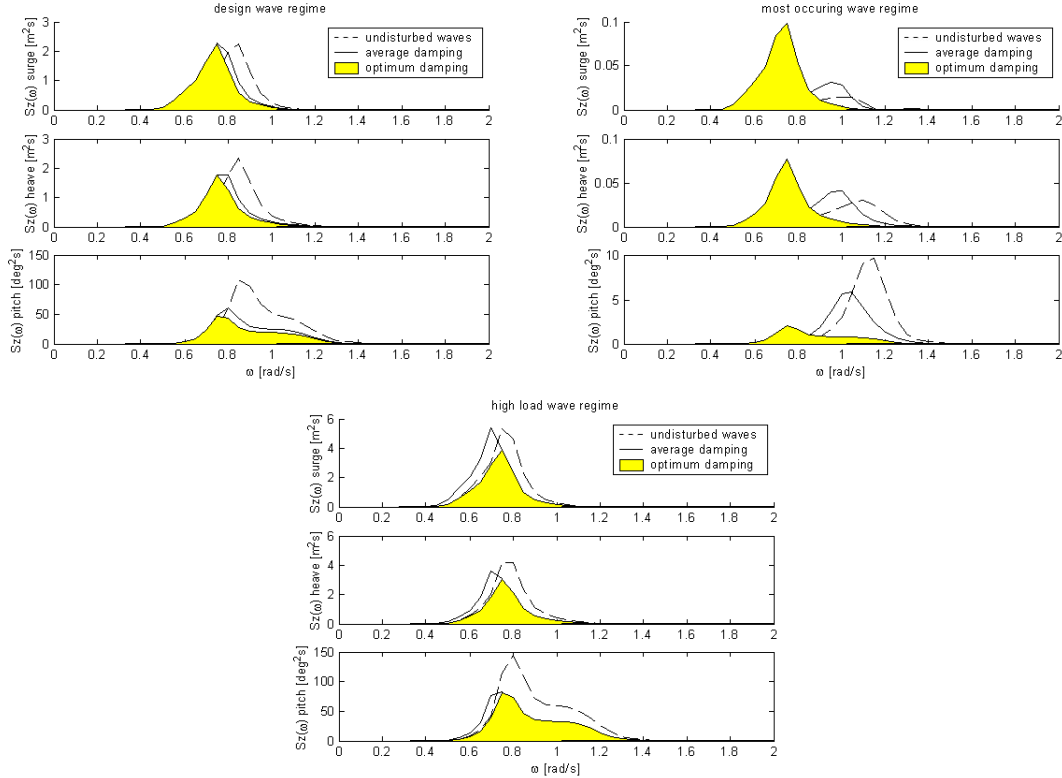
Figure 6.14: New motion spectra of the ecoboat for different wave regimes

To compare motion spectra in numbers the maximum value of the spectrum and the significant value of the spectrum are used (compare paragraph 4.4). Table 6.9 gives the maximum and the significant values for the different motions for the undisturbed, averagely damped and optimally damped waves for each of the three wave regimes.

Design wave regime

	max $S_x(\omega)$	max $S_z(\omega)$	max $S_\theta(\omega)$	$x_{a_{1/3}}[m]$	$z_{a_{1/3}}[m]$	$\theta_{a_{1/3}}[°]$
undisturbed waves	2.25	2.33	107.5	1.39	1.37	10.99
average damping [%]	+0.89	-23.61	-43.17	-2.59	-10.6	-23.38
optimum damping [%]	0	-24.03	-55.51	-5.91	-16.07	-31.23

	max $S_x(\omega)$	max $S_z(\omega)$	max $S_\theta(\omega)$	$x_{a_{1/3}}[m]$	$z_{a_{1/3}}[m]$	$\theta_{a_{1/3}}[°]$
undisturbed waves	0.01	0.03	9.58	0.13	0.19	2.89
average damping [%]	+200	+33.33	-38.41	+33.29	+8.53	-17.58
optimum damping [%]	+900	+166.67	-78.29	+113.03	+28.12	-46.33

High load wave regime

	max $S_x(\omega)$	max $S_z(\omega)$	max $S_\theta(\omega)$	$x_{a_{1/3}}[m]$	$z_{a_{1/3}}[m]$	$\theta_{a_{1/3}}[°]$
undisturbed waves	5.35	4.2	145	2.06	1.88	12.95
average damping [%]	+0.93	-14.52	-42.66	-3.32	-11.26	-21.73
optimum damping [%]	-28.04	-28.10	-43.70	-17.13	-19.87	-23.83

Table 6.9: Characteristic values of the new ecoboat motions

For all motions in all wave regimes the peak has shifted to a lower frequency. This corresponds to the overall increase in wave period for the damped situation. The damping effects at the optimum location (optimum damping) are larger than the damping effects averaged over the grid (average damping) for all three wave regimes. Therefore the explanation of the effects is a comparison between the motions in undisturbed waves and the motions at the optimum location.

Surge
The surge motion is least affected by the damper. The maximum amplitude remains the same for the design wave regime with or without damping and the significant amplitude is only reduced with 6% for the optimum location. The surge motion in the most occurring wave regime is increased 10 times. This seems a disadvantage of the presence of the damper, but both the maximum value and the significant value remain very small. This increase in surge motion for the most occurring wave regime is an effect of the change in zero-crossing period. The response to larger periods is stronger than to smaller wave periods as illustrated in figure 4.3 in chapter 4 and in this situation the increase in response is more important than the reduction of the wave height. For the high load wave regime the maximum amplitude is decreased by 28% and the significant amplitude by 17% which is beneficial in severe situations.

Heave
The heave motion is affected in a similar manner as the surge motion. For the design and high load wave regime the maximum value of the motion is decreased by 24 and 28% and the significant value by 16 and 20% respectively. While the heave motion is increased for the most occurring wave regime due to the shift in wave period. Although this is a disadvantage the maximum value and the significant value both remain very small and are not considered a serious draw back for the damper.

Pitch
The most important effect of the damper is the reduction of the pitch motion the ecoboat. This motion is very unpleasant for the inhabitants and is crucial to determine the living conditions. The reduction of the maximum spectral value for the design wave regime is 56% and 31% for the significant amplitude. The significant value for optimum damping is 7.56°which is still a high value and might require active damping, but the reduction is significant. In the most occurring wave regime the reduction is even stronger with a 78% reduction of the maximum value and 46% for the significant value that now becomes 1.55°which is very reasonable to

endure. The pitch motion is also reduced in high load conditions by the presence of the dampers with 44 and 24% for the maximum and the significant value respectively. But the resulting significant value of 9.87° is not acceptable for habitation and active damping of this motion will be required.

The actual limitations of motions for human inhabitance should be examined before a definite conclusion can be given.

Chapter 7

Sustainability of the ecoboat and dampers as households

This chapter will concentrate on the broader context of the ecoboat as a projected solution to fulfil future need of space, water and energy. First the global trends are discussed that create these needs and some of the fundamental principles and methods of sustainable development are introduced (7.1). Next a comparison is made of the use of resources of the ecoboat and dampers to a reference land-based building to be able to compare living at sea to living at land (7.2). This includes a calculation of the energy conversion capabilities of the damper designed in chapter 6. The comparison between land and sea-based living should help to answer the main question of this chapter: is living at sea a sustainable form of living?

7.1   Global trends towards living at sea

The ecoboat is designed as a combined solution to the need for water, energy and living space because global trends predict a shortage of these three basic needs in densely populated areas.

First the population growth is considered. Figure 7.1 demonstrates the population growth as estimated by the United Nations Population Division in 2004. Different scenario's of female fertility (number of children per woman) are shown as different growth prospects (low, medium, high and constant fertility). The most likely scenario (medium) shows a population increase from 6.5 billion in 2004 to 9.1 billion in 2050.
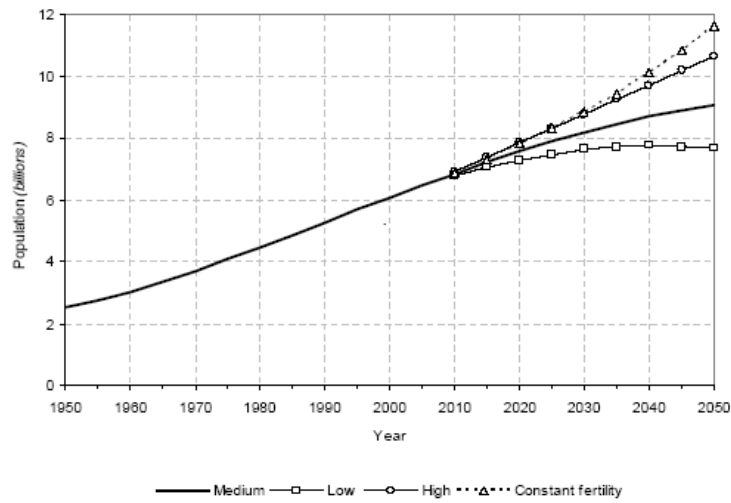
Figure 7.1: Population growth projection of the United Nations 2004 [15]

Another important global trend to be considered is of a demographic nature. The migration from rural areas to urbanized areas enforces the natural population growth of the cities. Figure 7.2 demonstrates that the population growth of figure 7.1 will be almost entirely concentrated in the urbanized areas. Migration will even lead to a slow decline of the rural population after 2015.

Figure 7.2: Urbanization prospects of the United Nations 2003 [16]

This concentrated population growth in urbanized areas will lead to a specifically high strain on these areas to provide for its inhabitants. Most of the larger cities are situated in river deltas or ocean bays and overall coastal areas are more densely populated than the regions inland. The increasing demand for space of growing urban populations will be hard to meet

79

and the water surface will in time be often considered space for expansion. This thesis is based on the assumption that living at sea will be part of future urban settlements. Timely investigation of the different aspects of living at sea as promoted by the ecoboat foundation, can help to shape the actual settlements.

Next to the need for space the need for water, energy, food and materials will increase in urbanized areas. Economies of scale can make an urbanized area ecologically more efficient than less densely populated areas. Provisions like public transport, apartment buildings or recycling of raw materials are only feasible for certain levels of population density. This could make an urban environment more ecological efficient than a rural environment. But at the moment the amount of natural resources required to sustain an urban resident (ecological footprint) is larger than the ecological footprint of a rural resident. The average level of prosperity of an urban resident is higher which allows more consumption and their attitude towards consumption is also often more positive. While the effects of the use of natural resources are less visible. Therefore at present both population growth and urbanization increase the request for natural resources.

Fossil fuels are a typical example of the consumption of natural resources at this moment as illustrated in figure 7.3. It can be seen that the consumption is steadily increasing and that fossil fuels represent and enormous global need for energy.
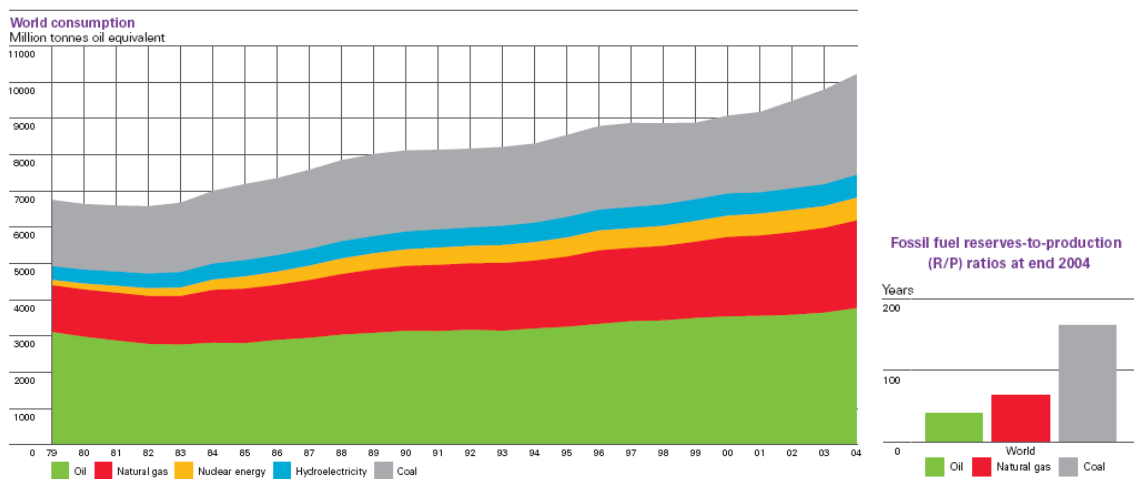
Figure 7.3: Global energy use and reserves divided by energy source [2]

Recent studies confirm the conclusions of the Club of Rome[1] that fossil fuels are limited and will be depleted within the next decades. Comparable graphs can be given for many other natural resources.

These trends illustrate the challenge to find solutions that take into account the increasing

---

[1]The Club of Rome wrote 'The limits to growth (1972)'. This report stressed the relation between economic growth and environmental problems like depletion of natural resources and pollution. It is considered the starting point of most environmental policies

population and increasing prosperity, but at the same time decrease the use of natural resources. This thesis is concentrated on the combination of increasing the available living space by investigating living at sea but also reducing the ecological footprint of its inhabitants.

7.2   Sustainability of living at sea

Sustainable development is defined by the Brundtland Commission[2] as development *'that meets the needs of the present without compromising the ability of future generations to meet their own needs'* [13]. Equation 7.2.1 can be used to quantify this principle.

$$I = P \cdot C \cdot T \tag{7.2.1}$$

with I environmental impact, P population, C level of consumption and T technology. This illustrates the direct relation between environmental impact, population, consumption level and the efficiency of the technology used for that consumption. To decrease the impact on the environment to halve the current level the technology T should be a factor-10 more efficient with raw materials and energy. This presumes a population growth according to figure 7.1 and an increase of consumption to four times the current level to achieve a more equal distribution over the world. With equation 7.2.1 this yields

$$0.5 = 1.4 \cdot 4 \cdot T \Rightarrow T = 0.09$$

The leaps in technology required for such improvements in efficiency can only be achieved with long term developments aimed at fulfilling needs rather then improving current systems. This means that the functional level of needs are considered (eg. 'transport', 'cleaning' or 'data exchange') to find a solution rather than improving the current solutions that fulfil these needs ('car', 'soap', 'fax-machine'). Fulfilling needs not only requires new technology, but also cultural and structural changes. For example living at sea could be one of the ways to fulfil the need for space, water and energy in densely populated areas while reducing the load on the environment considerably. But this would not only require a technological change, but also cultural and structural changes. A cultural change is required to accept living at sea as a save and desirable expansion of living space. Structural changes are needed to incorporate living units at sea in daily routines. This could require for instance a new form of working environments where local offices provide facilities for employees of various companies. The cultural and structural aspects are fundamental to the success of new technology and should be incorporated in multidisciplinary development teams. For this thesis only the technological aspects are considered.

Is living at sea such a leap in technology and a sustainable form of living? Four aspects of households at sea are compared to average land-based households to compare the use of raw materials and energy: water, natural gas, electricity consumption and the building materials. These aspects should demonstrate a reduction of 90% in material and energy use or otherwise meet the definition of a sustainable system as given by the Brundtland Commission. The

---

[2]Influential commission of the United Nations. Their definition ('Our common future', 1987) is generally accepted although not uniquely used.

ecoboat is compared to current forms of land-based living although some of the energy saving systems could also be used in land-based households. It should be clear that a possible sustainable household at sea is not considered the only sustainable form of living but an addition to sustainable land-based households.

Next to these four aspects of living at sea the required infrastructure, sewage, waste disposal and other systems should be investigated for a complete indication of the material and energy required. But the extend of such an investigation is beyond the scope of this thesis and therefore only those aspects are incorporated that can be quantified with the ecoboat and the damping system designed in the previous chapters. This means that the comparison presented in the next paragraphs can only give an indication of the opportunities of living at sea as a sustainable form of living and cannot give a conclusive answer wether living at sea is a sustainable form of living or not.

7.2.1 Land-based living: a reference building

To compare living at sea to land-based living an average land-based household is defined based on the statistics of the Dutch Energy Center (ECN) of the current consumption of Dutch households and the requirements for new buildings as given by the government.

The requirements for water, natural gas and electricity consumption and material use can be summarized as presented in table 7.1. The use of natural gas is wide spread in the Netherlands for central heating systems, tap water and cooking and is therefore also used in this comparison. To be able to compare natural gas consumption to other forms of energy-use the equivalent electrical value is included.

electricity	3402 kWh/year	average 2003 [4]
water	$108.4 m^3/year$	average 2004 [18]
natural gas	$1000 m^3$/year	Dutch legislation for new buildings
	(=8792 kWh/year)	($\sim 600 m^3$ for heating, $400 m^3$ tap water)
materials	€ 1030/year	Additional environmental costs
		according to GreenCalc [30]

Table 7.1: Energy and material use of an average land-based, 2.4 person household

Electricity, water and natural gas
The values for electricity, water and natural gas presented in table 7.1 are based on an average household size of 2.4 persons [4]. Electricity and water consumption are overall Dutch averages (old and new buildings) since these mainly depend on the choices of the inhabitant. Natural gas consumption and material use depend for an important part on building characteristics and are therefore compared to new buildings.

Materials
To be able to compare the material characteristics of land-based houses to the ecoboat a reference building is defined with an equal number of households and inhabitants as the ecoboat (as will be determined in paragraph 7.2.2).

An average household has a floor surface between 100 and $120 m^2$ and some external space

associated with the house. This yields a reference building of 16 houses of which each house is $5.4m$ wide, $9.6m$ deep, $7m$ high and has a garden of $6m$ deep (see appendix F for an illustration). The environmental costs given in table 7.1 are calculated for houses located in the West of Holland for a time span of 75 years.

The comparison of materials is based on GreenCalc calculations of the additional environmental costs required for the buildings per year. Environmental costs of buildings are not incorporated in the building costs but payed by society or future generations to restore or compensate natural resources, degradation, waste, pollution, hindrance, etc. GreenCalc is developed to calculate the effects of different materials and quantities of materials required for buildings and is a standard computational tool at the faculty of Architecture of Delft University of Technology. Appendix F gives a breakdown of the environmental costs of the reference building and more information about GreenCalc and its use.

7.2.2 Living at sea: the ecoboat and dampers

To be able to compare a sea-based household to a land-based household the ecoboat should be further detailed. A constellation of ecoboat and dampers is chosen to define the number of dampers to one ecoboat and the number of households on one ecoboat is also defined. These design choices have a large impact on the required material use and the available electricity for one household and should be reconsidered in a next design phase.

A constellation of ecoboats and dampers is illustrated in figure 7.4. The optimum location of the ecoboat with respect to the damper as calculated in chapter 6 is used to define the distance between ecoboat and damper ($50m$, see figure 6.13). The relative angle between the two is not considered, because the waves can come from all directions and an angle is only optimal for one wave propagation direction. A distance of $50m$ between the dampers is chosen. This is equal to half the grid size used in chapter 6 and the waves are expected to more or less equalize. This assumption should be confirmed by calculation in a next design phase.

The distance between the dampers and between the damper and ecoboat (both $50m$) yields the required number of dampers for one ecoboat. As illustrated in figure 7.4 one ecoboat requires six dampers. This is not a feasible solution to achieve a sustainable form of living, but initial living at sea will be in small settlements. Therefore a constellation with seven ecoboats is considered (see figure 7.4). This constellation uses a high percentage of the area and has a minimal circumference with respect to the enclosed area. One additional requirement is necessary to be able to calculate the number of dampers for these seven ecoboats: the distance between the ecoboats. Since interference effects have not been calculated yet a distance of $70m$ between the centerlines is chosen, equal to $35m$ of water between the boats. This is close enough for infrastructure to be feasible, but also far enough to neglect the effects of standing waves in this design phase. This yields 15 dampers or a ratio of 15/7.

The floor surface of the ecoboat is equal to $\sim 1000m^2$ and the overall height of $7m$ allows two stories of living space. Infrastructure is expected to use 20% of the available space. Therefore a first approximation is made of 16 households per ecoboat each with two stories of $50m^2$ (see appendix F.
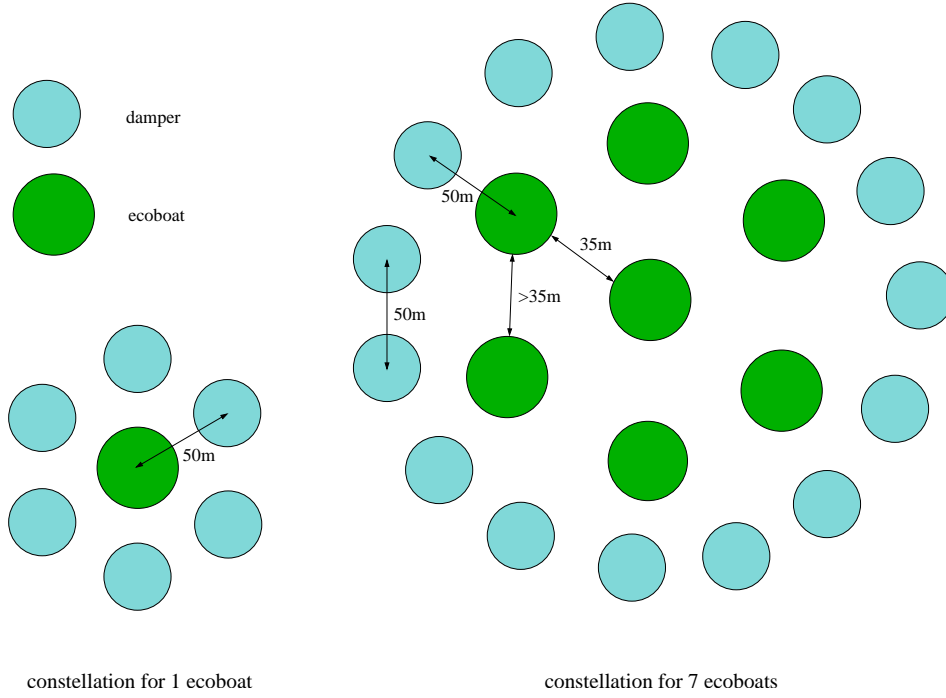
Figure 7.4: Possible ecoboat-damper constellations

To accommodate this many households some additional facilities are required. Therefore 6 ecoboats are considered inhabited and the seventh (middle) ecoboat is reserved for community services. This could include capacity for water storage and waste disposal systems, but also sport facilities etc. This means that the settlement will provide housing for 96 households with 230 inhabitants. The motivation of these choices and their effect on the comparison are given in paragraph 7.2.3.

Electricity
To calculate the available power from the dampers for transformation the force times the stroke is averaged over the time

$$\overline{P}_{heave} = \frac{1}{T} \int_0^T \beta_{heave}\,\dot{z}\,\dot{z}dt \quad [W] \tag{7.2.2}$$

With $\overline{P}_{heave}$ the average available power over one period in heave direction, T the wave period, β_{heave} the applied damping in heave as calculated in equation 6.2.1 and $\dot{z}$ the velocity of the damper in heave. $\beta_{heave}\dot{z}$ is equal to the force in heave direction and $\dot{z}dt$ is the distance dz; the combination yields the amount of work. Integrated and divided by T this yields the power in Watts.

The motion of the damper is given in equation 3.2.11 as

$$z = z_a \cos(\omega t + \epsilon_{z\zeta})$$
$$\dot{z} = -z_a \omega \sin(\omega t + \epsilon_{z\zeta})$$
$$\dot{z}^2 = z_a^2 \omega^2 \sin(\omega t + \epsilon_{z\zeta})^2 \quad \text{averaged over } T \Rightarrow \dot{z}^2 = \frac{1}{2} z_a^2 \omega^2 \qquad (7.2.3)$$

Equation 7.2.2 can now be written as

$$\overline{P}_{heave} = \frac{1}{2} \beta_{heave} z_a^2 \omega^2 \quad [W] \qquad (7.2.4)$$

An equivalent derivation can be used for the pitching motion to find

$$\overline{P}_{pitch} = \frac{1}{2} \beta_{pitch} \theta_a^2 \omega^2 \quad [W] \qquad (7.2.5)$$

> *Numerically this can be written as*
>
> $$\overline{P}_{heave} = \beta_{heave} \sum_{n=1}^{N} \frac{1}{2} z_{a_n}^2 \omega_n^2$$
>
> *and equation 3.3.2 can be rewritten to*
>
> $$\frac{1}{2} z_{a_n}^2 = S_z(\omega)\Delta\omega$$
>
> *with $\Delta\omega$ the step size of the calculations of $0.05\,rad/s$. Equal to the initial step size used in the DELFRAC calculations (see paragraph 3.4).*

This yields the available power that can be transformed for heave and pitch in the most occurring wave regime ($T = 4.25s$ and $H_{1/3} = 1.03m$ see paragraph 6.2.2). A conversion process from mechanical to electrical energy can have an efficiency of 90% [12], but the overall motion of the damper should first be converted to a direct mechanical force on the generator. Therefore the power delivered to the ecoboats is estimated to be 70% of the calculated power.

Power is expressed in Watt $[W]$ with $W = J/s$. Therefore the total energy yield in a year $[J/year]$ can be calculated by multiplying the power with the number of seconds in a year. This amount of energy can be rewritten to $kWh/year$ with the standard relation $1\,kWh=3.6\,MJ$. Table 7.2 gives the power and the energy yield in a year for both heave and pitch motion for a conversion efficiency of 70%.

A more accurate result of the energy yield per year can be obtained with the scatter diagram (see appendix B), but the most occurring wave regime defined as 'the prevailing wave period with the average wave height for that period' yields a feasible first approximation.

	$\overline{P}\ [kW]$	kWh/year	conversion efficiency
heave	0.01	67	70%
pitch	31.39	384937	70%

Table 7.2: Average power and yearly yield of 1 damper for most occurring wave regime

Table 7.2 confirms the observation of chapter 6 that the pitch motion is most relevant. It is recommended that in a next design phase the heave motion is neglected and that the damping applied in that direction is removed. The required investment to capture the heave energy is unacceptable compared to the yield. The pitch motion does give a relatively large energy yield compared to the energy requests from the households and should be optimized for maximum excitation and maximum conversion efficiency in a next design phase.

Other sources of electricity can be added to the electricity from the dampers to create a more robust system that is less dependent on weather circumstances. Solar panels can be mounted on top of the dampers. An average electricity yield for solar panels is $100kWh/year$ per square meter and the surface of each damper is $615m^2$ adding another possible $61500kWh/year$ of electricity. A third source of electricity could be the waste from the households. 96 households produce a considerable amount of waste that can be burned for electricity generation. Although a combination of energy sources will have a more constant yield in time, the variation in time of the electricity generation should be considered more carefully in a next design phase.

Finally the electricity consumption should also be reduced. Energy saving devices like LCD screens, laptop technology and new lighting devices all offer possibilities to reduce the household need of electricity.

Water
Fresh water can be generated with reverse osmosis. In this process salt water is pushed through a membrane at high pressure. An advanced reverse osmosis system uses $2kWh$ per m^3 of water [27] requiring $216.8kWh/year$ for the total water need of a household. The required energy can be reduced if the damper is used directly to yield the necessary pressure instead of transforming the movements of the damper to electricity and then using the generated electricity to create pressure.

The water need can also partly be fulfilled by rain water collection and the use of salt water for systems that do not involve direct human contact. Water saving systems like water saving shower heads, taps and toilet flushers also present an important opportunity to reduce the overall water need.

Natural gas
The need for climate control and warm tap water can be fulfilled by a heat pump and a solar boiler. The solar boiler should be mounted on top of the ecoboat to use the warmth of the sun for heating water. The current systems of a few square meters and a boiler reduce the consumption of natural gas for heating tap water by 50% [29], this reduces the consumption of natural gas for heating tap water to $200m^3$. It should be noted that the orientation and angle of a solar boiler are important to its overall effectiveness while the orientation of an ecoboat might not be constant.

To calculate the required electricity input for the heat pump the need for heating is split between tap water and climate control. The equivalent of $200m^3$ of natural gas used for heating tap water is $6330MJ$ net calorific value[3] or $1758.3kWh$. The equivalent of $600m^3$

---
[3]The calorific value of natural gas is the amount of Joules per unit of volume created by complete combustion. As part of the combustion process the hydrogen is transformed into water vapour. The net calorific value does not include condensation of this water vapour.

of natural gas used for climate control is $18.990MJ$ or $5275kWh$. Both are calculated with the net calorific value for natural gas of $31.65MJ/m^3$ [28] and the standard relation that the calorific value of electricity is $3.6MJ/kWh$. A current central heating system will have an efficiency η of 0.96

$$\eta = \frac{Q_{warmth}}{Q_{natural\ gas}} = 0.96 \tag{7.2.6}$$

with Q_{warmth} the heat added to the building in Joules and $Q_{natural\ gas}$ the calorific value of the natural gas in Joules.

This can be compared to a coefficient of performance (COP) = 3 of a heat pump for tap water that yields a temperature increase from the average sea water temperature of $12°C$ [26] to $90°C$

$$COP = \frac{Q_{warmth}}{W_{electric}} = 3 \tag{7.2.7}$$

with $W_{electric}$ the work in kWh applied to the system.

This should be combined with a COP=4 for a heat pump used for climate control that yields a temperature increase to $40°C$. This reduces the required energy input to $1828.7kWh$. See appendix G for a more detailed calculation of the COP of the heat pump. The calculation of the required electricity for the heat pump is very basic and should be reconsidered if a more detailed layout of the ecoboat is available.

The climate control system will have to be incorporated in an early stage of design, because the heat pump has a much higher efficiency for a small increase in temperature requiring a large contact region to transfer sufficient heat. Floor heating is a well known example of such a large contact region that requires a limited water temperature, but needs to be integrated with the construction. If the flow in the heat pump is reversed the system can also be used as a cooling system in summer.

The overall need for heating and cooling can be reduced if special care is taken in the design of the isolation and ventilation of the ecoboat.

Materials
The material use for the ecoboat is calculated in a similar manner as the material use for the reference building. A large concrete shell is assumed for the outer wall of $50cm$ thick and the inner ring is also considered a bearing element of the structure. In this way the internal layout can be kept relatively flexible. The shared space at the middle is covered with glass that can be opened for circulation. This in combination with sensible material choices yields an environmental cost per household of $\sim€\ 700/year$. See appendix F for a more detailed description of the environmental costs.

7.2.3 Comparison

The land-based and sea-based households are compared to determine the relative improvement. For a sustainable form of living the sea-based households should reduce the use of energy and raw materials by 90% or more compared to the land-based households or should otherwise comply with the definition of a sustainable system of the Brundtland Commission.

The comparison of the effects is strictly limited to the household consumption. Many aspects should be considered in more detail to find their life time use of raw materials and energy. Current solar panels require more energy during production than their life time yield. Waste burning systems will generate pollution. Material use for one damper has not been compared to the material use of an equivalent part of a conventional power plant. Another important aspect is the required facilities for one citizen. How much office space, sports grounds, etc. should be associated with one citizen and how does that change for sea settlements? All these uncertainties pose large restrictions on the comparison presented in this paragraph, but the comparison is still considered an important starting point for further investigation.

The aspects considered in this comparison are listed in table 7.3. The equivalent energy value is used to be able to include an overall comparison of the different aspects. The proposed savings in electricity and water use are not incorporated at this stage, because they depend on the choices of future inhabitants or on a more detailed design of the ecoboat. To indicate the opportunities of future savings a '<' sign is used in table 7.3.

	need land-based household per year	need ecoboat household per year	reduction ecoboat household per year
electricity	3402 kWh	<3402 kWh	from renewables
water	108.4 m^3 (∼217 kWh)	<108.4 m^3 (217 kWh)	from salt water
natural gas (heating)	1000 m^3 (∼8792 kWh)	0 m^3 (1828.7 kWh)	100% (79%)
combined energy need	12410 kWh	<5448 kWh	56% + renewables
materials	€ 1030	€ 704	32% + full cost pricing

Table 7.3: Comparison of the need of a land-based household to the ecoboat

Electricity and combined energy need
The constellation of ecoboat and dampers only hosts electrical provisions. It uses electricity to fulfil the direct electricity need, to provide fresh water from the available salt water and for heating. Therefore the water and natural gas consumption are rewritten to their equivalent electrical values to replace them and their combination yields the combined energy need in kWh.

The combined system of wave dampers, solar panels and waste burning system will yield more than 69756 kWh of electricity per household per year[4]. This is an overcapacity of 12.8 times the calculated energy need per household. Part of this overcapacity could be used to actively stabilize the ecoboat for long wave periods with high waves. The dampers will always have a surplus of energy for these wave regimes and that could be used directly for stabilization. The surplus of energy could also be used for the electricity demand of 1800 average land-based households, but transport to a land-based grid would require extensive infrastructure and should be considered very carefully.

A direct comparison between the electricity consumption of a land-based and an ecoboat household demonstrates an increase from 3402 to 5448 kWh (+62%), but the more relevant combined energy need is reduced with 56%. This reduction is not the factor-10 improvement

---

[4]Yield of 15 wave dampers with solar panels on top divided over 96 households

required for a sustainable solution. However all of the required energy is generated with renewable resources and thus sustainable within the original definition of the Brundtland Commission. Their definition emphasized that future generations should not be compromised to fulfil their needs. Renewable resources allow continuous use and therefore the ecoboat electricity need is a sustainable part of sea-based living.

Water

The water consumption is not yet reduced. The proposed systems (rain water collection, salt water for certain systems and water saving devices) would reduce the use of water and more particulary of fresh water considerably, but are not yet incorporated. A major change is the use of renewable energy to purify the water and the use of salt water which is a far more abundant resource globally than fresh water. Fresh water is no longer used as a resource. Therefore the ecoboat water consumption is considered sustainable compared to the land-based water consumption.

Natural gas

The use of natural gas is abandoned entirely. Tap water is produced by the combination of a solar boiler and a heat pump with electrical compression and the water for central heating is also produced by a heat pump. On an energy level a reduction of 79% is achieved by the application of these systems. The reduction on an energy level is not sufficient for a sustainable system as defined in paragraph 7.2, but the shift from natural gas to renewable resources is.

Materials

The environmental costs of the materials are reduced by 32%. This is only a small improvement compared to the required 90% reduction proposed in paragraph 7.2, but the total environmental costs of the materials are relatively low. A sum of € 704 per household per year could be incorporated in the prices of the materials or the construction and used to compensate society and future generations. In this way the environmental costs would be part of the building and maintenance costs and the relative impact of different materials and construction methods more visible to both owner and builder. This principle, also known as full cost pricing, should replace the taxes now used to compensate environmental costs. In this way the initial definition of the Brundtland Commission applies, because future generations will no longer be affected by the fulfilment of current needs.

7.2.4 Conclusions

Overall it can be seen that the consumption of energy and raw materials is not reduced sufficiently to achieve a 90% improvement, but the nature of the consumption is changed to a more sustainable form. The shift from fossil fuels to renewable energy and from fresh water to salt water both decrease the environmental load. Full cost pricing of materials will connect the environmental costs directly to the users. Therefore, based on the present investigation, living at sea is considered a sustainable form of living.

Chapter 8

Conclusions and recommendations

This study is concerned with the feasibility of the use of floating dampers to protect and sustain housing at sea. The possibility of this use is examined by designing wave dampers with the required properties. This shows that it is possible to design wave dampers that can be used to create a region of calm water that can host housing (ecoboats) and provide energy to sustain these houses.

8.1 Conclusions

Protection

Floating wave dampers can be designed to create much calmer water for the ecoboat, but should be combined with active internal stabilization of the ecoboat itself for the longest wave periods. This conclusion is based on the following considerations:

The damper is designed to calm the waves that yield the strongest motions for the ecoboat at the Dutch coast. The longest 5% of the wave periods are not included, because dampers for these waves would need to be too large. Therefore an active stabilization system is assumed within the ecoboat for the longest wave periods. Next it is presumed that a wave damping system designed for a specific wave period, will also damp waves with a shorter but not with a longer wave period. Therefore the longest wave period within the 95% of the waves is the design wave period. Combined with the scatter diagram of the Dutch coast this yields

$$\text{design wave regime:} \quad T_2 = 5.75s$$
$$H_{1/3} = 4.1m$$

The motions of the ecoboat in the design wave regime demonstrate a strong pitching motion. This is the critical motion for the design, because pitching motion is very unpleasant for inhabitants. The peak of this motions defines the design frequency at

$$\text{design frequency:} \quad \omega_0 = 0.85 \ rad/s$$

There are two wave energy conversion principles can be used for such a damping system. Both heaving and pitching bodies and oscillating water columns can fulfill the requirements. The difference in performance is very uncertain, therefore reliability is used to choose the heaving and pitching bodies principle for the wave energy conversion.

Five damper geometries are investigated to find the most suitable combination of diameter, draught and total height. They illustrate that larger diameters impose larger damping on the waves, but to match the pitch resonance to the design frequency the larger diameters need to be very high. Therefore a damper geometry is selected with

$$\text{damper geometry:} \quad \begin{aligned} diameter &= 28 \ m \\ draught &= 4.2 \ m \\ total \ height &= 5.45 \ m \end{aligned}$$

The selected damper geometry has a pitch resonance peak for $\omega = 1 \ rad/s$, which is not an exact match with the design frequency yet. This means that the performance of the damper will improve if a better match is found.

The damper reduces motions of the ecoboat, because the average wave height behind the damper is reduced. This reduction is not equal for each position behind the damper, therefore the ecoboat should be placed $50m$ behind the damper and between 11 and $17m$ next to the centerline to achieve a maximum reduction of wave height. The range of possible conditions for the ecoboat is represented by three different wave regimes: the design wave regime ($T_2 = 5.75s$, $H_{1/3} = 4.1m$), the most frequently occurring wave regime ($T_2 = 4.25s$, $H_{1/3} = 1.0m$) and a high load wave regime ($T_2 = 6.25s$, $H_{1/3} = 5.1m$). The reduction of the ecoboat motions is compared to the motions in undisturbed waves in table 8.1

	surge $x_{a_{1/3}}$	heave $z_{a_{1/3}}$	pitch $\theta_{a_{1/3}}$
design wave regime [%]	-5.91	-16.07	-31.23
most occurring wave regime [%]	+113.03	+28.12	-46.33
high load wave regime [%]	-17.13	-19.87	-23.83

Table 8.1: Reduction of ecoboat motions

Surge The surge motion is reduced for the design and high load wave regime, but increased for the most occurring wave regime. This increase is large in percentage, but the actual motion remains very small. The reduction of surge motion for high load circumstances is therefore considered more important.

Heave The heave motion is affected in a similar manner. In the design and high load wave regimes the motions are reduced, while the heave motion is increased in the most occurring waves. The average amplitude of the highest one third of the amplitude of this motion is still less than 25 centimeters and is therefore not considered a problem.

Pitch The most important effect of the damper is on the pitching motions of the ecoboat. The damper reduces the pitching motions of the ecoboat in all circumstances with up to 46% for the most occurring wave regime. The damper has thus a clear beneficial effect on the most critical motion of the ecoboat: the pitch and can be an important part of the safety system of the ecoboat.

Sustainability

A floating wave damper is a feasible solution to create a sustainable form of living at sea if household consumption is considered. This can be understood from the following considerations:

Living at sea is a future necessity. Population growth, urbanization and increasing prosperity require more space, water and energy while natural resources decline. Therefore the use of raw materials and energy should be reduced with at least a factor-10 compared to current technology or the technology should be changed in a way that does not limit the opportunities of future generations to fulfil their needs.

The feasibility of the ecoboat and dampers as a sustainable form of living is investigated by comparing the consumption of electricity, water, natural gas and building materials of the ecoboat with the consumption of a land-based reference building. The sea-based settlement consists of 7 ecoboats surrounded by 15 dampers. 6 of these ecoboats are inhabited and provide space for 96 households in total, the 7-th is reserved for general facilities. The land-based reference building is comparable to one ecoboat.

A more robust energy system is created by adding solar panels on top of the dampers and a burning system of the household waste at the 7-th ecoboat. This system is less dependent on the weather than with only wave dampers, but will still need some sort of energy storage. One damper with solar panels yields 446437kWh/year which is sufficient for 16 ecoboat households, but can also provide electricity for another 105 average land-based households.

Other important features for the ecoboat households are the use of reverse osmosis to create fresh water from salt water. The use of an electrical heat pump for heating and full cost pricing of materials. Full cost pricing means that all (environmental) costs associated with a material are part of the material price and thus paid by the user. This yields a change in consumption for the ecoboat household as presented in table 8.2.

	reduction of raw materials and energy per ecoboat household per year
electricity	from renewables
water	from salt water
natural gas (heating)	-100% (-79%)
combined energy need	-56% + renewables
materials	-32% + full cost pricing

Table 8.2: Reduction of household consumption for the ecoboat

Overall the consumption is reduced, but not with a factor-10. However, the shift from fossil fuels to renewable energy sources and from fresh to salt water makes the consumption of electricity and water sustainable in time. The shift to full cost pricing also protects future generations from the effects of current use and is therefore sustainable.

8.2   Recommendations

The feasibility of using a floating wave damper to protect and sustain sea-based housing can not be determined solely on this study. However, this thesis shows that the use of floating wave dampers for this purpose cannot be dismissed as wishful thinking either. It proves that there is a realistic change that such a use may be possible in the future, provided further research is done. In particular many more variables should be considered for the set of values used in this study. This further research should focus on:

Protection
- A stabler ecoboat should be used as a starting point. This means that the ecoboat configuration (diameter, draught, total height) should be reconsidered.
- The location should be further specified, because the design wave regime has a major effect on the design and is location specific.
- Active stabilization should be investigated to estimate the motions of the ecoboat including active stabilization.
- Overtopping devices should be reconsidered as a wave energy conversion principle for larger sea settlements if sufficient funding is available to use an experimental design approach.
- The change with frequency of the added mass should be used in calculations.
- The match between the frequency of the pitch resonance peak and the design frequency should be improved. This requires an iterative design approach of the damper geometry.
- The phase of the radiated waves from a structure should become part of the DEL-FRAC calculations.
- Multiple bodies should be evaluated simultaneously in DELFRAC to calculate the interactions of ecoboats and dampers. This will improve the results for the ecoboat motions, the wave pattern behind the dampers and the distance between the ecoboats.
- The grid used for calculations should be enlarged towards the damper, because the waves decrease in that direction.
- The boundaries of the ecoboat motions should be defined, therefore the maximum accelerations for permanent human habitation need to be determined.

Sustainability
- Cultural and structural aspects should be assessed by multidisciplinary development teams, because they are fundamental to the success of new technology.
- The comparison between land and sea-based living should be extended to include the required infrastructure, sewage, waste disposal and other systems.
- The size of the houses on one ecoboat should be reconsidered based on the wishes and expectations of future inhabitants. This will affect the use of materials for one household.
- The energy yield per year should be recalculated with the scatter diagram for higher accuracy.

- The heave motion of the damper should be neglected and no damping applied in that direction.
- The time variation of the electricity yield should be considered more extensively to determine the need for energy storage.
- The required electricity and water should be reduced by implementing frugal devices.
- All aspects of an ecoboat settlement should be considered to find the life time use of raw materials and energy.

Appendix A

List of wave energy converters

Table A gives an overview of the existing energy conversion devices for near-shore to offshore and offshore situations both operational and those in advanced stages of development. Main information sources are Wave Energy Conversion by John Brooke in 2003 ([1]) and the assessment on Offshore Wave Energy Conversion Devices of the Electricity Innovation Institute by Mirko Previsic from June 2004 ([11]). The devices are split between the different conversion techniques and small pictures give an indication of their functioning.
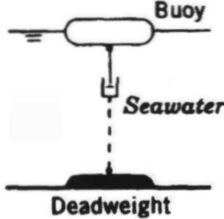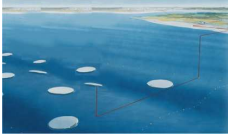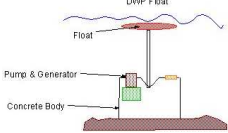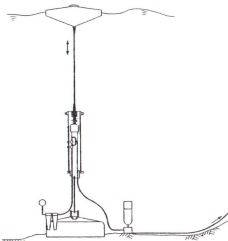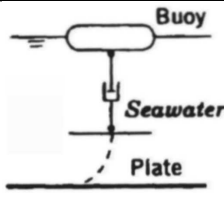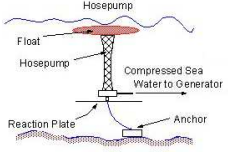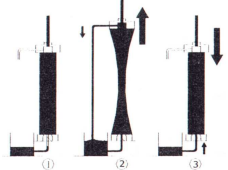
Definition of 'operational' energy conversion devices and 'advanced stage of development' by John Brooke:
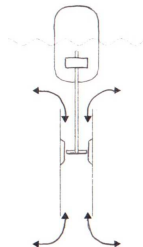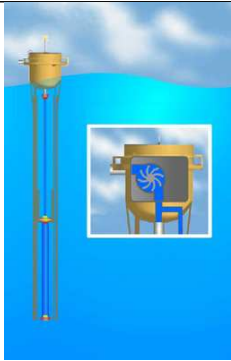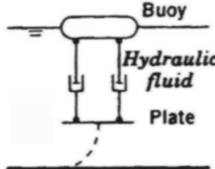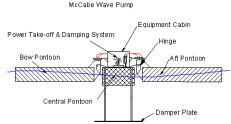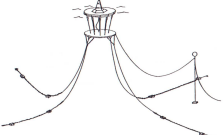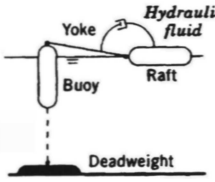
"The operational category comprises full-scale devices, chiefly prototypes, that are currently operating (or have operated) where the energy output is utilized for the production of energy or other purpose; also includes full-scale devices at an advanced stage of construction ."
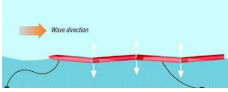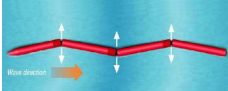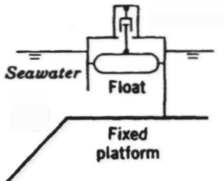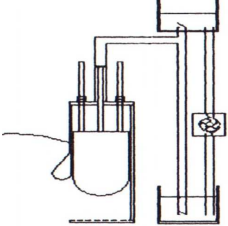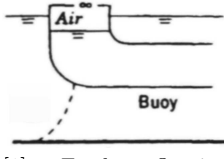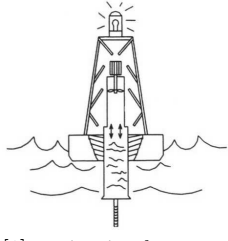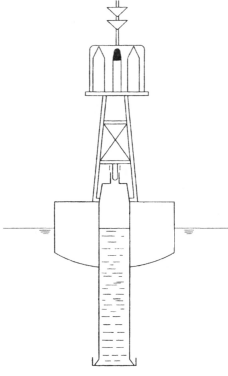
"The advanced-stage-development category comprises: (a) devices of various scales including full-scale, that have been deployed and tested in situ for generally short periods, but where the energy output has not been utilized for the production of electricity or other purpose (in most cases plans call for such devices to be further developed and deployed as operational wave energy systems); and (b) full-scale devices planned for construction where the energy output will be utilized for the production of electricity or other purpose."
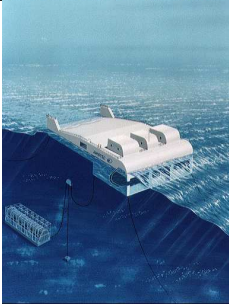
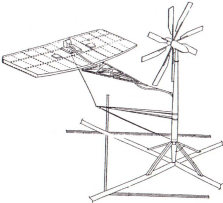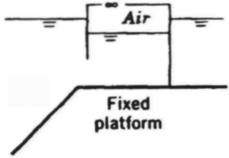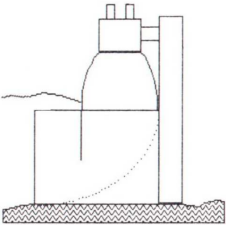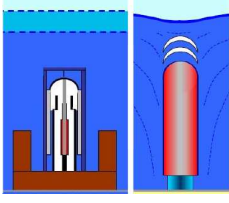| Classification of basic energy conversion principles	
A	Heaving or pitching bodies
B	Oscillating water column
C	Pressure devices
D	Surging-wave energy converters
E	Particle motion converters
F	Overtopping devices
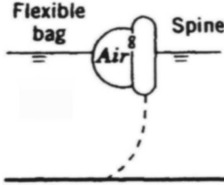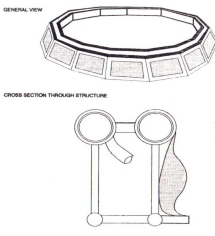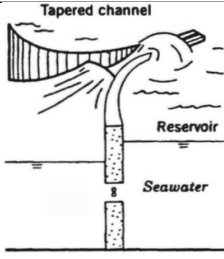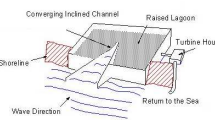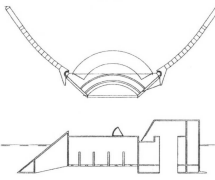
Table A.1: Summary of all operational wave energy converters and those in advanced stages of development

category	specific energy conversion process	device	device information
A	[1] Freely heaving float with sea-floor reaction point	[21] OPT PowerBuoy [21] OPT farm	developed in the USA and Australia, prototype testing in Portland, Australia
	,,	[22]Danish heaving buoy	developed in Denmark, prototype testing in Hanstholm
	,,	Phase-controlled power buoy	developed in Norway, prototype testing in the Trondheim fjord, minimum water depth is 40m for a device diameter of 10m, pneumatic power take off
	,,	[1] DELBUOY	developed in the U.S. to provide fresh water in remote areas by reverse osmosis
	[1] Freely heaving float with inertial reaction point	[22] Hosepump [1] Hosepump principle	developed in Sweden

category	specific energy con-version process	device	device information
	"	 [1] IPS buoy	developed in Sweden, tested device had a diameter of 3m
	"	 [25] AquaBuoy	developed in Sweden and the USA based on the hosepump and the IPS buoy, minimum water depth is 50m, device diameter is 6m with a draught of 30m, part of the E2I EPRI assessment
	 [1] Contouring float with inertial reaction point	 [22] McCabe wave pump	developed in Ireland, prototype testing in the Shannon river estuary, designed for fresh water production by reverse osmosis for remote islands
	"	 [1] Wave energy module	developed in the USA
	 [1] Contouring float with sea-floor reaction point	Kaiyo jack-up rig	developed in Japan, prototype testing on Iriomote Island, Okinawa
	"	Cockerell Contouring raft	developed in the UK
	"	Hagen Contouring raft	developed in the USA

category	specific energy conversion process	device	device information
	Floating articulated cylinder with mutual force reaction	 [11] Pelamis side view [11] Pelamis top view	developed in the UK, test site: Shetland/Isle of Islay, designed for water depth ¿50m, device diameter 4.6m, total device length 150m part of the E2I EPRI assessment
A/B	 [1] Heaving float in bottum-mounted or moored floating caisson	 [1] ConWEC	developed in Norway
B	 [1] Freely floating OWC	 [1] navigation buoy	developed in China based on Masuda navigation buoy, in operation at various sites
	"	 [1] Masuda navigation buoy	developed in Japan, in operation at various locations, device diameter of 3m with a draught of 3.75m
	"	 [24] Kaimei floating platform	developed in Japan, prototype testinf: Yura

category	specific energy conversion process	device	device information
	Fixed floating OWC	 [23] Mighty Whale	developed in Japan, tested in Gokasho bay, minimum water depth of 40m, device is 30m wide and 50m long
	”	 [1] Sperbuoy	developed in the UK, prototype tested in Plymouth
	”	 [1] Shim wind-wave system	developed in South Korea
	[1] Bottum-mounted OWC	 [1] Osprey	developed in UK, testsite is Thurso
C	Submerged pulsating-volume body with seafloor reaction point	 [1] Archimedes wave swing	developed in the Netherlands, fullscale prototype testing at Viano do Castello, Portugal, minimum water depth is 30m, device diameter is 9,5m, part of the E2I EPRI assessment

category	specific energy conversion process	device	device information
D	 [1] Flexible pressure device	 [1] SEA Clam	developed in the UK
F	 [1] Reservoir filled by direct wave action	 [22] Floating wave-power vessel	developed in Sweden
	"	 [1] Wave Dragon	developed in Denmark, minimum water depth is 25m, device is between 260 and 300m wide, part of the E2I EPRI assessment

Appendix B

Scatter diagram of Randstad wave regime

Randstad wave regime

The Randstad wave regime for the ecoboat location is compiled from three measuring sites: Noordwijk, IJmuiden munition deposit and Lightship Goeree. 30 Years of measurements are combined into a probability distribution of wave height and wave period [20].

The averaged scatter diagram for the wave regime of the ecoboat location

$$\text{Wave regime}_{\text{ecoboat}} = \frac{\text{data}_{\text{Noordwijk}} + \text{data}_{\text{IJmuiden}} + \text{data}_{\text{Goeree}}}{3} \tag{B.0.1}$$

This scatter diagram is given in figure B.1

Wave height at projected location

The wave height $H_{1/3}$ from the scatter diagram is corrected for the difference in water depth between measuring sites and the location for the ecoboat with the use of the average shoaling coefficient K_{sh} of the three measuring sites.

$$K_{sh\,\text{measurement}} = \frac{K_{sh\text{Noordwijk}} + K_{sh\text{IJmuiden}} + K_{sh\text{Goeree}}}{3} \tag{B.0.2}$$

The direct relation between the shoaling ratio and the wave height ratio yields the wave height at the projected location.

$$\frac{K_{sh\,\text{measurement}}}{K_{sh\,\text{projected location}}} = \frac{H_{1/3\,\text{measurement}}}{H_{1/3\,\text{projected location}}} \quad \Leftrightarrow$$

$$H_{1/3\,\text{projected location}} = H_{1/3\,\text{measurement}} \cdot \frac{K_{sh\,\text{projected location}}}{K_{sh\,\text{measurement}}} \tag{B.0.3}$$

Significant wave height (H1/3) and wave period (T2) avaraged over three measuring points

H1/3 \ T2	0.00-0.20	0.20-0.40	0.40-0.60	0.60-0.80	0.80-1.00	1.00-1.20	1.20-1.40	1.40-1.60	1.60-1.80	1.80-2.00	2.00-2.20	2.20-2.40	2.40-2.60	2.60-2.80	2.80-3.00	3.00-3.20	3.20-3.40	3.40-3.60	3.60-3.80	3.80-4.00	4.00-4.20	4.20-4.40	4.40-4.60	4.60-4.80	4.80-5.00	5.00-5.20	5.20-5.40	5.40-5.60	5.60-5.80	5.80-6.00	6.00-6.20	6.20-6.40	6.40-6.60	6.60-6.80	total
0.00-0.50	0	0	0	0	0	0	0	0	0	0	0	0	0	0	0	0	0	0	0	0	0	0	0	0	0	0	0	0	0	0	0	0	0	0	0
0.50-1.00	0	0	0	0	0	0	0	0	0	0	0	0	0	0	0	0	0	0	0	0	0	0	0	0	0	0	0	0	0	0	0	0	0	0	0
1.00-1.50	0	0	0	0	0	0	0	0	0	0	0	0	0	0	0	0	0	0	0	0	0	0	0	0	0	0	0	0	0	0	0	0	0	0	0
1.50-2.00	0	0.001	0	0	0	0	0	0	0	0	0	0	0	0	0	0	0	0	0	0	0	0	0	0	0	0	0	0	0	0	0	0	0	0	0.001
2.00-2.50	0.004	0.035	0.022	3E-04	0	0	0	0	0	0	0	0	0	0	0	0	0	0	0	0	0	0	0	0	0	0	0	0	0	0	0	0	0	0	0.061
2.50-3.00	0.026	1.292	1.313	0.328	0.031	0.003	0	0	0	0	0	0	0	0	0	0	0	0	0	0	0	0	0	0	0	0	0	0	0	0	0	0	0	0	2.994
3.00-3.50	0.195	3.753	4.362	2.924	1.161	0.303	0.057	0.004	0	0	0	0	0	0	0	0	0	0	0	0	0	0	0	0	0	0	0	0	0	0	0	0	0	0	12.758
3.50-4.00	0.319	3.826	4.205	4.827	4.039	2.435	1.051	0.381	0.115	0.023	0.001	0.001	0	0	0	0	0	0	0	0	0	0	0	0	0	0	0	0	0	0	0	0	0	0	21.223
4.00-4.50 (most occurring wave regime)	0.077	1.771	2.564	3.239	3.953	3.894	3.065	1.951	0.97	0.387	0.165	0.059	0.015	0.002	0	0	0	0	0	0	0	0	0	0	0	0	0	0	0	0	0	0	0	0	22.111
4.50-5.00	0.01	0.614	1.388	1.85	1.972	2.288	2.733	2.705	2.203	1.493	0.842	0.387	0.172	0.08	0.03	0.007	0.001	0	0	0	0	0	0	0	0	0	0	0	0	0	0	0	0	0	18.776
5.00-5.50	3E-04	0.196	0.581	0.957	0.995	0.855	0.89	1.134	1.402	1.551	1.426	1.075	0.687	0.37	0.174	0.07	0.034	0.012	0.002	0.0003	0	0	0	0	0	0	0	0	0	0	0	0	0	0	12.413
5.50-6.00 (design wave regime)	0	0.061	0.177	0.335	0.367	0.332	0.295	0.27	0.287	0.351	0.523	0.643	0.693	0.618	0.451	0.297	0.147	0.078	0.033	0.013	0.0057	0.0003	0	0	0	0	0	0	0	0	0	0	0	0	5.976
6.00-6.50 (high load wave regime)	0	0.026	0.055	0.075	0.082	0.093	0.064	0.063	0.054	0.065	0.075	0.097	0.159	0.199	0.275	0.297	0.261	0.18	0.1187	0.059	0.0363	0.015	0.007	0.0023	0.0013	0.001	0.001	0	0	0	0	0	0	0	2.361
6.50-7.00	0	0.005	0.021	0.019	0.013	0.012	0.018	0.014	0.012	0.013	0.012	0.015	0.025	0.03	0.042	0.056	0.089	0.103	0.1013	0.085	0.081	0.043	0.0253	0.0103	0.008	0.005	0.0023	0.001	0	0	0	0	0	0	0.861
7.00-7.50	0	7E-04	0.008	0.005	0.003	0.003	0.002	0.002	0.004	0.004	0.003	0.004	0.004	0.002	0.006	0.01	0.018	0.017	0.0247	0.034	0.0367	0.0373	0.0357	0.023	0.0177	0.0063	0.0043	0.002	0.0007	0.001	0	0	0.0003	0	0.319
7.50-8.00	0	0	0.002	0.003	0.001	0.002	0.001	0.001	0.001	0.001	0	0	0.001	0.001	0.001	0.002	0.002	0.002	0.002	0.005	0.0063	0.01	0.0087	0.011	0.011	0.0093	0.005	0.0043	0.0027	0.0023	0.0003	0	0	0	0.100
8.00-8.50	0	3E-04	7E-04	0.001	7E-04	0	3E-04	3E-04	3E-04	0	0	0	3E-04	3E-04	0.001	0	3E-04	0.001	0	0	0.0013	0.002	0.002	0.0023	0.004	0.0037	0.0037	0.0033	0.0013	0.003	0.0003	0.0003	0.0003	0	0.034
8.50-9.00	0	0	0	3E-04	0	0	0	0	0	0	0	0	3E-04	0	0	0	0	0	0	0	0	0	0	0	0	0.0003	0.001	0.001	0.0003	0.0003	0	0	0	0.0003	0.004
total	0.631	11.58	14.7	14.56	12.62	10.22	8.177	6.524	5.049	3.888	3.047	2.281	1.757	1.303	0.981	0.737	0.552	0.393	0.2817	0.196	0.1667	0.1077	0.0783	0.0493	0.0423	0.0263	0.018	0.0117	0.0053	0.0073	0.002	0.0013	0.0013	3E-04	100

Figure B.1: Probability distribution of wave height for the ecoboat location [20]
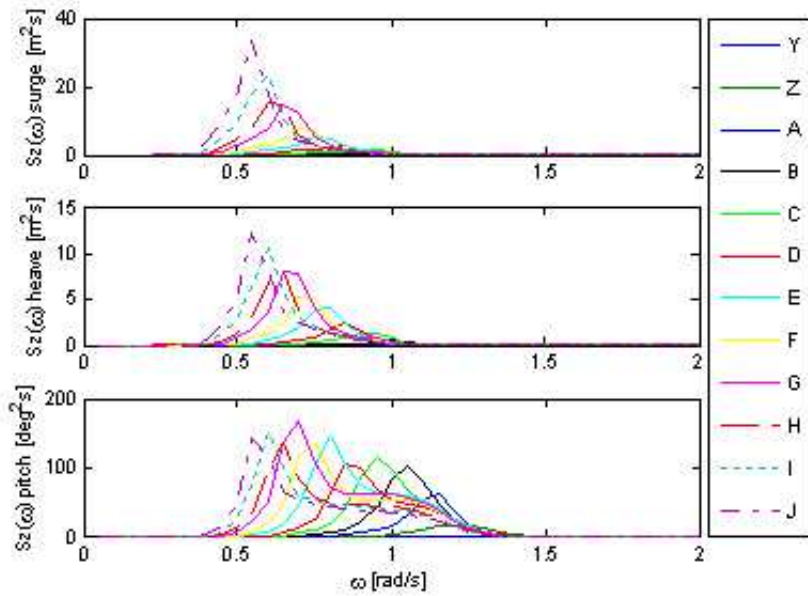
Appendix C

Ecoboat response to limit loads

Figure C.1: Ecoboat responses to limit load wave regimes

	T_2 [s]	$H_{1/3}$ [m] (including shoaling)		T_2 [s]	$H_{1/3}$ [m] (including shoaling)
Y	3.00-3.50	1.5	E	6.00-6.50	5.1
Z	3.50-4.00	2.3	F	6.50-7.00	5.3
A	4.00-4.50	2.6	G	7.00-7.50	6.2
B	4.50-5.00	3.2	H	7.50-8.00	5.8
C	5.00-5.50	3.8	I	8.00-8.50	6.2
D	5.50-6.00	4.1	J	8.50-9.00	6.4

Figure C.1 illustrates that the limit loads increase for surge and heave with increasing wave length (decreasing frequency) but have a maximum for pitch at G for a smaller wave period.

Appendix D
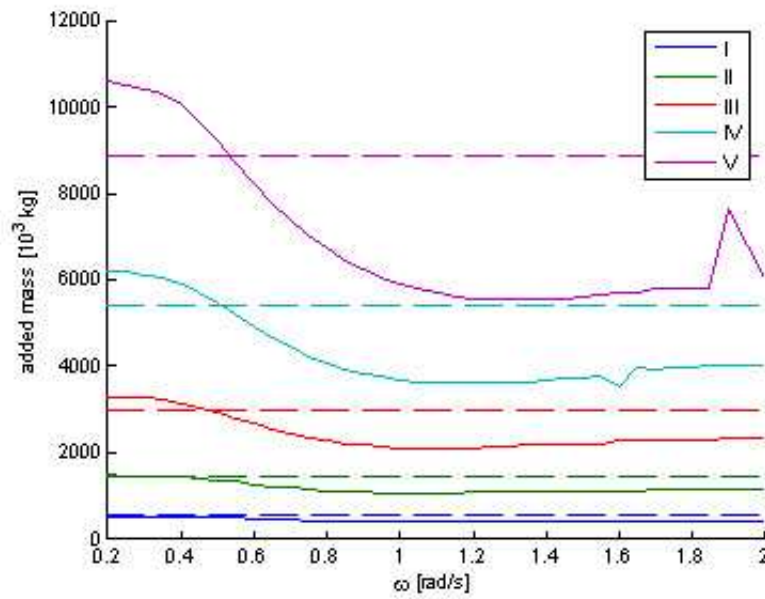
Added mass calculations versus analytical estimates

Figure D.1: Change of added mass with frequency for geometry I-V

Dotted line is analytical approximation of the added mass ($a = \frac{1}{12}\pi D_d^3 \rho_{sea}$), solid line is DELFRAC calculation of the added mass.

geometry	diameter D_d [m]	draught d_d [m]	height H_d [m]
I	12	9.6	22.8
II	17	7.9	21.5
III	22	6.2	20.1
IV	27	4.6	18.6
V	32	2.9	17

Appendix E

Damping ratio of the heave and pitch motion
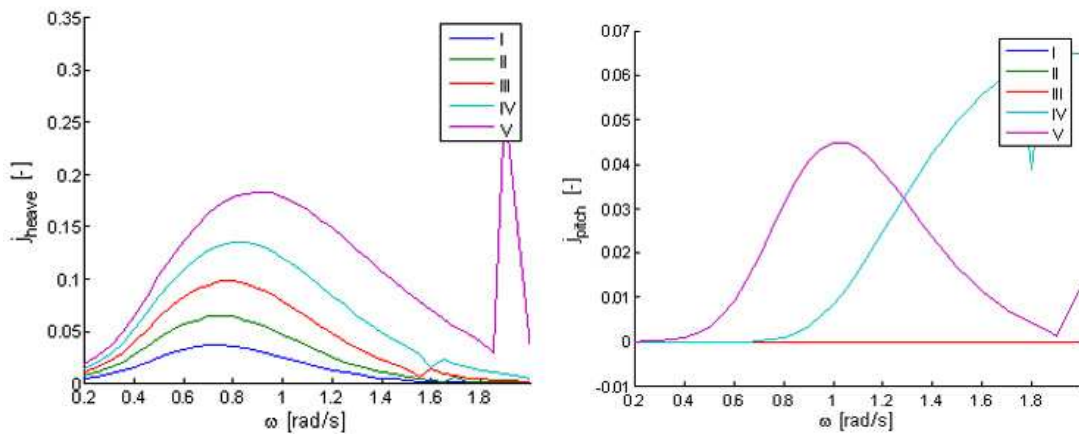
Figure E.1: Damping ratio for heave and pitch motion

geometry	diameter D_d [m]	draught d_d [m]	height H_d [m]
I	12	9.6	22.8
II	17	7.9	21.5
III	22	6.2	20.1
IV	27	4.6	18.6
V	32	2.9	17

---

[1]The damping ratios for pitch of geometry I, II and III are complex
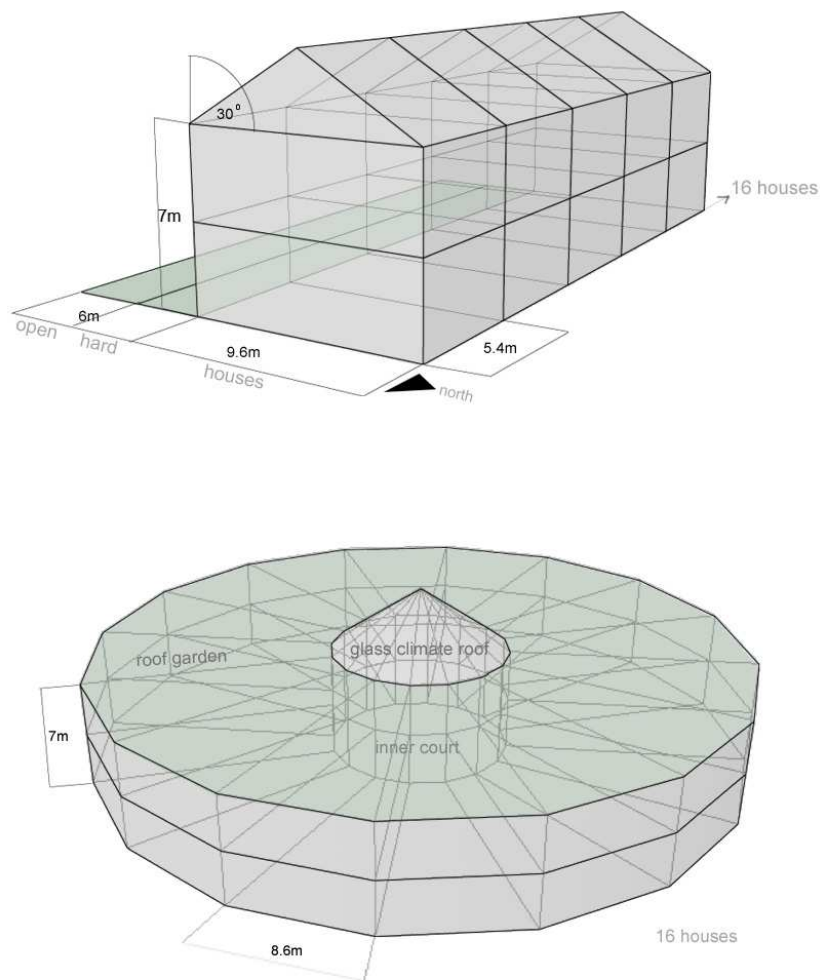
Appendix F

Environmental costs of material use

Figure F.1: Lay-out of land-based reference building and ecoboat households

Overview of environmental costs

Environmental costs of materials

	Ecoboat	Land-based reference
Foundations	-	311,718
Exterior	640,791	488,663
Bearing construction	143,471	347,884
Finish	57,719	76,603
Grounds	2,885	12,022
Total costs	844,866	1,236,890

Specification of environmental costs of materials

Resources	8,510	25,653
Pollution	256,825	352,146
Waste	357,487	473,550
Hindrance	28,059	42,584
Degradation	108,341	184,607
Energy	85,644	158,349
Total costs	844,866	1,236,890

The calculations of the costs are done with GreenCalc [30] developed to calculate the environmental costs of buildings. The input of the program consists of the specific materials and quantities of materials required for different sections of the building (foundations, exterior, bearing construction, etc). For the comparison between the ecoboat and the land-based houses only those sections that differ are included.

The choice of specific materials and their required quantity is largely build on experience. Therefore the calculations are performed by dr. ir. A. van den Dobbelsteen specialized in the environmental costs of buildings of the faculty of Architecture of the Delft University of Technology. The basic design of the ecoboat and the land-based reference building as illustrated in figure F.1 was made in cooperation with the author and then further detailed by Andy van den Dobbelsteen.

Some points of interest: the environmental costs of the mooring of the ecoboat are considered comparable or less than the environmental costs of infrastructure surrounding land-based buildings and therefore not included. The 'grounds' referred to of the ecoboat is the patio in the middle.
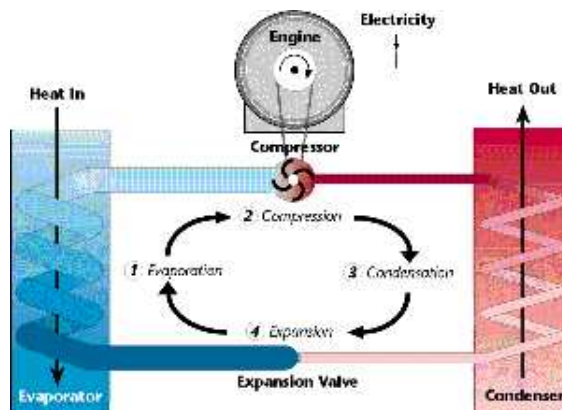
Appendix G

Heat pump

Figure G.1: Components of a heat pump cycle [31]

A heat pump for the ecoboat uses the temperature of the surrounding water to evaporate a refrigerant (ammonia or other) at low pressure, compresses the refrigerant vapor increasing both pressure and temperature, the vapor then condenses in the warm region and transports its heat, next the pressure is reduced in the expansion valve to complete the cycle.

The heat pump cycle illustrated in figure G.1 has a coefficient of performance equal to

$$COP = \frac{Q_{heat\ out}}{W_{electrical}} \quad [8] \tag{G.0.1}$$

with $Q_{heat\ out}$ the heat delivered to the building and $W_{electrical}$ the work required for the compressor.

The first estimation for the COP is made based on the statistics of the Heat Pump Center [31] as illustrated in figure G.2
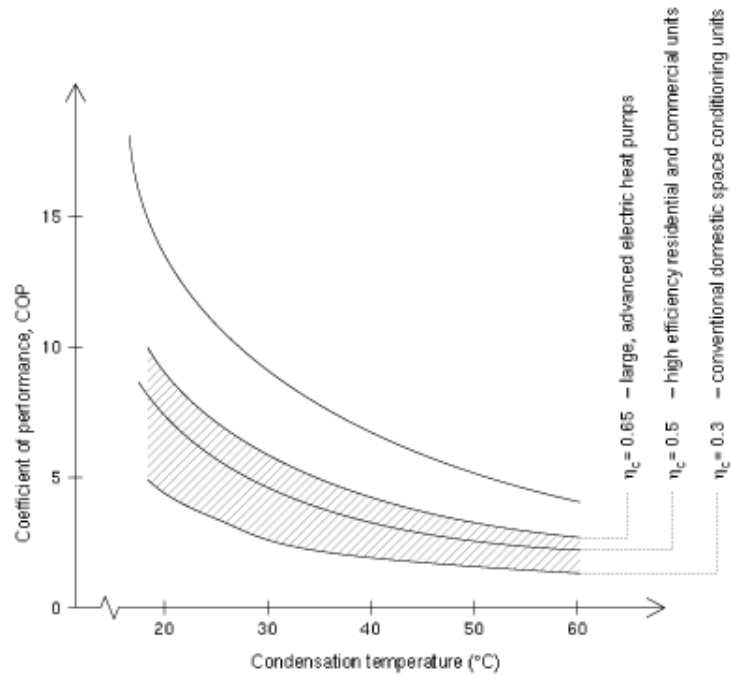
Figure G.2: Coefficients of performance of a heat pump [31]

The scale of the ecoboat allows relatively large and thus more efficient systems, therefore the Carnot efficiency (η_c) is considered comparable to those of large, advanced electric heat pumps. This yields a COP for the central heating (condensation temperature=45°C) of 4 and for tap water (average condensation temperature=55°C) COP=3.

Bibliography

[1] John Brooke (2003), *Wave Energy Conversion*, Elsevier Ocean Engineering Book Series Volume 6.

[2] Brittish Petroleum (June 2005), *Putting energy in the spotlight: BP Statistical Review of World Energy*, www.bp.com.

[3] Michael E. McCormick (1981), *Ocean Wave Energy Conversion*, (Alternate Energy) A Wiley-Interscience publication, John Wiley & Sons, New York.

[4] EnergieNed (2004); *Energie in Nederland*

[5] Prof. ir. J. Gerritsma (September 2002); *Bewegingen en Sturen I, Golven*; Report nr. 473-K reprint; Faculty of Mechanical Engineering and Marine Technology, Delft University of Technology.

[6] J.M.J. Journee and W.W. Massie (January 2001), *Offshore Hydromechanics*, first edition, Delft University of Technology.

[7] J.M.J. Journee and Jacob Pinkster (April 2002), *Ship Hydromechanics, Part I: Introduction*, draft edition, Delft University of Technology.

[8] M.J. Moran and H.N. Shapiro (1988); *Fundamentals of Engineering Thermodynamics*; John Wiley & Sons, Inc., New york.

[9] J.A. Pinkster, *Prediction of loads and motions of structures in waves*, Ship Hydromechanics Laboratory, Delft University of Technology.

[10] J.A. Pinkster (1995), *Hydrodynamic Interaction Effects in Waves*, Proceedings of the Fifth (1995) International Offshore and Polar Engineering Conference, June 11-16, 1995, Ship Hydromechanics Laboratory, Delft University of Technology.

[11] Mirko Previsic (June 16, 2004), *Offshore Wave Energy Conversion Devices*, E2I IPRI Assessment,Electricity Innovation Institute, report [E2I EPRI WP-004-US-Rev 1].

[12] Ronald Shaw (1982), *Wave Energy a design challenge*, Ellis Horwood Energy and Fuel Science Series, Ellis Horwood Limited, Chichester, England.

[13] Paul Weaver et al (2000); *Sustainable Technology Development*; Greenleaf Publishing Limited, Sheffield, United Kingdom.

[14] Peter Wellens (December 2004); *Wave Energy, study to determine the optimal performance of a floating wave energy converter*; OE5690 MSc thesis report offshore engineering, Delft University of Technology.

[15] United Nations Department of Economic and Social Affairs Population Division (2004); *World Population Prospects: The 2004 Revision*; United Nations, New York.

[16] United Nations Department of Economic and Social Affairs Population Division (2003); *World Urbanization Prospects: The 2003 Revision*; United Nations, New York.

[17] United Nations Department of Economic and Social Affairs Population Division (2001); *Population, Environment and Development: The Concise Report*; United Nations, New York.

[18] Vewin (2005); *Watergebruik thuis 2004*

[19] http://www.bp.com

[20] http://www.golfklimaat.nl

[21] http://www.oceanpowertechnologies.com/energy

[22] http://europa.eu.int/comm/energy_transport/atlas/htmlu/wavint4.html

[23] http://www.jamstec.go.jp/jamstec/myt.html

[24] http://www.jamstec.go.jp/jamstec/MTD/Whale/

[25] http://www.aquaenergygroup.com/home.htm

[26] http://www.knmi.nl

[27] http://urila.tripod.com/Seawater.htm

[28] http://home.hetnet.nl/ vanadovv/Energ.html

[29] http://www.ecn.nl/dego/index.en.html

[30] http://GreenCalc.com

[31] http://www.heatpumpcentre.org/

[32] http://roland.lerc.nasa.gov/ dglover/dictionary//content.html